NUREG/CR-6369, Vol. 2
SEA 97-3105-A:15

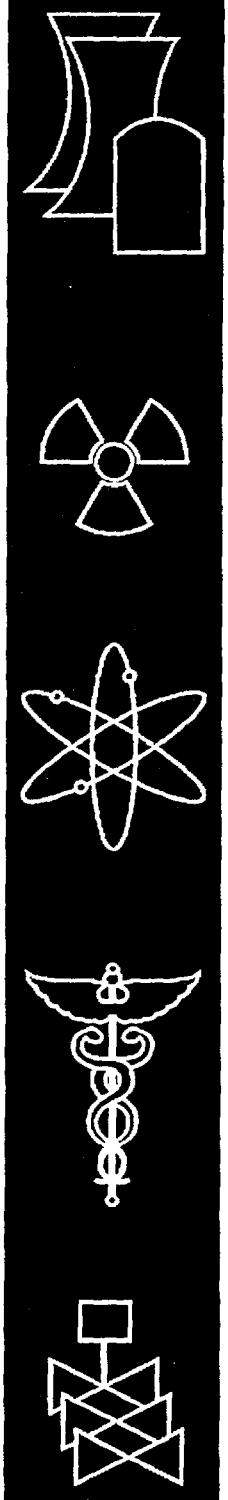

Drywell Debris Transport Study: Experimental Work

Final Report

Science and Engineering Associates, Inc.

U.S. Nuclear Regulatory Commission
Office of Nuclear Regulatory Research
Washington, DC 20555-0001

AVAILABILITY NOTICE

Availability of Reference Materials Cited in NRC Publications

NRC publications in the NUREG series, NRC regulations, and *Title 10, Energy,* of the *Code of Federal Regulations,* may be purchased from one of the following sources:

1. The Superintendent of Documents
   U.S. Government Printing Office
   P.O. Box 37082
   Washington, DC 20402–9328
   <http://www.access.gpo.gov/su_docs>
   202–512–1800

2. The National Technical Information Service
   Springfield, VA 22161–0002
   <http://www.ntis.gov/ordernow>
   703–487–4650

The NUREG series comprises (1) brochures (NUREG/BR-XXXX), (2) proceedings of conferences (NUREG/CP-XXXX), (3) reports resulting from international agreements (NUREG/IA-XXXX), (4) technical and administrative reports and books [(NUREG-XXXX) or (NUREG/CR-XXXX)], and (5) compilations of legal decisions and orders of the Commission and Atomic and Safety Licensing Boards and of Office Directors' decisions under Section 2.206 of NRC's regulations (NUREG-XXXX).

A single copy of each NRC draft report is available free, to the extent of supply, upon written request as follows:

Address: Office of the Chief Information Officer
Reproduction and Distribution
Services Section
U.S. Nuclear Regulatory Commission
Washington, DC 20555–0001
E–mail: <DISTRIBUTION@nrc.gov>
Facsimile: 301–415–2289

A portion of NRC regulatory and technical information is available at NRC's World Wide Web site:

<http://www.nrc.gov>

All NRC documents released to the public are available for inspection or copying for a fee, in paper, microfiche, or, in some cases, diskette, from the Public Document Room (PDR):

NRC Public Document Room
2120 L Street, N.W., Lower Level
Washington, DC 20555–0001
<http://www.nrc.gov/NRC/PDR/pdr1.htm>
1–800–397–4209 or locally 202–634–3273

Microfiche of most NRC documents made publicly available since January 1981 may be found in the Local Public Document Rooms (LPDRs) located in the vicinity of nuclear power plants. The locations of the LPDRs may be obtained from the PDR (see previous paragraph) or through:

<http://www.nrc.gov/NRC/NUREGS/
SR1350/V9/lpdr/html>

Publicly released documents include, to name a few, NUREG-series reports; *Federal Register* notices; applicant, licensee, and vendor documents and correspondence; NRC correspondence and internal memoranda; bulletins and information notices; inspection and investigation reports; licensee event reports; and Commission papers and their attachments.

Documents available from public and special technical libraries include all open literature items, such as books, journal articles, and transactions, *Federal Register* notices, Federal and State legislation, and congressional reports. Such documents as theses, dissertations, foreign reports and translations, and non-NRC conference proceedings may be purchased from their sponsoring organization.

Copies of industry codes and standards used in a substantive manner in the NRC regulatory process are maintained at the NRC Library, Two White Flint North, 11545 Rockville Pike, Rockville, MD 20852–2738. These standards are available in the library for reference use by the public. Codes and standards are usually copyrighted and may be purchased from the originating organization or, if they are American National Standards, from—

American National Standards Institute
11 West 42nd Street
New York, NY 10036–8002
<http://www.ansi.org>
212–642–4900

NUREG/CR-6369, Vol. 2
SEA 97-3105-A:15

Drywell Debris Transport Study: Experimental Work

Final Report

Manuscript Completed: February 1998
Date Published: September 1999

Prepared by
D. V. Rao, C. Shaffer, B. Carpenter/SEA
D. Cremer, J. Brideau/SEA
G. Hecker, M. Padmanabhan, P. Stacey/ARL

Science and Engineering Associates, Inc.
6100 Uptown Blvd. NE
Albuquerque, NM 87110

Subcontractor:
Alden Research Laboratory
30 Shrewsbury Street
Holden, MA 01520

Prepared for
Division of Engineering Technology
Office of Nuclear Regulatory Research
U.S. Nuclear Regulatory Commission
Washington, DC 20555-0001
NRC Job Code W6325

NUREG/CR-6369, Vol. 2, has been
reproduced from the best available copy.

Abstract

This report describes three test programs undertaken as part of the DDTS to provide basic understanding regarding transport of insulation fragments in the drywell following a postulated LOCA. The first two tests focused on transport of debris by blowdown flow. They obtained data related to (a) inertial capture of insulation debris on typical BWR drywell structures while they are transported across the structures by the steam flow; and (b) degradation of large insulation pieces captured on floor gratings when exposed to high velocity steam flow with suspended droplets. These tests clearly established that wet floor gratings would capture significantly more debris than any other BWR drywell structures (e.g., pipes, I-beams and vents). The capture efficiency of all structures was found to be a strong function of debris size and structural wetness, but a weak function of flow velocity and local flow patterns. Floor gratings possess 100% capture efficiency for insulation pieces larger than 6"x4". These large pieces do not degrade or are not forced through the grating clearances (1.5"x4") when subjected to high velocity droplet flow, even though the differential pressure across them is as high as 1 psid.

The third test program addressed the issue of washdown of debris previously captured on floor gratings by break over flow or containment spray flow during ECCS recirculation phase. These tests concluded that majority of the small debris pieces captured on various structures would be washed down by break flow or spray flow. On the other hand, erosion is the only available mechanism by which large pieces deposited on the floor gratings would be transported. In three hours, as much as 25% of the larger pieces can be eroded and transported to the suppression pool.

Contents

Contents (Continued)

Contents (Continued)

Contents (Continued)

Figures

Figures (Continued)

Tables

Executive Summary

A postulated LOCA in a BWR whose primary piping is insulated with fibrous insulation will generate fibrous debris in a region close to the broken pipe. These insulation fragments, ranging in size from small fragments to partially damaged blankets, will be entrained by the ensuing steam flow and carried through the drywell to the suppression pool. However, the drywell is congested with numerous structural elements (e.g., pipes, gratings, I-beams and vents) that could impede such transport. The debris particles are expected to impact these structural elements, which are expected to be wet as a result of steam condensation and droplet deposition. It was not known if such a particle upon impact will be captured on the structural surface or will be sheared off by the high flow velocity (25-150 ft/s). It was also unknown whether the captured debris would be retained on the structures in spite of short-term (≈ 1 minute) exposure to high steam flow during the remaining blowdown or long-term exposure (15-180 minutes) to water from break overflow or containment spray flow. Three experiments were designed and conducted as part of the DDTS to provide basic understanding and insights related to short-term and long-term fibrous debris transport in the BWR drywells. The first two experiments focused on studying inertial capture of fibrous debris on typical drywell structures during airborne transport. The third experiment studied washdown of debris previously deposited on various drywell structures by break overflow and containment sprays.

A series of separate effects tests were conducted at ARL to obtain a basic understanding of fibrous insulation capture on typical BWR drywell structures due to inertial capture. Using an air flow tunnel with water spray nozzles, these tests studied debris capture as influenced by size of debris particles, mass loading of debris (gm/ft^2), shape and orientation of individual structures, congestion of structures, structural wetness, and gas fluid velocity. Low gas velocity tests, between 25 and 50 ft/s, were conducted using the full 4 ft by 4 ft cross-sectional area of the tunnel, and a smaller test section insert (2 ft by 2ft) was used to achieve velocities as high as 150 ft/s. Mechanically shredded and pre-weighed fibrous debris of different sizes was injected into flow stream using a debris injection gun. The debris capture fraction for each structure was estimated as the ratio of the debris deposited on the structure to the quantity of debris approaching that structure. The major findings of the study were that gratings captured more debris than any other drywell structures, that surface wetness strongly influenced debris capture, and that capture on vent plates and vent entrance is moderate.

While the ARL separate effects tests provided valuable data, the tests had notable limitations of relatively light debris loading on the structures compared to expected BWR conditions, modest assortment of debris sizes and non-prototypical congestion of structures. Also, the test data was obtained for simplified flow fields (plug flow approaching the structures). Application of such a data to BWR drywells would have required detailed understanding of the local flow fields in each region of the containment. These limitations prompted additional experiments of a more integrated nature. The principle objectives of these tests were two-fold: (1) to provide debris capture fractions for each structure that could be compared to ARL tests to quantify impact (if any) of the three dimensional flow patterns that are more typical of BWR drywells, and (2) to provide integrated data that could be used to benchmark analytical models and methods that are ultimately used to predict debris transport within a BWR drywell.

These integrated debris transport tests were carried out at the CEESI air blast facility by SEA. The test method selected was debris generation and subsequent transport by a dispersing 1100-psi air jet through a tunnel with structural characteristics scaled to a BWR drywell. The tunnel was 70 feet long and 10 ft in diameter. It was equipped with water fog-sprays to uniformly wet the structures with warm water and space heaters to pre-heat the structures and tunnel atmosphere. The debris were generated by jet impingement on an aged insulation blanket constrained on both sides to maximize debris generation. The debris was then carried by the airflow over 20-ft long structural congestion, a 90° bend, and a Mark I vent entrance, all of which were pre-wet fed by warm water to simulate surface wetness. The structural arrangement was designed to be representative of a BWR drywell based upon a survey of Mark I and Mark II containments. The design of the test section and the nozzle arrangement was based on computational fluid dynamics simulation of the drywell as well as that of the test facility. The tests demonstrated the ability of structural components to capture debris. The average overall transport fraction for small debris in the CEESI facility was 33% of the total debris generated. Once again gratings were found to be the most effective debris catcher. The average fraction of debris captured by each test structural component are given in Table E-1. The capture fractions were found to be relatively independent of the debris mass loading (lbm/ft2) impacting the

structures, at least within the range of interest to BWR drywells. The debris capture data are consistent with ARL test data indicating that the finer aspects of the local flow fields (e.g., eddies and wake) do not significantly influence debris capture.

The ARL and CEESI tests clearly established that a fraction of the small and large debris would be deposited as they are transported through the drywell during blowdown. Likely locations for the deposition are floor gratings located at different elevations. These pieces would then be subjected to remaining blowdown flow, which consists mainly of steam intermixed with water droplets, and washdown water flow. Short-term erosion or detachment of these pieces from the location where they were originally deposited was studied using the ARL test facility. In these tests, 6" by 6" pieces (1/4"-thick) were mounted on a grating normal to the flow direction and were exposed to airflow at a velocity of 150 ft/s and water drop quality as high as 10%. Under these conditions, the pressure drop across the pieces was as high as 0.5 psi. No noticeable degradation in the pieces was observed and nearly 100% of the debris was located at the original location where they were deposited by inertial capture.

Long-term erosion and relocation caused by water flows was studied at an SEA test facility. In these tests, debris of various sizes were placed on gratings and pipes and subjected to water flow typical of containment spray nozzles and break overflow. The structures were assembled in a 2-ft by 2-ft test section with clear glass to visualize test progression. The debris used were primarily generated by air jets, although a few large pieces of manually cut pieces were used in selected tests. The testing established that both containment sprays and break overflow are capable of washing down small debris deposited on various drywell structures during blowdown. The larger pieces do not undergo instantaneous degradation when subjected to water flow as high as 50 GPM/ft^2; instead, they erode continuously with time. Rate of erosion is negligible for containment sprays, but can be as high as 25% for break overflows, assuming continuous operation for three hours.

The results of the experiments were used in conjunction with analytical models and engineering judgement to obtain drywell transport fractions. Analyses of the experimental results also were used to identify important plant features that control debris transport in the drywell.

Table E-1. Debris capture efficiencies.

Structure Type	Capture Fraction Small Debris	Capture Fraction Large Debris
I-beams and Pipes arranged to prototypical congestion over a debris path length of 20 ft	9%	≈0%
Gratings V shaped grating (at an angle with flow) Other grating (normal to bulk flow)	 28% 24%	 100%
90° bend in the flow	17%	(None tested)
Mark I Vent Entrance	< 10%	(None tested)
Mark II Vent Entrance	15%	(None-tested)

Acknowledgements

The authors would like to acknowledge contributions of Mr. Michael Marshall, Mr. Robert Elliott, and Mr. Aleck Serkiz of US Nuclear Regulatory Commission for their enthusiasm and unwavering support to the experimental program. Review comments provided by the Phenomena Identification and Ranking Table (PIRT) panel members, Drs. Gary Wilson, Lothar Wolf, Brent Boyack, Ken Williams and Mark Leonard was instrumental in the design and conduct of the experiments.

Numerous individuals have contributed towards completion of this study. At SEA Mr. Kirk Weingardt, Ms. Kami Burr and Mr. Jerry Stockton played a key role conducting the experiments as well as during the data analysis. At CEESI, Mr. Roger Shaffer and Mr. Walt Seidel played a key role in preparing the experimental facility for testing.

The ARL staff performed excellently to design and conduct the separate effects experiments on-time and within budget. Their contribution is especially impressive and has made this test program a pleasure to coordinate.

Finally, SEA would like to recognize Mr. Bruce Alpha and Mr. Edward Wolbert of Transco Products, Inc. for their support of the experimental program. All of the target insulation blankets used in the integrated effects test were manufactured specifically for these tests and provided by Transco.

Acronyms

ARL	Alden Research Laboratory Inc.
BWR	Boiling water reactor
BWROG	Boiling Water Reactor's Owners Group
CEESI	Colorado Engineering Experiment Station
DDTS	Drywell debris transport study
ECCS	Emergency core cooling system
LOCA	Loss of cooling accident
MSLB	Main steam line break
PVC	Polyvinyl chloride
SEA	Science and Engineering Associates, Inc.

1. Introduction

1.1 Background and Objectives

A LOCA in a BWR would generate piping insulation debris, ranging in size from small fibrous insulation pieces to partially torn insulation blankets. These debris would be transported from the drywell (where they are generated) to the suppression pool by the high velocity steam flow during blowdown. During their transport, there is a potential that some of these debris may be captured by inertial or other means on various drywell structures (e.g., pipes, gratings, I-beams and cable conduits), whose surfaces are expected to be wet due to steam condensation and droplet deposition. Following blowdown, debris transport can also occur during long-term ECCS recirculation mode when water is introduced into drywell as a result of break overflow or containment spray operation. As this water cascades down various structures, it may erode and wash down some of the debris previously deposited during blowdown phase, and deposit them on the drywell floor where they would be subjected to pool dynamics. Figure 1-1 illustrates these potential debris transport pathways.

Tests were conducted as part of the DDTS to obtain experimental data related to: (a) debris capture on various drywell structures due to inertial impact while they are transported by steam-gas flow during blowdown and (b) washdown and erosion of such captured debris by water flow during long-term ECCS Recirculation phase. The overall objectives of the test program were to obtain experimental data that could be used in conjunction with analytical models to predict transport of debris in BWR drywells and to draw insights related to controlling phenomena and plant features that influence debris transport.

1.2 Program Overview

Three different test programs were undertaken to compile the required experimental program. All these tests studied transport of low-density fiberglass insulation commonly used in US nuclear power plants. All tests were conducted at ambient temperatures. Air-was used to simulate steam in the inertial capture tests. Figure 1-1 illustrates the transport pathway studied in each test program.

The first series of tests, conducted at ARL, are separate effects tests, in that they were designed to provide basic understanding of the phenomena that control inertial capture of fibrous debris pieces of different sizes on typical drywell structures. Air was used to simulate steam and water sprays were used to wet the structural surfaces. These tests employed a 4-ft x 4-ft test section through which ambient air was forced by a blower. Insulation debris were transported by that airflow across the real size drywell structural elements, where a fraction of them were deposited due to inertial impaction. Associated inertial capture efficiencies were measured for typical drywell structures (I-beams, pipes, and floor gratings of various sizes and orientations, and vent assemblies) as a function of airflow velocity (over a range of 25-150 ft/s), surface wetness and debris size. The debris used in these tests were produced by mechanical shredding of the aged insulation blanket, using procedures previously established as part of NUREG/CR-6224 study [Refs. 1.1 and 1.2]. Figure 1-2 compares the size distribution of debris used in these tests with the debris size descriptions provided in NUREG/CR-6224 and the nomenclature used by the BWROG [Refs. 1.2 and 1.3]. Section 2 provides a description of these tests and the results of the test program.

The second series of tests were conducted at CEESI to determine inertial capture efficiency of drywell structures assembled to prototypical congestion levels[1]. In these tests ambient temperature 1100-psi air jets were used to generate insulation debris and transport them over the structural assembly whose surfaces were pre-wet by warm water sprays. The transport velocities varied between 25-fts/s and 50-ft/s, which were determined to be prototypical transport velocities in the lower regions of the drywell following a MSLB. Transport efficiencies were measured as a function of debris size and structural surface wetness. Figure 1-2 compares size distribution of debris used in these tests, with those used in other tests [Refs. 1.2 and 1.3]. A complete description of these tests, the scaling rationale used in their design and the experimental data are presented in Section 3.

The final series of tests were conducted at SEA to obtain experimental data related to erosion and washdown of insulation debris previously deposited on various

[1] Prototypical congestion levels were determined from a BWROG survey of Mark I and Mark II drywells.

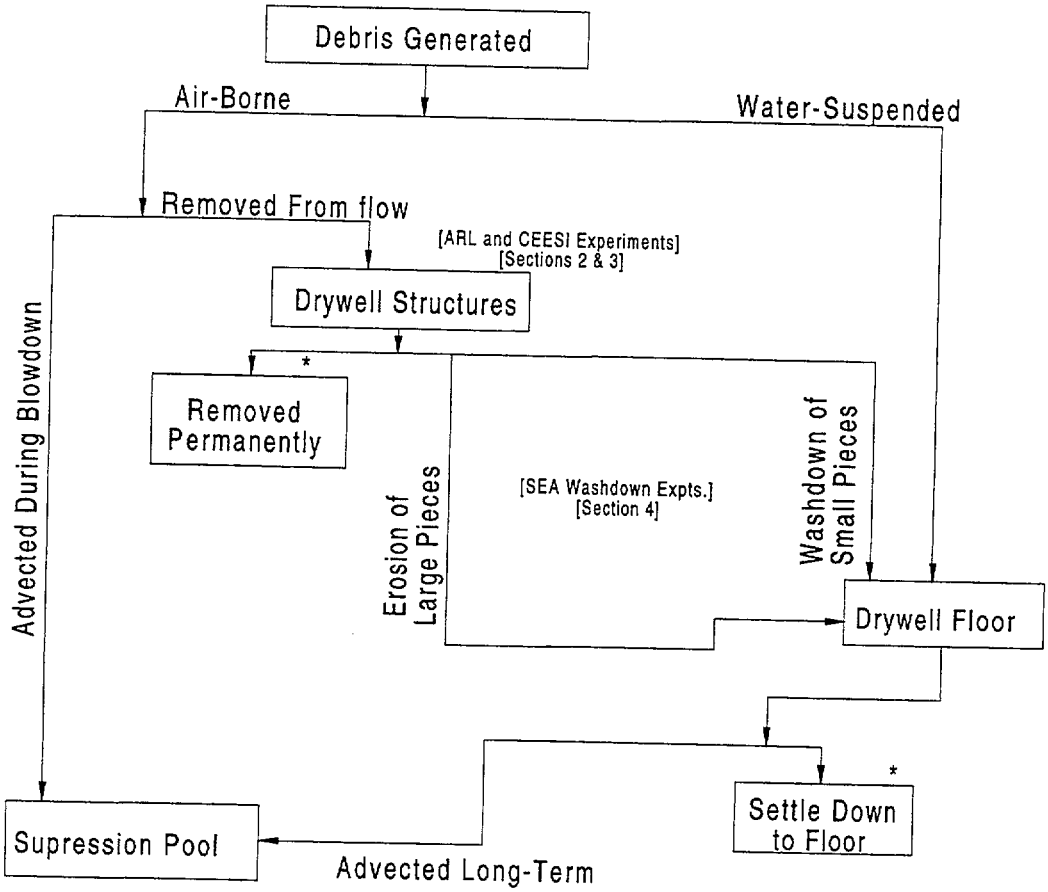

Figure 1-1. Potential debris transport pathways studied.

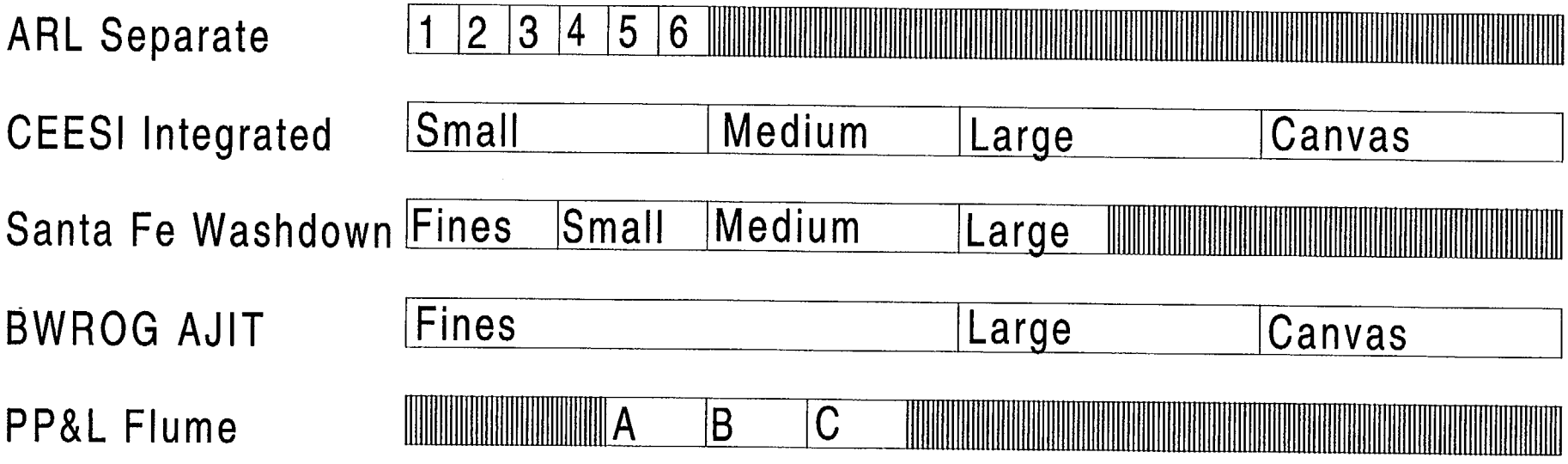

Figure 1-2. Debris sizes and distrubitions used in study.

structures when subjected to break overflow or containment spray flow. In these experiments, insulation debris fragments placed on various structures (e.g., gratings and pipes) were subjected to water flow scaled to be representative of containment sprays and break overflow. The fraction of debris transported due to a combination of washdown and erosion phenomena was measured as a function of debris size and time. Figure 1-2 compares the size distribution of debris used in these tests, with those used in other tests [Refs. 1.2 and 1.3].

Section 4 provides further details on test description, test procedures, and test results.

Section 5 discussed overall findings of the experimental study and their recommended usage. This section also provides a comparison of the data with that obtained from previous experiments (e.g., BWROG test program).

The results from these tests were used to quantify appropriate logic tree branches as described in the main body of this report.

1.3 References

1.1 D. V. Rao and F. Souto, "Experimental Study of Head Loss and Filtration for LOCA Debris," NUREG/CR-637, Science and Engineering Associates, Inc., 1996.

1.2 G. Zigler, et al., "Parametric Study of the Potential for BWR ECCS Strainer Blockage Due to LOCA-Generated Debris, NUREG/CR-6224, Science and Engineering Associates, Inc., 1994.

1.3 Boiling Water Reactors Owners' Group, "Utility Resolution Guidance for ECCS Suction Strainer Blockage," NEDO-32686, 1996.

2. Separate Effects Test Program to Evaluate Inertial Debris Capture on BWR Drywell Structures

2.1 Phenomena Selected for Study

The objective of these tests was to provide a basic understanding related to inertial capture of small insulation debris generated by a postulated MSLB. Past analyses and bench-top experiments have shown that debris generated by MSLB tend to be mostly dry with traces of wetness on the surface [Ref. 2.1]. Furthermore, it is estimated that these debris possess enough inertia to impact objects located in their pathway. It is also known that the structures would be wet due to a combination of steam condensation on their relatively cool surfaces and deposition of water droplets resulting from jet expansion. [Ref. 1.2] However, it was not known if surface forces introduced by surface wetness would be sufficient to capture the debris. These tests were designed to provide the necessary insights regarding the importance of inertial capture on various drywell structures.

A secondary objective of these tests was to study possible degradation and erosion mechanisms for large pieces during blowdown. Large pieces (typically larger than 6" x 4") are expected to be captured on the floor gratings whose clearances are 1" x 3". Such pieces would then be exposed to high velocity steam flow intermixed with water droplets for about a minute. A series of tests were conducted to study potential for degradation of the insulation pieces under these conditions.

The parameters selected for study were: flow velocity, surface wetness, structure type, debris size and debris loading. Flow velocity was varied between 24-150 ft/s to be representative of flow velocities in various regions of the drywell. Experiments were conducted using small debris, categorized according to NUREG/CR-6224 nomenclature (see Figure 1-2). The structures simulated included: I-beams, piping of various diameters, gratings, and Mark II vents. Finally, the wetness was varied qualitatively between dry to draining water film conditions.[1] The debris loading, expressed as concentration of debris per unit cross-sectional area approaching the structures, was varied over a narrow range of 6.3 to 12.5 g/ft^2.

2.2 Test Facility

2.2.1 Flow Tunnel

Components of the test air tunnel are shown in Figure 2-1. To avoid recirculation of the debris, the tunnel had a once through flow system, with the blower at the upstream end and an air filtering plenum downstream of the test section. The tunnel was constructed using full panels of medium density overlay plywood with an external wood stud framework, such that the inside cross section dimension was 4 ft x 4 ft. Steel strapping was used to prevent seams from opening up when the tunnel was pressurized by the blower. To achieve a uniform velocity distribution, a combination of perforated plates and a honeycomb structure was used. The head loss across this flow conditioning device was calibrated with respect to measured tunnel velocities and this correlation was later used to set the test velocities.

Two ranges of test velocities could be established based on the cross sectional area of the test section. Relatively low speed tests, up to 50 ft per second, were conducted using the full 4 ft x 4 ft area of the tunnel. A smaller 2 ft x 2 ft test section was inserted within the large test section to achieve velocities up to 150 ft per second. As shown in Figure 2-2A, the large test section was 8 ft long, as defined by the length of the acrylic viewing panels on the ceiling and one side, whereas the smaller high velocity test section was 5 ft long and fit within the larger test section.

About 2 ft downstream of the test section(s), the 4ft x 4ft tunnel section entered an 8ft x 8ft, 16 ft long filter box shown in Figure 2-2B. The roof and rear wall were covered with two inch rubberized "hog hair" filter media. After the hog hair became clogged with insulation debris, the filter media was replaced with corrugated paper filter panels.

A flow conditioning structure was installed just downstream of the blower, and this conditioner consisted of two 40% open perforated plates, spaced 4 inches apart, upstream of an 81 cell, 2 ft long, plywood honeycomb

[1] Surface wetness was not quantified in terms of water film thickness.

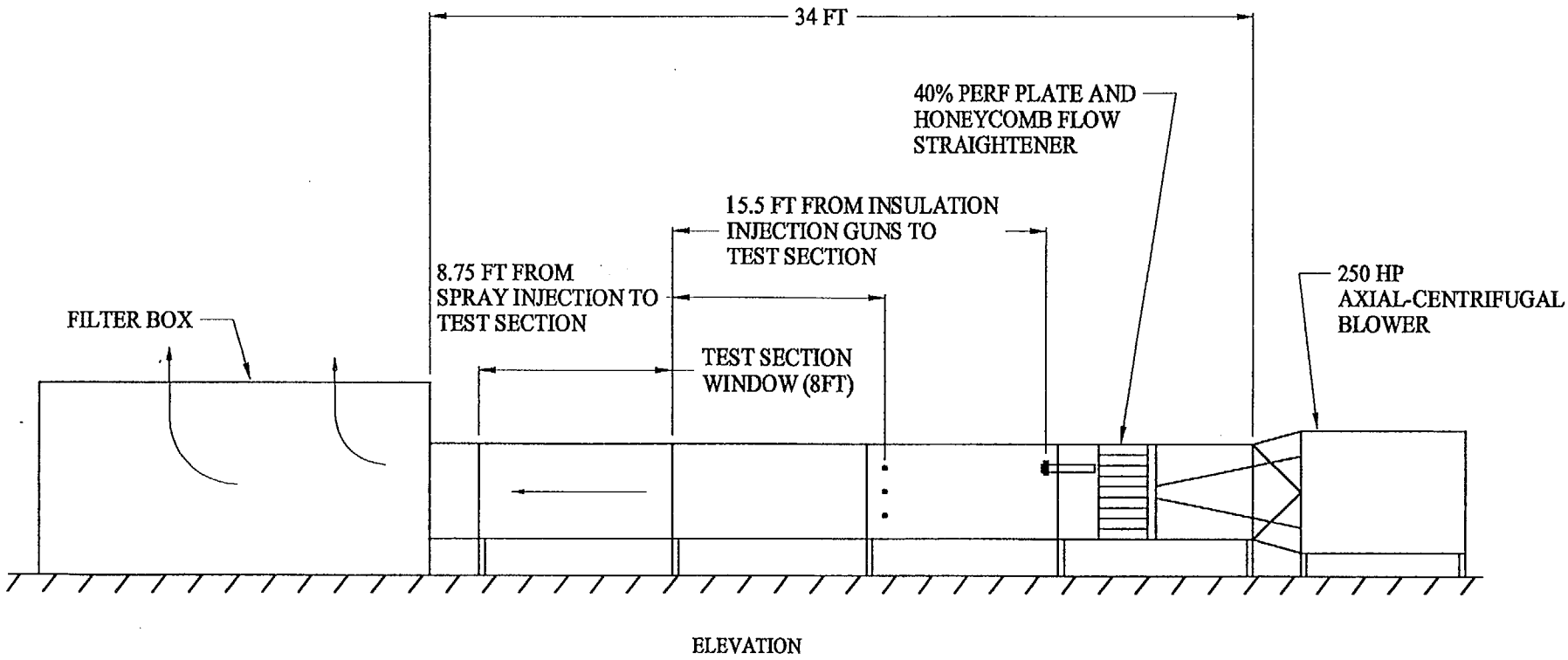

Figure 2-1. General arrangement of test tunnel.

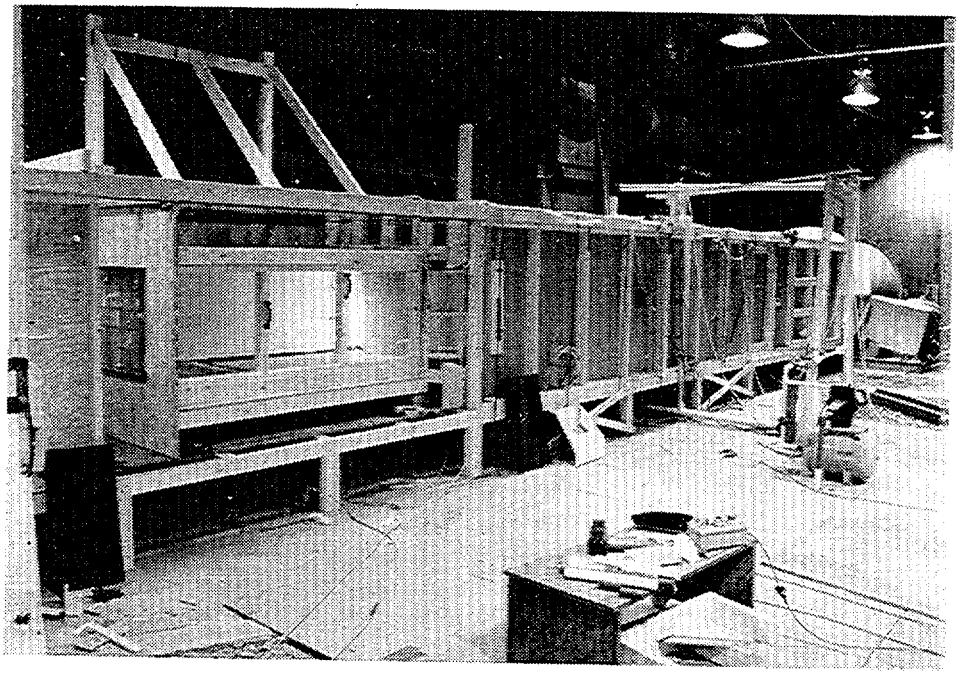

A) SHOWING THE SMALLER 2 FT X 2 FT TEST SECTION MOUNTED INSIDE THE 4 FT X 4 FT SECTION; BLOWER IS FAR RIGHT

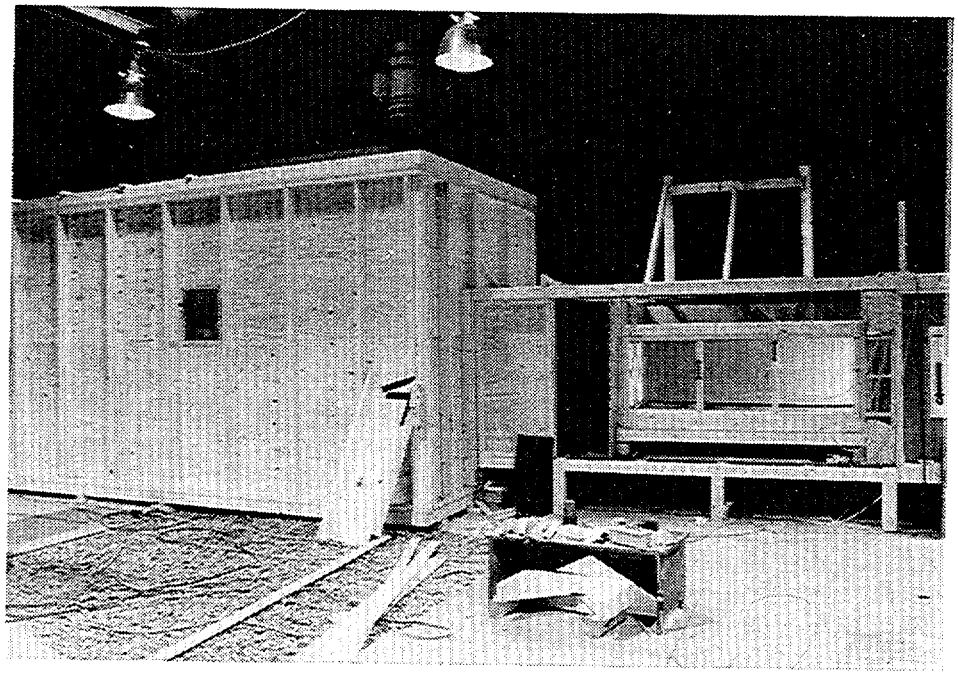

B) FILTER BOX; FLOW EXITS THROUGH TOP AND REAR PANELS

Figure 2-2. Test tunnel components showing test sections and filter box.

honeycomb structure (which can be seen in Figure 2-5B). Figure 2-3 shows the velocity distribution at the test section with the conditioner in place, indicating that essentially all velocities were within about ±10% of the average.

To provide a non-intrusive means to set the tunnel velocity using an air-over-water U-tube manometer, the head loss across the flow conditioner was calibrated to velocity measurements taken in the tunnel over a range of blower speeds. The resulting relationship for the large test section is shown in Figure 2-4.

2.2.2 Insulation Injection

The fibrous insulation debris was introduced within the tunnel by pressurizing sections of four inch PVC pipes capped at one end and with a rupture disk at the discharge end. A schematic of the debris injection system is shown in Figure 2-5. The pipe sections were suspended from the tunnel ceiling downstream of the flow conditioning structure and filled with preshredded insulation. Air was pumped into the capped end of the pipe sections until the rupture disk failed, and the jet of escaping air dispersed the insulation debris. Adequate insulation dispersal and complete discharge of debris required the rupture disk to burst at an appropriate pressure. Through experimentation with different rupture disk materials from metals to paper, a single sheet of 3M brand overhead transparency plastic material produced a rupture disk which reliably burst at 50 to 52 psi. In addition, this material did not disintegrate and contaminate the insulation upon rupture, but rather, consistently split into three to four flower-like petals. The position of the injection pipes was selected by preliminary testing to produce a relatively uniform pattern of debris on a fine screen placed across the test section.

2.2.3 Geometry of Objects Tested

Two categories of obstructions were tested, referred to in this report as single member tests and combined member tests. Single member tests involved mounting up to two objects of the same type (identical cross section) side by side within the test tunnel, both similarly aligned to the flow. In cases where the projected or frontal area of the test member was small, for example, I-beams with the web parallel to the flow, two identical pieces were mounted to increase the material capture and the accuracy of weighing the dried material.

Combined member tests included mounting several shapes with different orientations or more than one of a common member section, each aligned differently to the flow. By design, the arrangement of individual members in each combination was related to the single member tests, so that debris capture on individual components used in combinations could be compared to the capture when tested alone. Effects of member proximity, wake effects, and shielding could thereby be evaluated.

The surface finish of the test obstructions varied from slightly rusted (not flaking) for the I-beam sections to newly painted for the 1 ft and 2 ft pipes. The floor grating was galvanized steel which made the surface rough and purposely non-skid.

2.2.4 Insulation Debris Generation

The fibrous insulation debris was generated from heat treated NUKON base wool blankets. The blankets were cut up manually and then subjected to a leaf shredder following a prescribed procedure (Ref. 2-2) to produce the desired fragment sizes. A classification of debris sizes (Ref. 2-3) was used to grade and separate the insulation debris into two groups, Classes 3 & 4 and Classes 5 & 6. Debris sizes larger than Class 6 are termed in this report as Class 6+ and mainly included fragments 3 to 4" in size, obtained manually by pulling pieces from a NUKON blanket. As further fragmentation of debris was caused by the injection system in the facility, the originally introduced Classes 3 & 4 resulted in debris of Classes 2 through 4, while the original Classes 5 & 6 debris was further fragmented to give a size range of Classes 2 through 6. Further fragmentation of the larger pieces (Class 6+) was relatively negligible and is neglected. Figure 2-6 shows the pre-injection appearance of the debris comprising Classes 2 through 4, 2 through 6, and 2 through 6+.

Taking into account some additional fragmentation by the injection system, tests covered four different mixes of fragment sizes, as follows:

1. Classes 2 through 4 (injection pipes loaded with Classes 3 and 4).
2. Classes 2 through 6 (injection pipes loaded mostly with Classes 5 and 5; but also with some Classes 3 and 4).

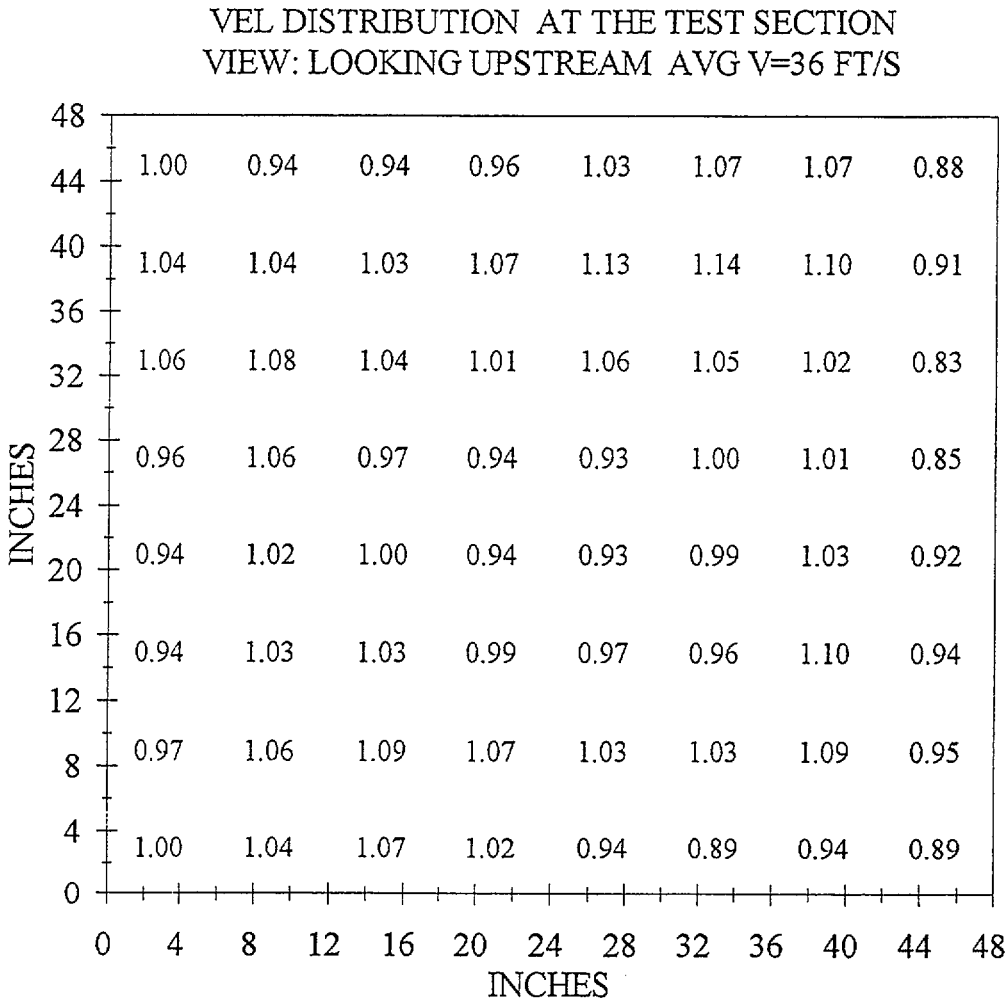

NOTE: VALUES ARE LOCAL VELOCITIES DIVIDED BY AVERAGE VELOCITY

Figure 2-3. Non-dimensional velocity distribution in large test tunnel with final flow conditioner.

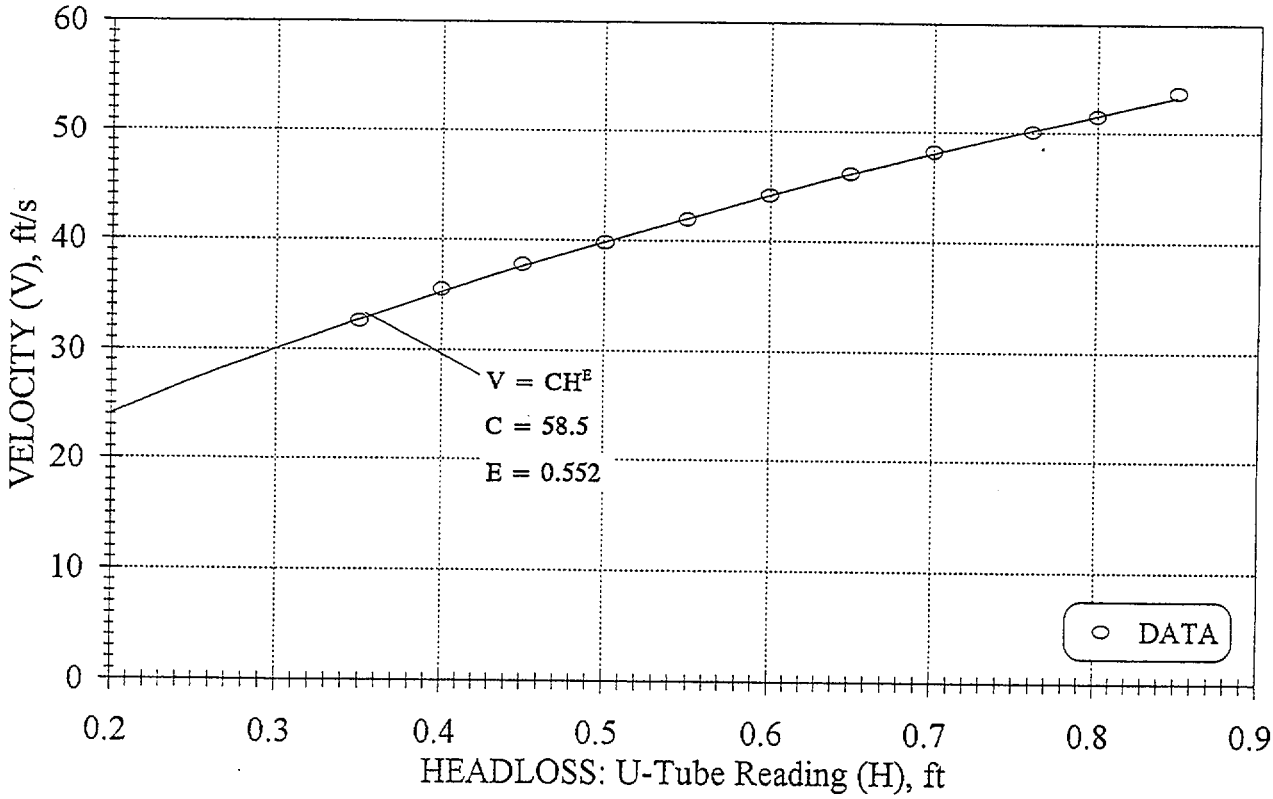

Figure 2-4. Head loss across flow conditioner versus average velocity in large (4ft x 4 ft) test section.

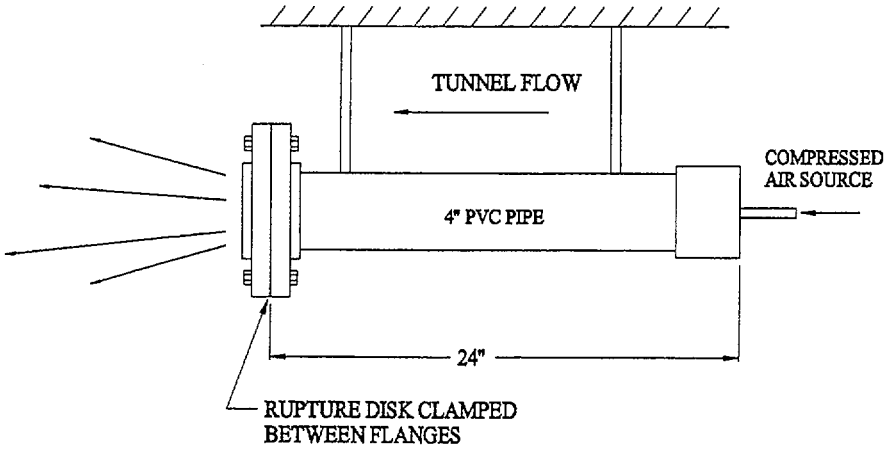

A) SIDE VIEW OF INJECTION PIPE

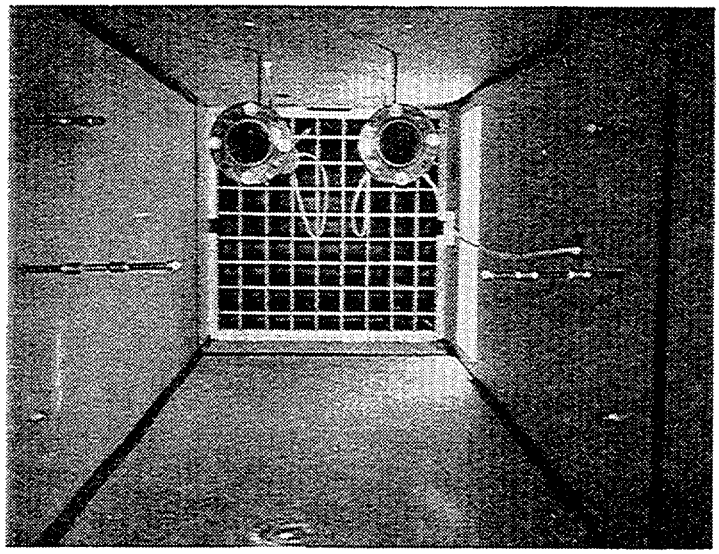

B) LOOKING UPSTREAM AT DEBRIS INJECTION PIPES, WATER SPRAY NOZZLES ON SIDE WALLS AND HONEYCOMB FLOW CONDITIONER

Figure 2-5. Debris injection system

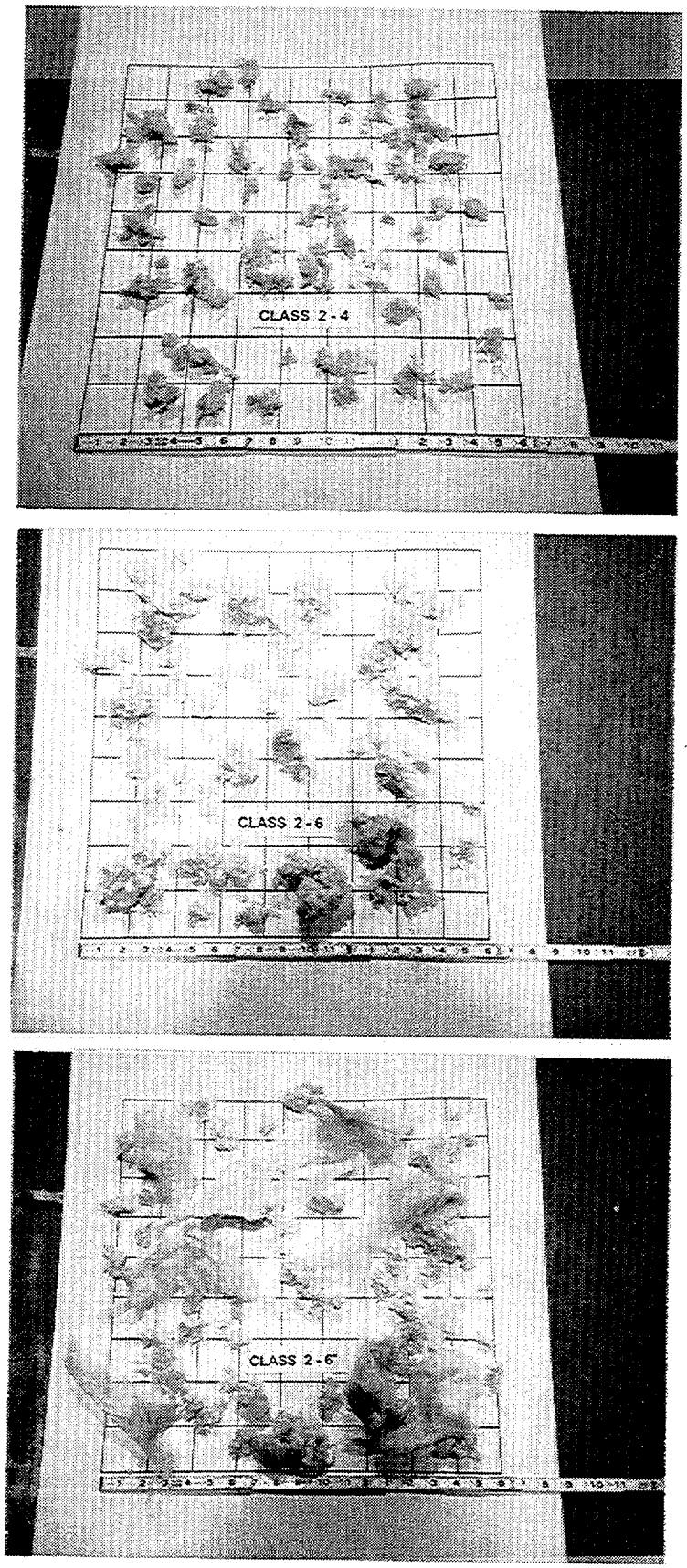

Figure 2-6. Pre-injection sizes of shredded NUKON fibrous insulation debris shown on a 2" x 2" grid.

3. Classes 2 through 6+ (injection pipes loaded with Classes 3 & 4, 5 & 6, and 6+ using the same weight from each group, and
4. Class 6+ only.

2.3 Test Plan and Procedure

2.3.1 Test Matrix

A test matrix (see Table 2-1) was developed to evaluate the effect of the following variables on debris capture:

a. Gas velocity
b. Wetness of structure surfaces
c. Debris size
d. Structure geometry
e. Structure orientation to the flow direction
f. Flow through a typical BWR Mark II vent opening

As shown in Table 2-1, 44 tests were conducted in total, including 4 repeat tests. Tests requiring gas velocities of 50 ft/s or less were conducted with the larger 4 ft x 4 ft duct section, while the higher velocity tests were conducted with the 2 ft x 2 ft duct section. Tests 1 through 22 covered various drywell structures, such as pipes, I-beams, and gratings, and were all conducted for an injected debris weight of about 100 gm. A few tests to ascertain the effects of debris size (Classes 2 to 4 versus 2 to 6) and wetness of structure surfaces were also included among these tests. The structures were tested individually (single member tests) in Tests 1 through 13 and 19 through 21, while Tests 14 through 18 and Test 22 were with combinations of structures (combined member tests). Tests 1 through 18 and Test 22 were conducted with an approach air velocity of 50 ft/s, while Tests 19 through 21 were conducted with 25 ft/s velocity.

BWR drywells typically have two floor gratings significant distances apart relative to the grating thickness and, hence, tests were conducted with two gratings placed at a distance of 4 ft apart in the test facility to examine the relative debris capture at an upstream and downstream grating. Tests 23 through 26 and 31 through 34 were formulated to test the two grating arrangement for different approach velocities, debris masses (concentration) and sizes.

Tests 27 through 30 were conducted with a typical Mark II vent geometry to ascertain debris capture on the vent cover or on the floor, as influenced by surface wetness and debris size. Since gravity had only a minor influence on fibrous debris transport and capture (i.e., the fibrous debris fall velocity is low compared to the gas flow velocity), the vent was oriented horizontally for testing convenience. These tests were conducted with an approach velocity of 25 ft/s in the 4 ft x 4 ft test section, which resulted in a vent velocity of about 185 ft/s. With the higher system losses generated by the vent, higher flows were not tested due to blower capacity limitations.

Additional single grating tests to cover a range of velocities and debris masses resulted in Tests 35 through 38. Tests 39 and 40 were included to evaluate debris capture on solid objects at higher velocities of 100 to 150 ft/s, but with the same debris concentrations as the previous tests at 50 ft/s. Tests 1R, 2R, 20R and 29R were repeats of Tests 1, 2, 20, and 29, respectively.

Tests 41 through 44 were conducted to investigate the potential for insulation debris to degrade or disintegrate when subjected to a wet high velocity gas flow. These tests were conducted in the small (high velocity) test section using 1/8" to ½" thin layers of rough-cut (approximately 6" x 6") insulation pieces placed on a single floor grating.

2.3.2 Test Procedure

The following lists the step by step test procedure. Tests that required variations to the procedure are noted on an individual basis in Section 2.4.

a. The desired test structures were installed in the test section of the air tunnel.

b. Both injection pipes were filled with the selected pre-weighed mass of insulation debris (maximum of 50 gm/pipe at a time).

c. The desired air velocity was set by measuring the head loss across the flow conditioner and adjusting the blower speed.

d. Video cameras to record debris capture were turned on.

e. The surfaces of the objects were wetted by turning the sprays on for the selected duration.

f. Within a maximum of 10 seconds after stopping the water sprays, the first debris injection pipe disk was ruptured and the second disk rupture occurred about 10 seconds later.

Table 2-1. Debris capture testing matrix for completed tests.

Test No.	Obstruction description	Prewet time (sec)	Air velocity in conduit (ft/s)	Approximate debris size (type)	Weight of injected insul. (gm)
1	2ft dia pipe parallel to flow	10	50	2 to 4	100
2	2 ft dia pipe @ 90 deg. to flow	10	50	2 to 4	100
3	1 ft dia pipe @ 90 deg to flow	10	50	2 to 4	100
4	(1) grating @ 26 deg. to flow	10	50	2 to 4	82
5	(1) grating @ 45 deg. to flow	10	50	2 to 4	87
6	(2) 10 x 4 I-beam flange to flow	10	50	2 to 4	100
7	(2) 10 x 4 I-beam web to flow	0	50	2 to 4	100
8	(2) 10 x 4 I-beam web to flow	10	50	2 to 4	100
9	(2) 10 x 4 I-beam web to flow	30	50	2 to 4	100
10	2 ft dia pipe @ 90 deg. to flow	0	50	2 to 4	100
11	(2) 10 x 4 I-beam web to flow	10		2 to 4	100
12	(1) grating @ 90 deg. to flow	10	50	2 to 4	100
13	(1) grating @ 90 deg. to flow	10	50	2 to 6	100
14	combination #1	10	50	2 to 4	100
15	combination #2	10	50	2 to 4	100
16	combination #3	10	50	2 to 4	100
17	combination #3	30	50	2 to 4	100
18	combination #3	30	50	2 to 6	100
19	1 ft dia pipe @ 90 deg. to flow	10	25	2 to 4	100
20	(2) 10 x 4 I-beam flange to flow	10	25	2 to 4	100
21	(2) 10 x 4 I-beam web to flow	10	25	2 to 4	100
22	combination #3	30	50	2 to 4	100
23	(2) grating 90 deg. to flow	10	50	2 to 4	100
24	(2) grating 90 deg. to flow	10	50	2 to 4	200
25	(2) grating 90 deg. to flow	10	50	2 to 4	200
26	(2) grating 90 deg. to flow	0	50	2 to 4	100
27	vent with cover	0	25	2 to 4	100
28	vent with cover	10	25	2 to 4	100
29	vent with cover	10	25	2 to 6	100
30	vent with cover	10	25	6+	100
31	(2) grating 90 deg. to flow	10	100	2 to 6+	50
32	(2) grating 90 deg. to flow	10	140	2 to 6+	50
33	(2) grating 90 deg. to flow	10	100	2 to 6+	100
34	(2) grating 90 deg. to flow	10	140	2 to 6+	100
35	(1) grating 90 deg. to flow	10	132	2 to 4	50
36	(1) gating 90 deg. to flow	10	100	2 to 4	25
37	(1) grating 90 deg. to flow	10	100	2 to 4	100
38	(1) grating 90 deg. to flow	10	150	2 to 4	100

Table 2-1. Debris capture testing matrix for completed tests (continued).

Test No.	Obstruction description	Prewet time (sec)	Air velocity in conduit (ft/s)	Approximate debris size (type)	Weight of injected insul. (gm)
39	(1) 10 x 4 I-beam flange to flow	10	100	2 to 4	25
40	(1) 10 x 4 I-beam web to flow	10	100	2 to 4	25
1R	repeat of test 1	10	50	2 to 4	100
20R	repeat of test 20	10	25	2 to 4	100
29R	vent with cover	10	25	2 to 6	100
2R	repeat of test 2	10	50	2 to 4	100
41	debris on grating	60	134	½" thick	42
42	debris on grating	60	126	½" thick	42
43	debris on grating	60	138	1/4" thick	36
44	debris on grating	60	130	1/8" thick	100

g. The blower speed was ramped down to bring the air flow to zero in approximately 30 seconds.

h. Video cameras were turned off.

I. Black and white photographs were taken of the test obstructions with captured insulation.

j. The captured debris on each surface of the objects and the walls and floor was separately collected, dried and weighed.

k. The percent of debris captured was calculated.

Percent Capture was determined as follows:

1. The injection system produced a uniform cross-sectional distribution of insulation debris approaching the test objects. Based on the test tunnel cross sectional area and the total weight of the injected insulation, an approaching insulation concentration, gm/ft^2, (weight per area) was calculated.

2. The frontal, or projected, area of the test objects was calculated.

3. The maximum theoretical capture amount per test object was determined by multiplying the projected area of the object from item 2 by the approaching total debris concentration from item 1.

4. The Percent Captured was determined by dividing the dry weight of the insulation actually collected from the obstruction(s) by the maximumtal theoretical amount from item 3, multiplied by 100 to convert to a percent.

2.4 Results

The test results are summarized in Table 2-2. Photographs of debris capture for all tests were taken, and selected photographs are included in this section for discussion of basic phenomena. Conforming to the objectives of the tests, the effects of each test variable on debris capture are discussed separately based on the test data. Using the major findings, an overall evaluation of the application of these results to quantifying debris capture in a BWR drywell following a LOCA is also provided.

Table 2-2. Results of BWR drywell capture tests.

TEST #	OBSTRUCTION DESCRIPTION	PREWET TIME SEC	PROJECTED AREA OF OBSTN. SQ-FT	PERCENT OF AREA OBSTRUCTED	AIR VELOCITY IN CONDUIT FT/S	APPROXIMATE DEBRIS SIZE (TYPE)	WEIGHT OF INJECTED INSUL. gm	WEIGHT OF CAPTURED INSUL. gm	PERCENT** INSUL. CAPTURED ON OBSTRUCTION(S)
1	2ft dia pipe parallel to flow	10	3.1	20	50	2 to 4	100	3.6	18
1R	repeat of test 1	10	3.1	20	50	2 to 4	100	3.7	19
2	2ft dia pipe @ 90 deg. to flow	10	8.0	50	50	2 to 4	100	4.2	8
2R	repeat of test 2	10	8.0	50	50	2 to 4	100	4.8	10
3	1ft dia pipe @ 90 deg. to flow	10	4.0	25	50	2 to 4	100	1.1	4
4	grating @ 26 deg. to flow+	10	16.0	100	50	2 to 4	82	12.0	15
5	grating @ 45 deg. to flow+	10	16.0	100	50	2 to 4	87	14.6	17
6	(2) 10x4 I-beam flange to flow	10	2.7	17	50	2 to 4	100	2.0	12
7	(2) 10x4 I-beam web to flow	0	6.7	42	50	2 to 4	100	0.0	0
8	(2) 10x4 I-beam web to flow	10	6.7	42	50	2 to 4	100	9.6	23
9	(2) 10x4 I-beam web to flow	30	6.7	42	50	2 to 4	100	13.1	31
10	2ft dia pipe @ 90 deg. to flow	0	8.0	50	50	2 to 4	100	0.0	0
11	(2) 10x4 I-beam web to flow	10	6.7	42	50	2 to 6	100	2.7	6
12	grating @ 90 deg. to flow+	10	16.0	100	50	2 to 4	100	16.2	16
13	grating @ 90 deg. to flow+	10	16.0	100	50	2 to 6	100	26.7	27
14	combination #1	10			50	2 to 4			
	total of vertical beams		2.7	17			100	1.8	11
	total of horizontal beams		6.7	42			98	4.3	11
	total of combination #1		8.2	51			100	6.1	12

+ Grating approximately 75% open area

** Compared to the maximum possible capture amount; using the projected area of the obstruction and a uniform insulation distribution. Percent capture for individual componants in the combination tests is based on the available approaching weight of insulation: injected weight minus any material captured on upstream components.

Table 2-2. Results of BWR drywell capture tests (continued).

TEST #	OBSTRUCTION DESCRIPTION	PREWET TIME SEC	PROJECTED AREA OF OBSTN. SQ-FT	PERCENT OF AREA OBSTRUCTED	AIR VELOCITY IN CONDUIT FT/S	APPROXIMATE DEBRIS SIZE (TYPE)	WEIGHT OF INJECTED INSUL. gm	WEIGHT OF CAPTURED INSUL. gm	PERCENT** INSUL. CAPTURED ON OBSTRUCTION(S)
15	combination #2	10			50	2 to 4			
	total of upstream 10" pipe		3.3	21			100	2	10
	total of vertical beams		2.7	17			98	2	12
	total of horizontal beams		6.7	42			96	1	2
	total of downstream 12" pipe		4.0	25			95	1	4
	total of combination #2		9.9	62			100	7.4	12
16	combination #3	10			50	2 to 4			
	total of upstream 12" pipe		4.0	25			100	2	8
	total of upper beam		3.3	21			98	5	24
	total of lower beam		1.3	8			93	1	13
	total of grating+		16.0	100			92	9	10
	total of combination #3		8.6	100			100	16.1	16
17	combination #3	30			50	2 to 4			
	total of upstream 12" pipe		4.0	25			97	2	8
	total of upper beam		3.3	21			97	4	20
	total of lower beam		1.3	8			91	0	none
	total of grating+		16.0	100			91	12	13
	total of combination #3		8.6	100			97	18.3	19

+ Grating approximately 75% open area

** Compared to the maximum possible capture amount; using the projected area of the obstruction and a uniform insulation distribution. Percent capture for individual componants in the combination tests is based on the available approaching weight of insulation: injected weight minus any material captured on upstream components.

Table 2-2. Results of BWR drywell capture tests (continued).

TEST #	OBSTRUCTION DESCRIPTION	PREWET TIME SEC	PROJECTED AREA OF OBSTN. SQ-FT	PERCENT OF AREA OBSTRUCTED	AIR VELOCITY IN CONDUIT FT/S	APPROXIMATE DEBRIS SIZE (TYPE)	WEIGHT OF INJECTED INSUL. gm	WEIGHT OF CAPTURED INSUL. gm	PERCENT** INSUL. CAPTURED ON OBSTRUCTION(S)
18	combination #3	30			50	2 to 6			
	total of upstream 12" pipe		4.0	25			100	2	8
	total of upper beam		3.3	21			98	6	29
	total of lower beam		1.3	8			92	2	26
	total of grating+		16.0	100			90	13	14
	total of combination #3		8.6	100			100	22.4	22
19	1ft dia pipe @ 90 deg. to flow	10	4.0	25	25	2 to 4	100	1.2	5
20	(2) 10x4 I-beam flange to flow	10	2.7	17	25	2 to 4	100	1.6	10
20R	repeat of test 20	10	2.7	17	25	2 to 4	100	1.4	8
21	(2) 10x4 I-beam web to flow	10	6.7	42	25	2 to 4	100	4.3	10
22	combination #3	30			50	2 to 4			
	total of upstream 12" pipe		4.0	25			100	2.1	8
	total of upper beam		3.3	21			98	3.9	19
	total of lower beam		1.3	8			94	1	13
	total of grating+		16.0	100			93	7.7	8
	total of combination #3		8.6	100			100	14.7	15
23	(2) grating 90 deg to flow+	10	16.0		50	2 to 4	100		
	total on upstream grate			100			100	17.3	17
	total on downstream grate			100			83	10.6	13
	total for test 23			100			100	27.9	28

+ Grating approximately 75% open area

** Compared to the maximum possible capture amount; using the projected area of the obstruction and a uniform insulation distribution. Percent capture for individual componants in the combination tests is based on the available approaching weight of insulation: injected weight minus any material captured on upstream components.

Table 2-2. Results of BWR drywell capture tests (continued).

TEST #	OBSTRUCTION DESCRIPTION	PREWET TIME SEC	PROJECTED AREA OF OBSTN. SQ-FT	PERCENT OF AREA OBSTRUCTED	AIR VELOCITY IN CONDUIT FT/S	APPROXIMATE DEBRIS SIZE (TYPE)	WEIGHT OF INJECTED INSUL. gm	WEIGHT OF CAPTURED INSUL. gm	PERCENT** INSUL. CAPTURED ON OBSTRUCTION(S)
24	(2) grating 90 deg to flow+	10	16.0		50	2 to 4	200		
	total on upstream grate			100			200	38.2	19
	total on downstream grate			100			162	21.5	13
	total for test 24			100			200	59.7	30
25	(2) grating 90 deg to flow+	10	16.0		50	2 to 6+	200		
	total on upstream grate			100			200	96.5	48
	total on downstream grate			100			104	11.2	11
	total for test 25			100			200	107.7	54
26	(2) grating 90 deg to flow+	0	16.0		50	2 to 4	100		
	total on upstream grate			100			100	9	9
	total on downstream grate			100			91	5.9	6
	total for test 26			100			100	14.9	15

+ Grating approximately 75% open area

** Compared to the maximum possible capture amount; using the projected area of the obstruction and a uniform insulation distribution. Percent capture for individual componants in the combination tests is based on the available approaching weight of insulation: injected weight minus any material captured on upstream components.

Table 2-2. Results of BWR drywell capture tests (continued).

TEST #	OBSTRUCTION DESCRIPTION	PREWET TIME SEC	PROJECTED AREA OF OBSTN. SQ-FT	PERCENT OF AREA OBSTRUCTED	AIR VELOCITY IN CONDUIT FT/S	APPROXIMATE DEBRIS SIZE (TYPE)	WEIGHT OF INJECTED INSUL. gm	WEIGHT OF CAPTURED INSUL. gm	PERCENT** INSUL. CAPTURED ON OBSTRUCTION(S)
27	vent with cover++	0	3.4	21	25	2 to 4	100	0	none
28	vent with cover	10	3.4	21	25	2 to 4	100		
	tunnel floor u/s of cover							1.6	
	tunnel floor d/s of cover							7	
	face of cover			21			98	2.1	10
	back of cover							0	
	tunnel walls d/s of cover							3.7	
	outside of pipe							2.4	
	tunnel back wall							5.3	
	total for test 28++			100			88	9.8	11
29	vent with cover	10	3.4	21	25	2 to 6	50		
	tunnel floor u/s of cover							0	
	tunnel floor d/s of cover							4.7	
	face of cover			21			50	0.8	8
	back of cover							0	
	tunnel walls d/s of cover							0	
	outside of pipe							1.3	
	tunnel back wall							3.9	
	total for test 29++			100			45	6	13

+ Grating approximately 75% open area

** Compared to the maximum possible capture amount; using the projected area of the obstruction and a uniform insulation distribution. Percent capture for individual componants in the combination tests is based on the available approaching weight of insulation: injected weight minus any material captured on upstream components.

++ Percent captured was calculated using only the material collected from the vent cover, pipe and back wall.

Table 2-2. Results of BWR drywell capture tests (continued).

TEST #	OBSTRUCTION DESCRIPTION	PREWET TIME SEC	PROJECTED AREA OF OBSTN. SQ-FT	PERCENT OF AREA OBSTRUCTED	AIR VELOCITY IN CONDUIT FT/S	APPROXIMATE DEBRIS SIZE (TYPE)	WEIGHT OF INJECTED INSUL. gm	WEIGHT OF CAPTURED INSUL. gm	PERCENT** INSUL. CAPTURED ON OBSTRUCTION(S)
29R	vent with cover	10	3.4	21	25	2 to 6	100		
	tunnel floor u/s of cover							1.6	
	tunnel floor d/s of cover							8.4	
	face of cover			21			98	4.1	20
	back of cover							0	
	tunnel walls d/s of cover							0	
	outside of pipe							0	
	tunnel back wall							7.2	
	total for test 29R++			100			90	11.3	13
30	vent with cover	10	3.4	21	25	6+	100		
	tunnel floor u/s of cover							2.1	
	tunnel floor d/s of cover							8.8	
	face of cover			21			98	8.3	40
	back of cover							0	
	tunnel walls d/s of cover							0	
	outside of pipe							2.4	
	tunnel back wall							20.1	
	total for test 30++			100			89	30.8	35

+ Grating approximately 75% open area

** Compared to the maximum possible capture amount; using the projected area of the obstruction and a uniform insulation distribution. Percent capture for individual componants in the combination tests is based on the available approaching weight of insulation: injected weight minus any material captured on upstream components.

++ Percent captured was calculated using only the material collected from the vent cover, pipe and back wall.

Table 2-2. Results of BWR drywell capture tests (continued).

TEST #	OBSTRUCTION DESCRIPTION	PREWET TIME SEC	PROJECTED AREA OF OBSTN. SQ-FT	PERCENT OF AREA OBSTRUCTED	AIR VELOCITY IN CONDUIT FT/S	APPROXIMATE DEBRIS SIZE (TYPE)	WEIGHT OF INJECTED INSUL. gm	WEIGHT OF CAPTURED INSUL. gm	PERCENT** INSUL. CAPTURED ON OBSTRUCTION(S)
31	(2) grating 90 deg to flow +	10	4.0	100	100	2 to 6+	50		
	upstream grate		4.0	100			50	12.8	26
	downstream grate		4.0	100			37	6.2	17
	total for test 31			100			50	19	38
32	(2) grating 90 deg to flow +	10	4.0	100	140	2 to 6+	50		
	upstream grate			100			50	19.7	39
	downstream grate			100			30	3.6	12
	total for test 32			100			50	23.3	47
33	(2) grating 90 deg to flow +	10	4.0	100	100	2 to 6+	100		
	upstream grate			100			100	29	29
	downstream grate			100			71	12.2	17
	total for test 33			100			100	41.2	41
34	(2) grating 90 deg to flow +	10	4.0	100	140	2 to 6+	100		
	upstream grate			100			100	23	23
	downstream grate			100			77	9.4	12
	total for test 34			100			100	32.4	32
35	(1) grating 90 deg to flow +	10	16.0	100	132	2 to 4	50	3	6
36	(1) grating 90 deg to flow +	10	16.0	100	100	2 to 4	25	1.7	7
37	(1) grating 90 deg to flow +	10	16.0	100	100	2 to 4	100	7.6	8
38	(1) grating 90 deg to flow +	10	16.0	100	150	2 to 4	100	7	7
39	(1) 10x4 I-beam flange to flow	10	16.0	100	100	2 to 4	25	0.1	0
40	(1) 10x4 I-beam web to flow	10	16.0	100	95	2 to 4	25	3.7	15

+ Grating approximately 75% open area

** Compared to the maximum possible capture amount; using the projected area of the obstruction and a uniform insulation distribution. Percent capture for individual componants in the combination tests is based on the available approaching weight of insulation: injected weight minus any material captured on upstream components.

Table 2-2. Results of BWR drywell capture tests (continued).

TEST #	OBSTRUCTION DESCRIPTION	TOTAL WETTING TIME SEC	PROJECTED AREA OF OBSTN. SQ-FT	PERCENT OF AREA OBSTRUCTED	AIR VELOCITY IN CONDUIT FT/S	APPROXIMATE DEBRIS SIZE (TYPE)	PRETEST WEIGHT OF INSUL. gm	POST TEST WEIGHT OF INSUL. gm	TUNNEL PRESSURE DROP THROUGH DEBRIS psig
41	(1) grating 90 deg to flow++ with (5) pieces of debris	60	1.7	42	134	1/2" thick	35	35	0.43
42	(1) grating 90 deg to flow++ with (5) pieces of debris	60	1.7	42	126	1/2" thick	32	32	0.43
43	(1) grating 90 deg to flow++ with (5) pieces of debris	60	1.4	36	138	1/4" thick	16	15	0.41
44	(1) grating 90 deg to flow++ with (1) piece of debris	60	4.0	100	130	1/8" thick	30	30	0.45

++ Debris degradation test. Debris was placed in grating prior to starting the blower
The injection guns were not used for this test.

2.4.1 Gravitational Settling

The horizontal arrangement of the test facility simplified its construction and testing (compared to a vertical tunnel) but, the arrangement created the potential for gravitational settling, i.e., debris might settle and be captured on the tunnel floor upstream of the test obstruction(s).

To reduce the potential for capture on the tunnel floor, the water spray nozzles and debris injection pipes were positioned to minimize floor wetness and the amount of insulation injected upstream on the tunnel floor while maintaining an adequate distribution of both at the test section.

The effects of settling in the tunnel were found to be negligible for all of the test obstructions except the simulated Mark II vent geometry. With the vent geometry coupled with larger debris, some debris settled to the floor and to a lesser extent. As discussed in Section 2.4.8, because the tunnel surfaces did not simulate actual boundaries, the material attributed to gravitational settling was not included in the calculation of debris retention.

2.4.2 Effect of Obstructions Tested Individually

Test obstructions were classified as "solid" or "screen" objects. Flow went around solid objects, such as pipe and beam sections, whereas flow could pass through floor grating. Testing of individual objects involved mounting one or two of the same shapes in the tunnel. When two objects were used, the arrangement was such that both were in the same cross-sectional plane and neither was in the wake of the other.

Of the solid objects, an I-beam oriented with the web perpendicular to the flow, Test 8, produced the highest percent capture, 23% (percent capture was defined in Section 3.2 above). The same I-beam, oriented with the flanges perpendicular to the flow, i.e., the web parallel to the flow (Test 6), captured approximately half that amount. Post-test photos of these two tests are shown in Figure 2-7.

A 2-ft diameter pipe was tested parallel and perpendicular to the flow, with a hemispherical cap attached to the upstream end for the parallel-to-flow tests. In this parallel-to-flow configuration, the percent capture was 18% and 19% for Test 1 and 1R (a repeat test). When this pipe was oriented perpendicular to the flow, the percent captured reduced to 8% and 10% for Test 2 and 2R (a repeat test). Figure 2-8 shows photographs of typical capture on a 2-ft diameter pipe.

The floor grating was commercially available grating which consisted of 1" x 1/4" steel bars, 1" on center, supported by welded perpendicular rods every 4 inches. The whole grating was galvanized by dipping which produced a rough non-skid surface. The rough surface can be seen in Figure 18B. As oriented in the test tunnel, the open area was approximately 75%.

The floor grating produced the highest capture (mass) of the individual members tested. From Test 12, 16% (16 gm) of the approaching weight of Class 2 to 4 debris was retained on a single 4 ft x 4 ft panel of grating, see Figure 2-9A. With debris Class 2 to 6, the retention increased to 27% (27 gm), as shown in Figure 2-9B for Test 13.

For calculating percent capture on the grating, whether alone or in Combinations, 16 ft^2 (the total tunnel section area) was used for the projected area, which (by the definition in Section 3.2) means that the grating is exposed to 100% of the approaching debris. This method produces a low apparent percent retention on the grating, as compared to only using the solid portion of the grating.

2.4.3 Effect of Approach Velocity

The air velocity for the majority of the tests was 50 ft/sec. The floor grating and I-beam obstructions were also tested at velocities up to 140 ft/sec using the smaller test section inserted into the basic test tunnel (see Figure 2-3). With prewetting, 50 ft/sec through the floor grating with Class 2 to 4 insulation debris, Tests 12 and 23 (upstream grating) produced an average capture of 17%. The approach debris concentration for these tests was 6.3 gm/ft^2 (100 gm injected) and Figure 2-10 shows the debris capture for Test 23. Using the same approach concentration but at a velocity of 100 ft/sec (Test 36), the percent capture reduced to 7%. A similar reduction in capture occurred for a higher approach concentration (12.5 gm/ft^2); Test 24 at 50 ft/sec produced 19% capture compared to Test 35 at 132 ft/sec which produced 6% capture. These results indicate that for the smaller (2 to 4) class debris, the higher velocity appears to force the debris through the grate to reduce the capture percentage.

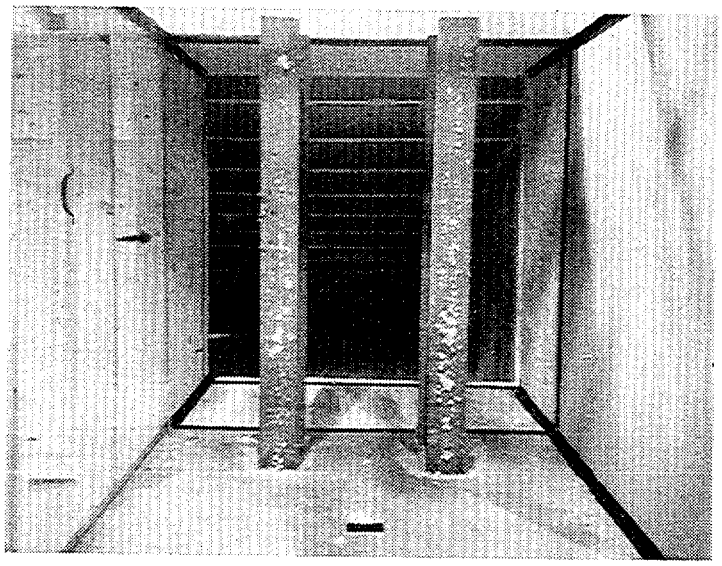

A) I-BEAMS MOUNTED FLANGE TO FLOW

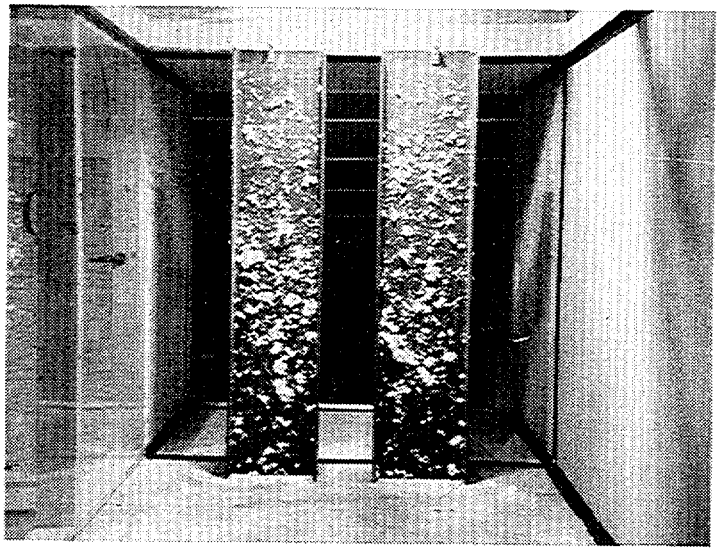

B) I-BEAMS MOUNTED WEB TO FLOW

Figure 2-7. Comparison of debris capture from A) test 6, and B) test 8.

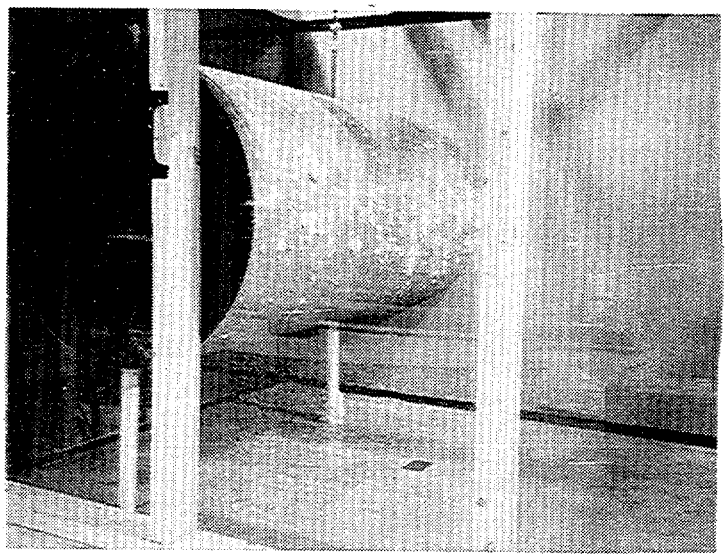

A) VIEW THROUGH TEST SECTION WINDOW

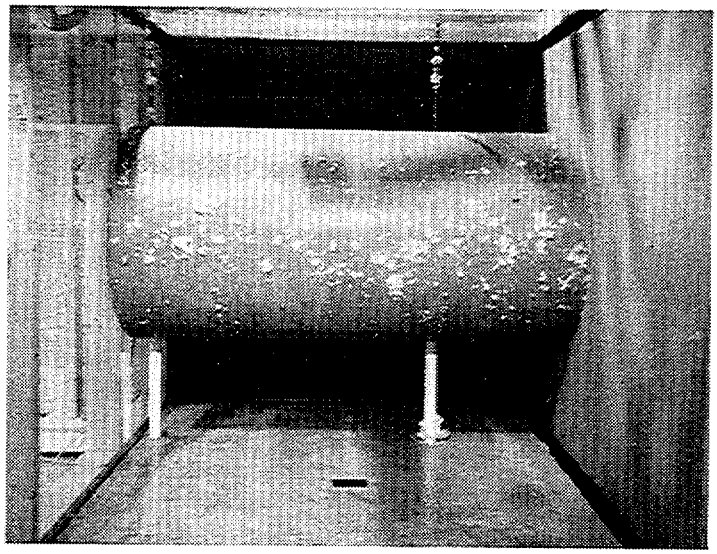

B) VIEW FROM INSIDE THE TEST TUNNEL

Figure 2-8. Debris capture on the 2-ft diameter pipe; 50 ft/sec, class 2 to 4 debris, and 6.3 gm/ft^2 approach concentration.

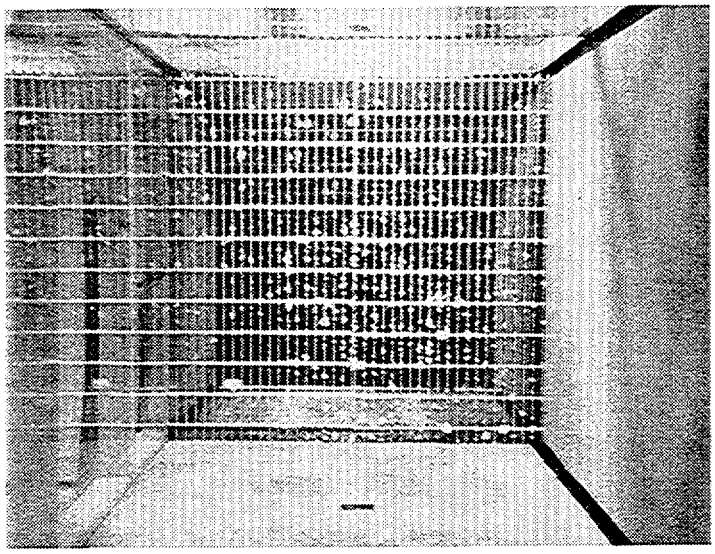

A) CLASS 2 TO 4 DEBRIS (TEST 12)

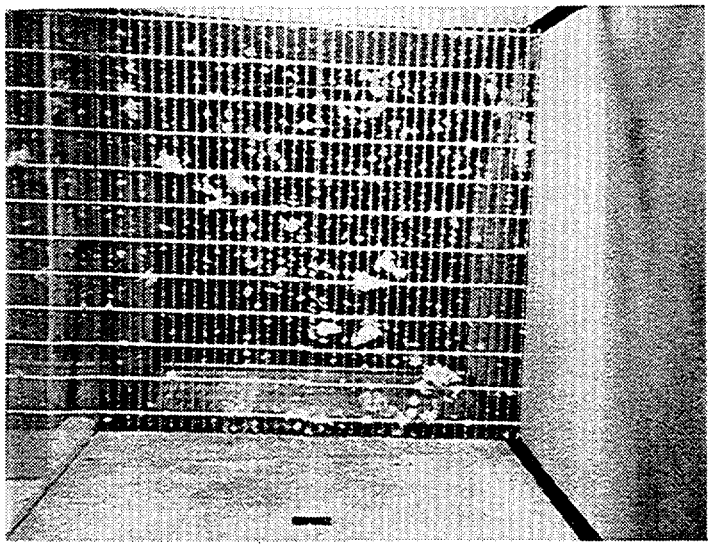

B) CLASS 2 TO 6 DEBRIS (TEST 13)

Figure 2-9. Debris capture on single grating at 50/ft sec.

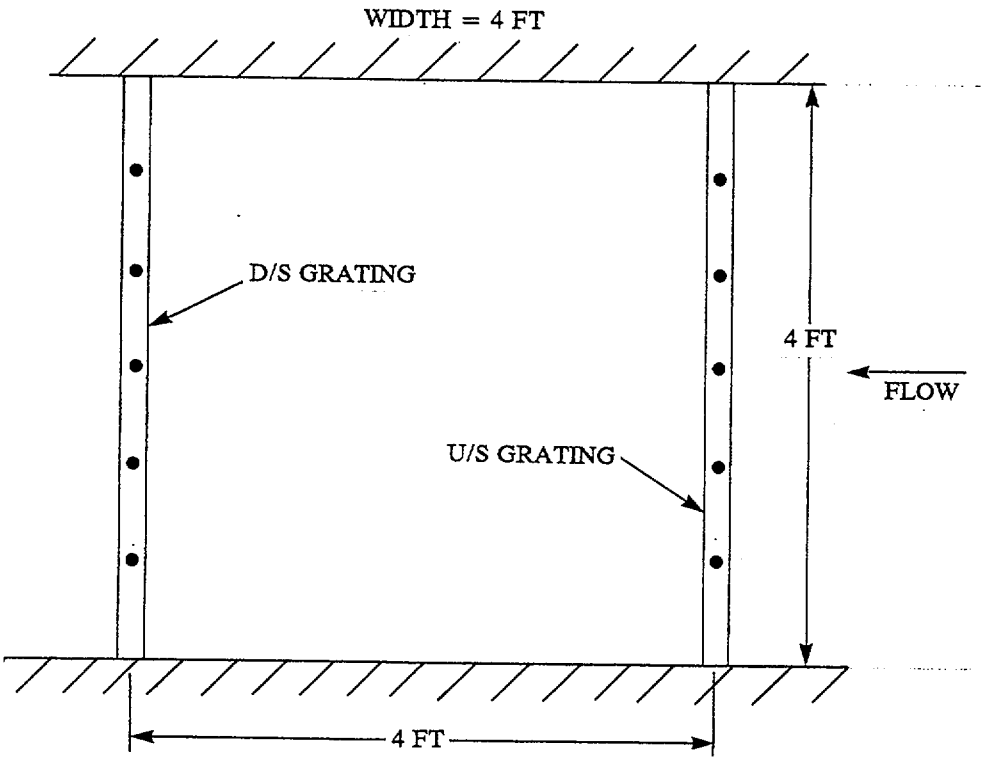

A) GRATING ARRANGEMENT

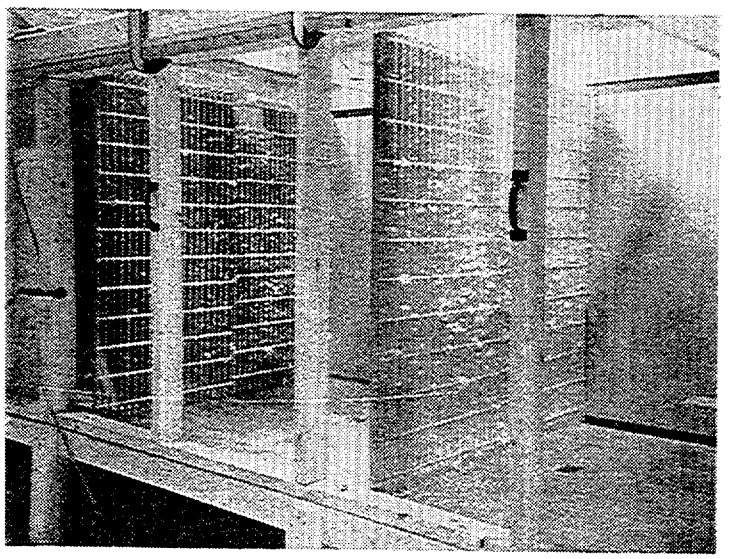

B) DEBRIS CAPTURE IN TEST 23

Figure 2-10. Arrangement and debris capture with two gratings; 50 ft/sec, class 2 to 4.

the upstream grate at 50 ft/sec, see Figure 2-11. When the velocity was increased to 100 ft/sec with other variables held constant (Test 31), the percent capture reduced to 26% for the upstream grate. But, when the velocity was increased to 140 ft/sec (Test 32), the percent capture on the upstream grate increased again to 39%. This percent capture is still lower, however, than the 48% measured at 50 ft/sec. The approach concentration was increased to 25 gm/ft^2 for Tests 33 and 34 with velocities of 100 and 140 ft/sec, respectively. The upstream grate percent capture for these two tests was 29 and 23, which agree with the results of Test 31 and support the trend that higher flow velocity reduces the capture potential of the floor grating.

The I-beam was tested with the web parallel to the flow (Test 39) and with the web perpendicular to the flow (Test 40) with velocities of 100 and 95 ft/sec, respectively. The insulation debris approach concentration and prewet times for these tests was identical to Tests 6 and 8, which had a flow velocity of 50 ft/sec. At 50 ft/sec, the upstream flange surface produced 12% capture, while at 100 ft/sec, the material captured on the same surface was immeasurable. From Test 8, with 50 ft/sec, the web of the beam produced 23% capture, which reduced to 15% when the velocity was increased to 95 ft/sec in Test 40.

In general, therefore, increasing the approach velocity above 50 ft/sec resulted in a decrease in the material captured.

2.4.4 Effect of Surface Wetness

Except for the floor grating, all of the obstructions required some prewetting for debris capture to occur. With no prewetting, Tests 7, 10, and 27 (see Table 2-2), an I-beam, pipe section, and vent cover, respectively produced no debris capture. Video documentation clearly shows debris impacting, but not adhering to the dry surfaces of these objects.

The majority of tests were conducted with a 10 second prewet time, although several tests were repeated with a 30 second prewet and this resulted in higher capture percentages; e.g., Test 9 was a repeat of an I-beam oriented with the web perpendicular to the flow. Test 8 of this geometry produced a capture of 23% with a 10 second prewet; with the 30-second prewet time of Test 9, the capture increased to 31%.

With combined obstruction geometries, the increased prewet time did not show the same trend. With a 10 second prewet time, Combination #3, (Test 16) shown in Figures 2-12 and 2-13, produced an overall 16% capture. When repeated with a 30-second prewet time in Tests 17 and 22, the overall capture was approximately the same, 19% and 15%, respectively.

Floor grating was tested in single panels, in dual panels, and in combination with other members. Tests with debris Class 2 to 4 showed that a single grate spanning the entire tunnel section (Test 12) produced a 16% debris capture. For the same test conditions with two parallel grates (Test 23), the upstream grate captured 17%. The performance of the downstream grate will be discussed in Section 4.9 below. The percent captured on the upstream grate reduced to 9% when there was no prewetting (Test 26). Because there was still 9% capture without prewetting, the grating material was less dependent on surface wetness compared to the solid objects, which did not capture any debris without prewetting.

2.4.5 Effect of Debris Size (Class of Insulation Debris)

Three ranges of debris size were tested, Classes 2 to 4, 2 to 6, and 2 to 6+. The following summary, drawn from Table 2-2, compares pairs of tests in which the only difference between the two tests in a pair was the insulation debris size (Class):

With the exception of Test 11, tests repeated with larger insulation debris produced higher capture percentages. The most dramatic increase was between the upstream grate of Test 33 and that of Test 37, both with a flow velocity of 100 ft/sec; the retention percentage increased by a factor of 3, from 8% to 29% with the larger debris size.

2.4.6 Effect of Debris Loading

The concentration of insulation debris per cross-sectional area approaching the obstructions, also referred to as debris loading, could be varied by adjusting the weight of insulation placed into the injection pipes. The maximum weight of insulation debris per pipe was 50 gm; in the 4 ft x 4 ft test section, this produced a 6.3 gm/ft^2 concentration. To inject more debris for a test required reloading the pipes, and this was accomplished by reducing the blower speed to a value that retained all captured material while allowing a technician to enter the tunnel. The blower was then adjusted back up to speed and the test continued. The water spray system was not used for the second injection to prevent captured material from the first injection from being washed off. For the

Table 2-3. Effect of debris size.

Obstruction description	Debris class	Percent capture	Test no.
(2) 10 x 4 I-beam web to flow	2 to 4	23	8
(2) 10 x 4 I-beam web to flow	2 to 6	6	11
Grating 90 deg to flow	2 to 4	6	12
Grating 90 deg to flow	2 to 6	27	13
Combination #3	2 to 4	16	16
Combination #3	2 to 6	22	18
(2) Grating 90 deg to flow	2 to 4	30	24
(2) Grating 90 deg to flow	2 to 6+	54	25
(1) Grating 90 deg to flow	2 to 4	8	37
(2) Grating 90 deg to flow	2 to 6+	29	33
*Upstream grate			

higher velocity tests which used the smaller test section, the injection pipes were operated with a lower mass of insulation debris to yield the same (or desired) concentration. For example, to produce a 6.3 gm/ft^2 concentration in the 2 ft x 2 ft high speed section, one injection pipe was loaded with 25 gm of debris, whereas 100 gm was used for the 4 ft x 4 ft cross-section.

Presumably, one effect of increasing the debris approach concentration is that the retention would increase towards a saturation point where material being striped off equals that being retained. Another possibility, especially applicable to the grating, is that higher approach concentrations might result in bridging of debris over the grate openings and, thus, produce a more effective screening device.

A configuration with two panels of floor grating, shown in Figure 2-10, was tested at high and low air speeds with different masses of injection debris. At 50 ft/sec, a comparison of Tests 23 and 24 indicated no appreciable change in total retention percentage when the approach concentration was increased from 6.3 gm/ft^2 to 12.5 gm/ft^2; the percentage capture varied from 28% to 30%. Similar results were obtained from Tests 31 and 33 with this configuration at 100 ft/sec, the total percent capture varied from 38% to 41%, respectively, when the approach concentration was increased from 12.5 gm/ft^2 to 25 gm/ft^2. An identical increase in approach concentration at 140 ft/sec reduced the total percent capture from 47% to 32% for Tests 32 and 34, respectively.

The results of these tests indicate that the effects of varying the approach concentration produced no appreciable change in retention on the floor grating.

2.4.7 Effect of Structural Combinations

Three configurations of combined obstructions (Figure 2-12) were tested. The method for determining the percent capture on downstream members in the combined structures accounted for insulation debris that was captured by upstream members. The first step was to separate the overall layout into a series of "planes" normal to the oncoming flow. For example, Combinations 1 consisted of two planes; the first being the two vertical beams, and the other, the two horizontal beams. Similarly, for Combination 3, the pipe and beams form the upstream plane, while the floor grating was the second plane. By the same method, Combination 2 was divided into four planes. If, for example, the members in the farthest upstream plane of obstructions retained 4 gm, the calculated approach concentration for the next downstream plane of members was adjusted to reflect the reduced weight of available debris.

Combination 1, shown in Figure 2-12, consisted of four 10 x 4 inch I-beams. The upstream vertical beams were oriented with the web parallel to the flow. The remaining two horizontal beams were located so as to be in the wake of the upstream beams and the downstream beams were oriented with the flanges parallel to the flow.

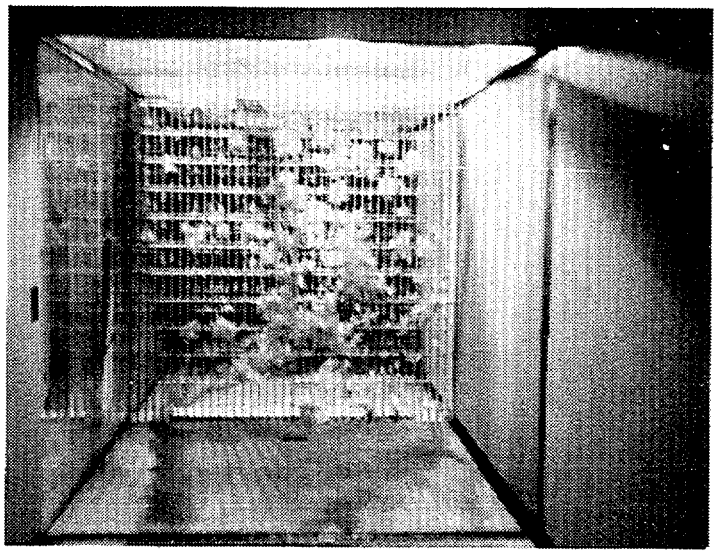

A) VIEW OF UPSTREAM GRATING

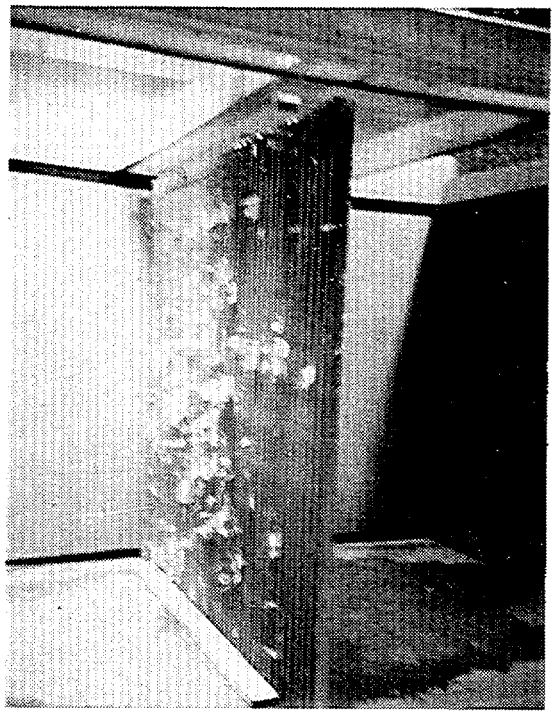

B) BACK SIDE OF UPSTREAM GRATING SHOWING DEBRIS FORCED THROUGH THE BARS

Figure 2-11. Debris capture on grating test; 50 ft/s, class 2 to 6+ debris, and 12.5 gm/ft2 approach concentration (test 25).

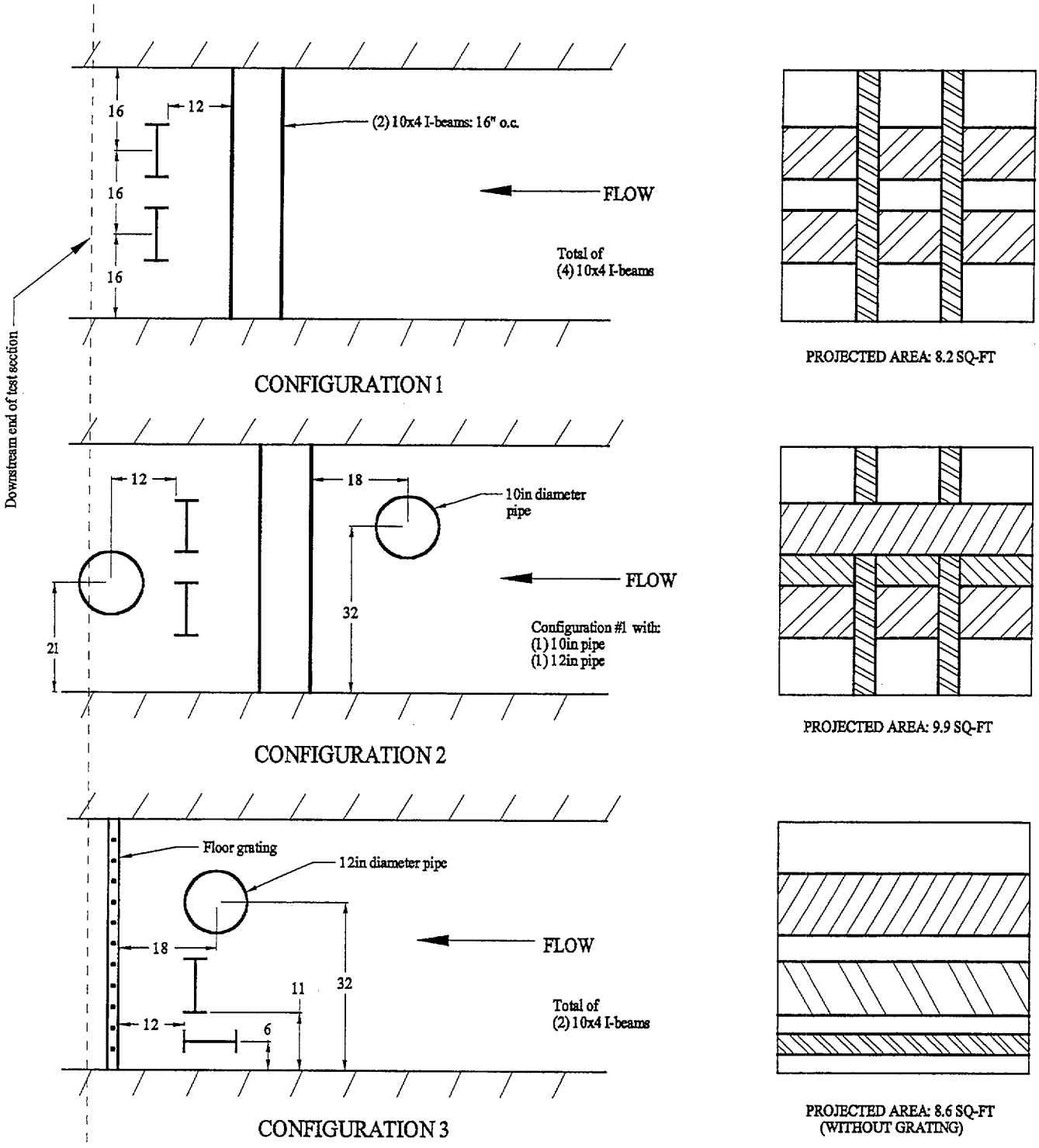

Figure 2-12. Combined member layouts

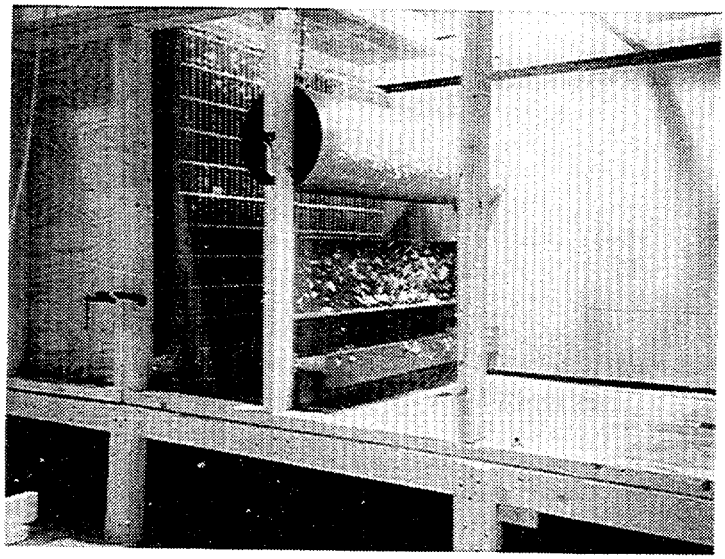

A) VIEW THROUGH TEST SECTION WINDOW

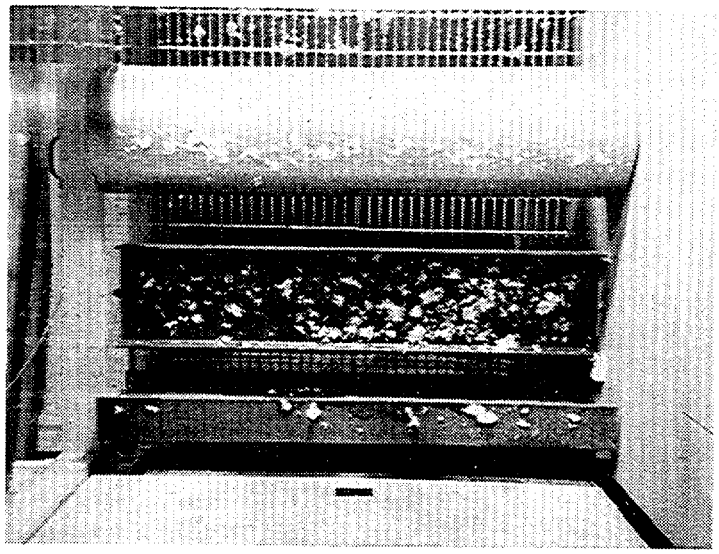

B) VIEW FROM INSIDE THE TEST TUNNEL

Figure 2-13. Debris capture on test combination 3, 50 ft/sec, class 2 to 4 debris, and 6.3 gm/ft^2 approach concentration (test 16).

Combination 1 was tested with Class 2 to 4 insulation at a velocity of 50 ft/sec (Test 14). The individual capture percentage for both upstream and downstream beams captured was 11%. The 11% retention on the upstream beams in Combination 1 agree well with those of Test 6 (at 12%) which indicates, as expected, that the downstream members in do not effect the retention performance of the upstream members. The upstream members, though, clearly reduced the retention found on the downstream beams. The beam orientation in Test 8 as identical to the downstream members in Combination 1. Test 8 produced a 23% capture compared to the 11% on the downstream beams in Test 14. Apparently, the debris retention ability of the beams is reduced when they are located in the turbulence of the wake region behind upstream members.

Combination 1 was modified by the addition of two 10-inch pipes to form Combination 2, as shown in Figure 2-12. Comparing the performance of individual members in Combination 2 (Test 15), as described above for Combination 1, the retention on downstream members was lower by approximately 50% than comparative tests with individual members. The upstream 10" diameter pipe in Test 15 retained 10%, which is an increase when compared to the 4% found when a 12" pipe was tested alone (Test 3). However, the results of Test 3 are suspect because tests with 12" diameter pipe in an upstream location, Tests 16, 17, and 18 produced 8% capture, similar to the 10% capture of Test 15 with a 10 inch pipe.

Combination 3 incorporated the pipe section, two orientations of the 10 x 4 inch beam, and the floor grating as shown in Figure 2-12. The pipe and beams forming the upstream members produced retention percentages similar to those from the independent obstruction tests. The retention on the downstream grating reflected the effects of being in the wake of the upstream members; from Test 12, the percent capture on the single floor grating was 16%, whereas the grate in Combination 3 retained 10% and 13% from Tests 16 and 17, respectively (for Test 17, the prewet time was 30 seconds but, as discussed in Section 4.4, debris retention on the grate was not strongly dependent on the extent of prewetting). Figure 2-13 shows the debris capture for Test 16 with Combination 3.

2.4.8 Vent Cover Testing

The general arrangement of the tested single Mark II vent entrance is shown in Figure 2-14A; although the vent pipe was installed horizontally in the test tunnel, as shown in Figure 2-14B. The approach velocity in the 4 ft x 4 ft section (simulating the drywell area per vent) was 25 ft/sec, which produced approximately 180 ft/sec in the downstream vent pipe. Even higher velocities occur at the vent entrance due to flow contractions. The vent surfaces, including the underside of the cover and inside the pipe, were pre-wetted by water spray nozzles positioned around and in the vent structure. Several size classes of fibrous debris were tested; Classes 2 to 4, 2 to 6, and 6+, each with an approach concentration of 6.3 gm/ft^2. The percent capture for the vent geometry was calculated by using only material collected from the vent cover, pipe and back wall of the test tunnel (the back wall representing the drywell floor). Some debris was collected from the tunnel side walls and floor, but because these surfaces were not simulating actual boundaries, material collected from these surfaces was subtracted from the total mass injected upstream before calculating the percent retention on other surfaces.

With no prewetting (Test 27), no insulation debris was captured on the vent entrance. With a 10 second prewet (Test 28) and Class 2 to 4 insulation, the capture was 11%, of which 5.3 gm or 54% by weight was collected from the back wall of the tunnel (which simulated the drywell floor). For Test 29, the injected approach concentration was 3.1 gm/ft^2 which produced a 13% capture of which, 65% by weight was from the back wall of the tunnel. The same retention was found when the approach concentration was increased to 6.3 gm/ft^2 for Test 29R, with 64%, by weight, collected from the back wall. Test 30 with class 6+ insulation produced 35% capture, with 65% by weight collected from the back wall.

2.4.9 Upstream and Downstream Gratings

Floor grating was found to retain the highest weight of insulation debris and, as described in Section 4.4, the dry floor grate did capture debris (unlike all other tested obstructions which captured no debris without prewetting). Also, as will be discussed further below, floor gratings alone captured nearly the same amount of debris as the total amount retained by floor gratings with other obstructions. For these reasons, the test program focus shifted toward investigating floor grating in different flow velocities with a range of debris size (classes), using both individual gratings and two gratings spaced several feet apart.

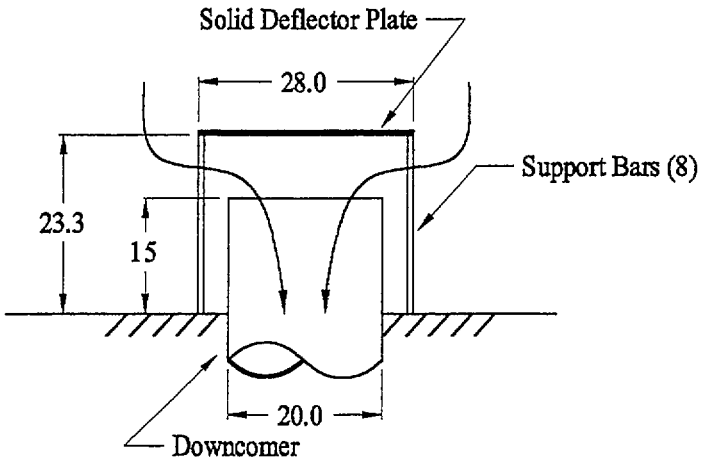

A) DIMENSIONED SKETCH OF VENT
(INCHES PROTOTYPE)

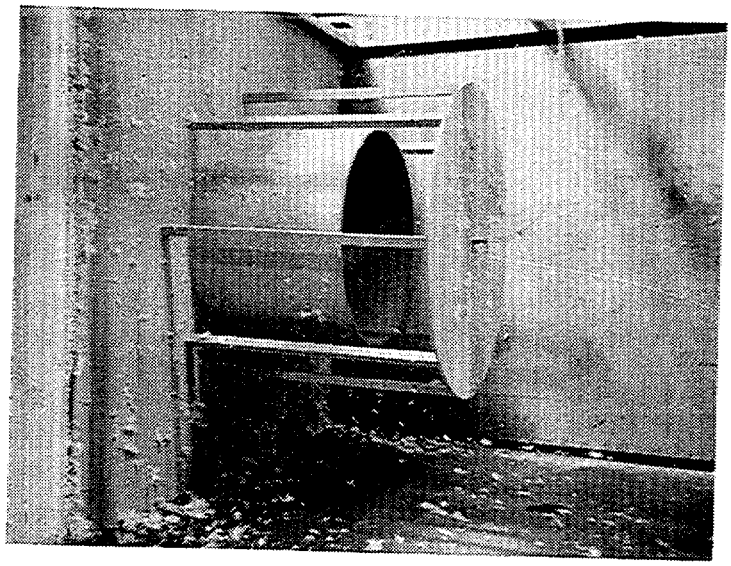

B) VENT AS INSTALLED IN TEST SECTION
SHOWING DEBRIS CAPTURE IN TEST 29R

Figure 2-14. Simulated Mark II vent geometry.

Early tests with a single grating at an angle to the flow with Class 2 to 4 debris; Tests 4 and 5, and perpendicular to the flow; Test 12, all produced 15% to 17% capture. Larger debris (Class 2 to 6) increased retention to 27% in Test 13.

A second panel of grating was installed 4 ft downstream from the first panel (see Figure 10A) to determine the retention characteristics of the second grating. With Class 2 to 4 debris and 50 ft/sec flow velocity and no prewet (Test 26), the overall (total) capture for both gratings was 15%. The upstream grate retained 9%, compared to 15% to 17% for tests described above with a 10 second prewet time. With a 10 second prewet time (Test 23), the overall capture was 28%. The upstream grate retained 17%, which agrees with previous single grate tests described above, and the downstream grate retained 13%, indicating a slight reduction in capture; possibly due to the fact that the first grate filters the larger pieces so that the debris approaching the second grate is composed of smaller, and more difficult to retain, debris sizes.

The injected concentration was doubled for Test 24, by injecting 200 gm of Class 2 to 4 insulation, and the overall capture was 30%, with 19% and 13% retained on the upstream and downstream grating, respectively. As the retention values did not appreciably increase with the higher injection weight (for Class 2 to 4 debris), the percent capture is not cumulative, i.e., a "saturation point" is reached, after which additional fibrous debris of this size passes through the grate.

Tests with dual gratings showed a substantial capture (up to 50% with larger size debris) on the upstream grating, but less capture (about 10% to 13%) in the downstream grating. Apparently, the upstream grating filters out the larger debris, and the remaining smaller debris can pass through the downstream grating. Plots of percent capture on gratings against tunnel velocity are given in Figure 2-15, comparing the capture on upstream and downstream gratings for various debris sizes. Generally, larger size debris and lower velocities resulted in more capture at the upstream grating, see Figure 2-15A. Photographs in Figures 2-10 and 2-11 also show this trend. For the downstream grating, no such trends are indicated, see Figure 2-15B. There was no consistent effect of debris concentration for either grating.

2.4.10 Grating Debris Degradation Tests

Additional tests were conducted with grating to investigate the potential for captured insulation debris to degrade or disintegrate when subjected to a wet, high velocity flow. First, tests were conducted in the small (high velocity) test section to establish a relationship between tunnel velocity and insulation-blocked area on the floor grating. Up to five roughly 6" x 6" pieces of NUKON insulation were distributed on a single panel of floor grating to vary the open area of the grate from 50% to 80%. With no prewetting, the tunnel velocity and pressure were recorded as the open area was decreased using 1/2" and 14" thin debris pieces. The resulting relationships between blockage area, velocity, and pressure are shown in Figure 2-16. From these results, a blockage of approximately 40% was chosen for the degradation testing.

Five 1/2" thin pieces of fibrous insulation debris were arranged on the floor grating as shown in Figure 2-17. This thickness was manually prepared by pealing off the appropriate layer from the standard 2" to 3" thick batts. Before the blower was turned on, the pieces were held in place by a layer of hardware cloth that was hinged at the bottom of the tunnel. When the air flow was sufficient to hold the debris against the grating, the hardware cloth was pivoted away from the grate and secured to the tunnel floor. The flow was adjusted, tunnel velocity and pressure were recorded, and the water spray system was turned on. The blower and spray system were both turned off after the spray had run for 60 seconds. The test procedure was repeated with 1/4" and 1/8" thin pieces of insulation debris.

No apparent breakdown of either the 1/2" or 1/4" insulation debris was seen, although the pieces bowed between the grating bars, Figure 2-18A, and the edges of the insulation pieces wrapped back around the grate bars to flap behind the grate, as shown in Figure 2-18B. The insulation was pushed back between the grate bars, but neither thickness tested showed signs of "blowing through." The pre- and post test weights of the insulation, shown in Table 2-2, confirm the observation that negligible debris was lost, i.e., no material was broken off and swept away from the sample pieces.

Based on the above results, a test with 100% blockage using a 1/8" thin layer of NUKON debris was conducted to determine if degradation would occur with this extremely thin layer. With 100% blockage using a 1/8" layer, the tunnel velocity was 130 ft/sec. After the 60-second air flow with water spray, several areas were found to have broken through and wrapped back around the grating bars as shown in Figure 2-19. However, the post-test dry weighing showed only negligible debris had been lost.

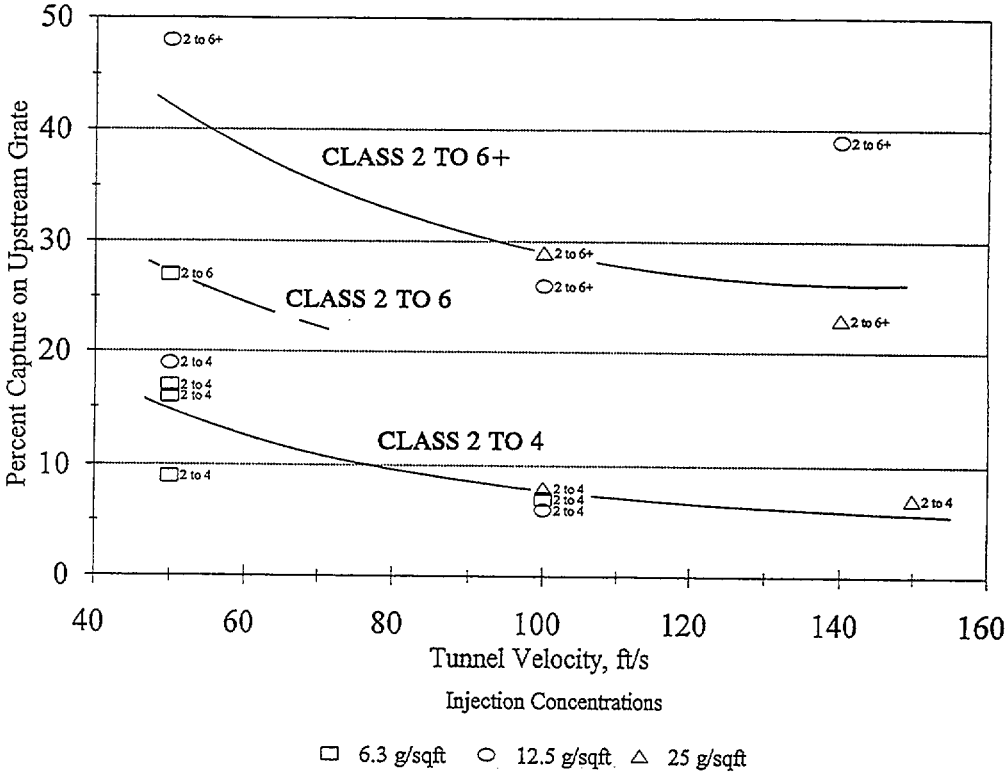

A) UPSTREAM GRATING

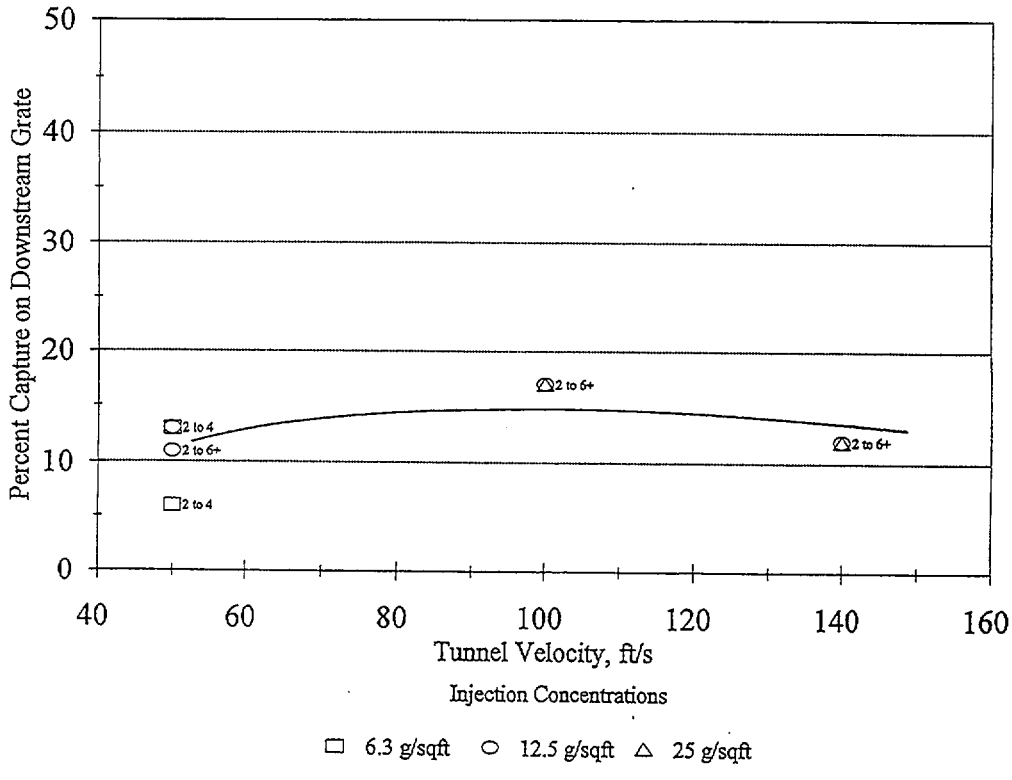

B) DOWNSTREAM GRATING

Figure 2-15. Effects of approach concentration and velocity on debris retention at gratings.

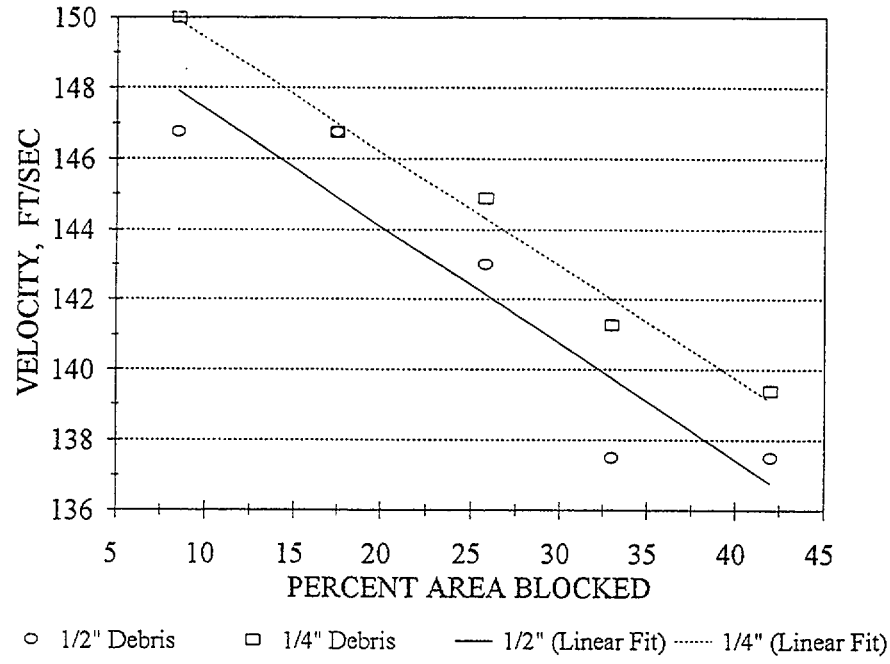

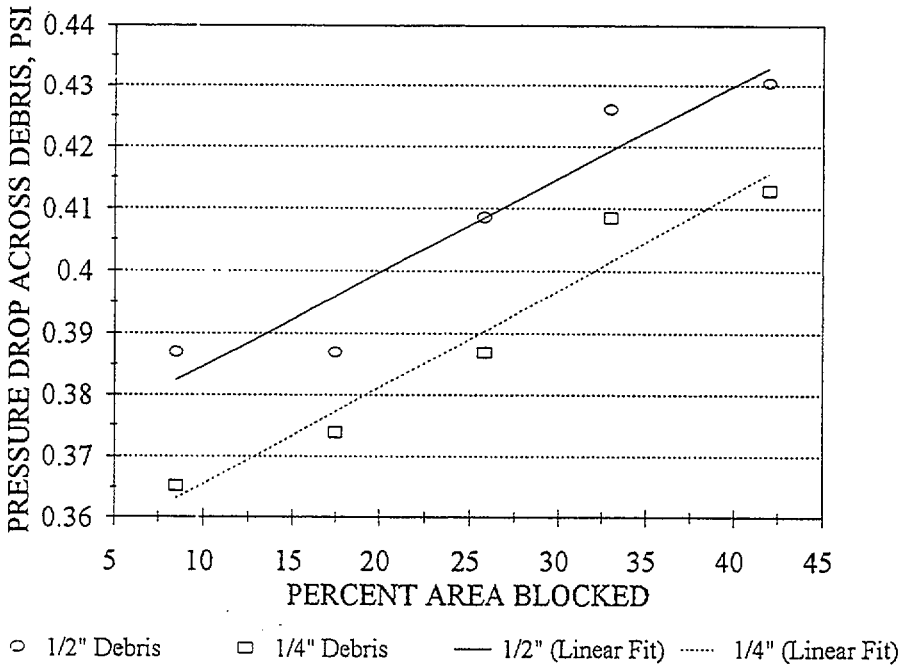

Figure 2-16. Effects of blockage of gratings on tunnel velocity and pressure drop through debris.

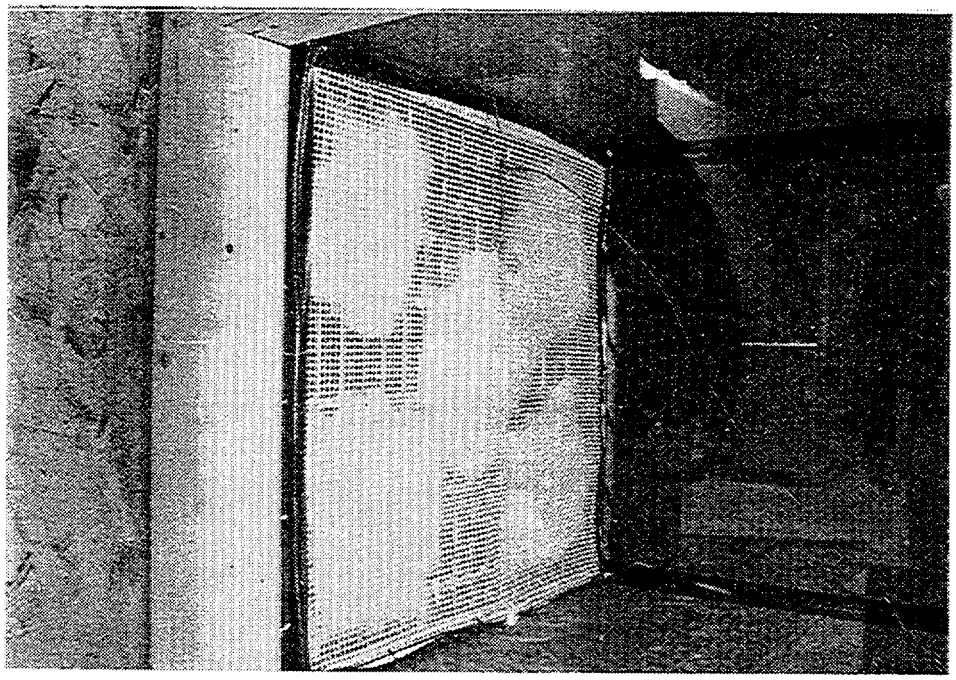

Figure 2-17. Insulation blockage with 5-1/2"-thick pieces held in place on floor grating prior to starting the blower.

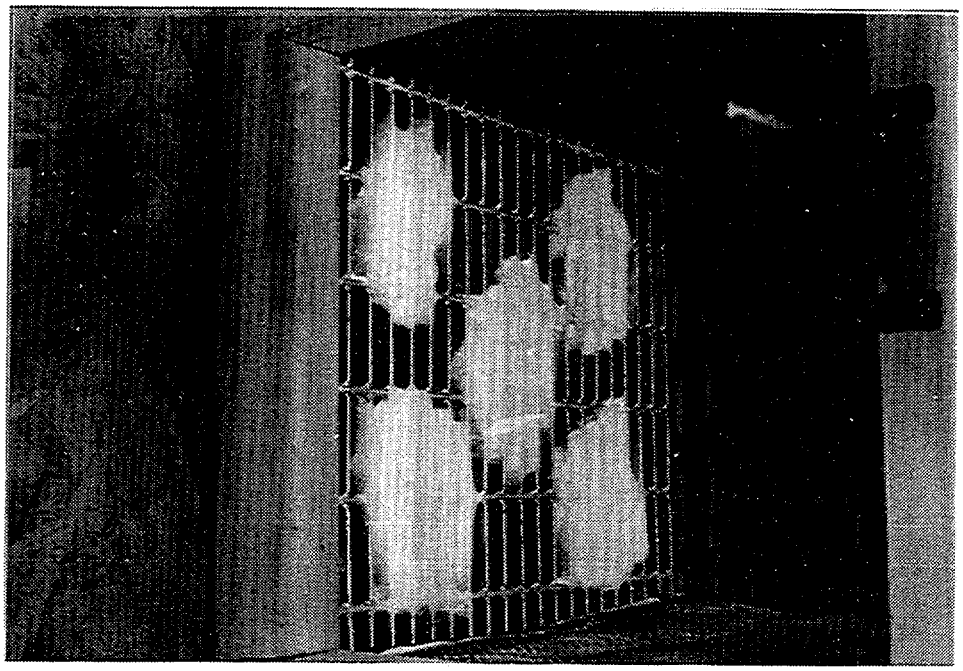

A) INSULATION BOWED BETWEEN THE GRATING BARS

B) VIEW FROM DOWNSTREAM; THE INSULATION EDGES WRAPPED AROUND AND THROUGH THE BARS

Figure 2-18. Results of blockage tests with ½"-thick insulation pieces: 40% initial blocked area.

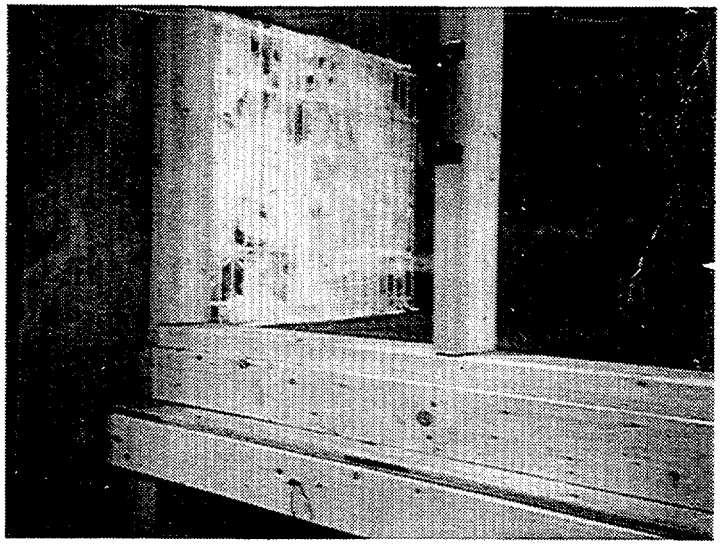

Figure 2-19. Debris blockage after test; 140 ft/s and 60 sec water spray on 100% blockage using 1/8" insulation layer.

Overall, these blockage tests indicate that at gas velocities up to 140 ft/sec, thin pieces of fibrous insulation do not further disintegrate after being captured on the floor grating.

2.4.11 Overall Evaluation of Application of Results

A major finding of the tests is that gratings captured significantly more debris by weight than any other objects tested. For example, the combination of objects in Test 17 showed that out of 100 gm of injected insulation debris, the grating captured 12 gm, while all other objects together collected only 6 gm. Also, comparing test data for a grating only with a combination of objects upstream of a grating (other test parameters identical), i.e., comparing Test 12 with Test 16, it is evident that the total capture for the combination of grating with upstream objects was essentially equal to the capture on a single grating only. This suggests that for debris capture evaluation, A first-order approximation could be to ignore all objects upstream and between gratings, and consider all deposition to be simulated by only the gratings. This would be a major simplification of the drywell debris capture evaluation, considering the numerous structures, their orientations and the complex flow patterns in an actual plant.

The above simplification is valid if the gratings cover the entire flow area, thereby forcing the flow to pass through the gratings without bypassing them. Also, it may be noted that the debris size plays a role in the amount of capture on the first grating, with higher capture of larger debris. Hence, some knowledge of actual debris sizes will help refine the evaluation. Test results showed a relatively small effect of velocity on debris capture on the first grating, although somewhat higher deposition occurred at lower velocities (see Figure 2-15).

Larger size but relatively thin insulation debris sheets (6" x 6" or larger) captured at gratings were found to be retained without further disintegration, even with approach gas velocities as high as 140 ft/sec.

2.5 Conclusions

The following conclusions are based on the test results, as summarized in Table 2-2, for fibrous insulation debris:

i. Gratings captured more fibrous insulation debris compared to other structural components. For example, the downstream grating in combined member Tests 16 through 18 captured more debris than all the other upstream obstructions combined, and the grating in Test 17 collected two-thirds of the total captured by this combination of obstructions.

ii. Under identical conditions of surface wetness, gas velocity, debris size and debris mass, a single grating captured as much debris as structural members combined with a downstream grating. Hence, one can approximate the total capture by neglecting upstream objects and considering only the downstream grating.

iii. Wetness has a clear influence on debris capture for objects like pipes and beams; when dry, these surfaces did not capture any debris. Floor grating capture was less sensitive to wetness.

iv. Dual gratings showed substantial capture (averaging about 25%) on the upstream grating, see Figure 2-15A, but less capture (about 12%) on the downstream grating, see Figure 2-15B. Generally, larger size debris and lower velocities resulted in more capture at the upstream grating, up to about 40%. For the downstream grating, no trends with initial upstream debris size or gas velocity was indicated, see Figure 2-15B.

v. Mark II vents with wetted surfaces showed debris capture on the cover plate and the simulated drywell floor totalling about 12%. The largest size debris tested, Class 6+, resulted in a total capture of 35%. No capture occurred on the downstream side of the cover nor inside the vent, even when prewetted.

vi. Negligible break up or disintegration of insulation debris captured on the grating was found when 1/8" to 1/2" thin pieces of insulation sheets (about 6" x 6") were subjected up to 140 ft/sec of approaching gas velocity.

vii Gravitational settling, i.e., loss of fibrous debris by capture on the tunnel floor, was negligible for all tests except the MARK II vent geometry. Material attributed to settling during the vent tests was not included in the calculation of percent capture.

2.6 References

2.1 D. V. Rao, et al., "Drywell Debris Transport Study: Draft Phase 1 Letter Report," SEA 96-3105-010-A:2, Science and Engineering, 1996.

2.2 Murthy, P., Padmanabhan, M., Weber, F.J., and Hecker, G.E., "Head Loss of Fibrous Nukon Insulation Debris and Sludge for BWR Suction Strainers," ARL Report No. 124-95/M787F, June 1995.

2.3 Zigler, G. et al. "Parametric Study of the Potential for BWR ECCS Strainer Blockage Due to LOCA Generated Debris," NUREG/CR-6224, Prepared by Science and Engineering Associates, Inc. for the U.S. Nuclear Regulatory Commission, August 1994.

3. Integrated Effects Test Program to Evaluate Inertial Debris Capture on BWR Drywell Structures

3.1 Background and Objectives

The separate effects tests described in Section 2 provided valuable data regarding inertial capture on BWR drywell structures. Those tests had notable limitations:

1. The debris loadings were light. The gun arrangement chosen for injection of the debris limited the amount of debris that could be introduced into the flow. The maximum debris loading achieved in the tests is 2 lbm/100 ft^2 compared to 2-10 lbm/100 ft^2 expected in the BWR plants. It was not clear if the findings of separate effects test regarding effectiveness of grating would be applicable to BWR plants.

2. Modest assortment of debris sizes. Separate effects tests were done using debris that were generally classified as small [see Figure 1-2]. No data were obtained on inertial capture of larger debris.

3. One dimensional flow fields. Debris were carried to the structural elements by a flow that is best described as plug flow. Direct application of such data to BWR plants is questionable.

4. Non-prototypical congestion of structures. Experiments have shown that structural congestion can significantly influence capture. However, prototypical congestion levels could not be reproduced in the test facility.

These limitations prompted experiments of a more integrated nature.

The integrated effects tests, reported herein, were designed to study debris transport under integrated and prototypical BWR drywell conditions following a postulated MSLB LOCA. These integrated debris transport tests were carried out by SEA for the NRC at the CEESI. Hereafter, these tests are referred to as the CEESI debris transport tests.

3.1.1 Objectives and Scope

The primary test objective was to gain insights into the transport of fibrous debris by means of small-scale experiments and to determine fibrous debris transport fractions under prototypical BWR drywell conditions following a postulated MSLB for use in analytical models. The test method selected to accomplish this objective was debris generation and subsequent transport by a dispersing air jet through a facility with characteristics somewhat similar to a BWR drywell.. The principal test results were debris capture fractions for the various structural components.

The main steam lines in BWRs exit the reactor vessel at relatively high elevations within the containment drywell and drop downward before penetrating the containment at about the mid-height level. Insulation debris generated at these higher elevations will be transported to the lower regions of the containment by the steam flow by reactor vessel depressurization. As the debris travels downward, it will contact drywell structures and equipment (e.g., gratings, beams, pipes, pumps, valves, ducts, and other structural supports). Some portion of the debris interacting with a structural component will be captured (stick) by that component. Other debris will pass through the downcomer vents into the suppression pool.

Prototypical operating conditions considered included flow velocities, surface wetness, debris transport path lengths, and congestion and type of structures along the debris transport pathway. The structural components placed in the transport pathway inside the test chamber included gratings, pipes, and I-beams. In addition, the debris transport pathway passed through a 90° bend. The diameter of the test chamber was approximately 10 ft and the total transport path length was approximately 70 ft. Bulk flow velocities entering the area containing the congestion of structural components generally ranged from 25 to 50 ft/sec. Because surface wetness of the structures was found in the ARL debris capture tests to strongly influence debris capture, and because structural surfaces with a BWR drywell following a LOCA would be expected to rapidly wet with steam condensate, the surfaces in the CEESI debris transport tests were artificially wet with a misting system prior to initiating each test. Insulation debris was maintained dry unless the debris picked up moisture upon interaction with a structural surface.

Insulation blankets were mounted and restrained to maximize the destruction of the blanket, i.e., generate the largest possible concentrations of debris passing through the congestion of structures. This was accomplished by restraining the blanket in front of the jet for as long as

possible. Obtaining data regarding debris generation, specifically the size distribution of the debris, was not an objective of this experiment.

The debris transport and capture data obtained from the CEESI tests was intended to serve as a means for benchmarking analytical methods and models applied to predicting debris transport within a BWR drywell. The CEESI test data was correlated with data from the ARL separate effects debris capture tests to provide a consistent data set. During the design of the experiment, scaling analysis determined the appropriate level of congestion for the structural components so that the congestion was somewhat typical of a BWR drywell. Further, one-dimensional jet expansion calculations and two- and three-dimensional CFD simulations determined the appropriate nozzle diameter of the air jet to obtain expected prototypical drywell bulk flow velocities.

3.2. Program Elements

The CEESI test program advanced in the following four steps:

1. Test development analyses and experimental design
2. Developmental tests,
3. Production tests, and
4. Data analyses.

3.2.1 Developmental Tests

Seven baseline tests were conducted to determine:

- The adequacy of the selected jet nozzle diameters to provide the desired bulk flow velocities,
- The duration of the air jet needed to complete debris transport,
- Optimal insulation mounting and location for maximum debris generation,
- Optimal test procedures such as prewetting structures using the misting system, and
- Optimal procedures for collecting and classifying debris

These development tests were instrumented with Pitot tubes connected to transducers to monitor and map flow distributions before the flow entered the congested test section. The measured flows (reported in Section 3.5) agreed well with the predicted flow velocities. Approximately 10 to 12 second of air jet duration was needed to complete debris generation and transport. For maximum debris generation, the insulation blankets needed to be steel banded and supported at both ends to hold the blanket in position longer for more complete destruction. Experience gained with these tests was applied to developing the operating procedures for the production tests and four of the seven tests provided useful debris transport and capture data.

3.2.2 Production Tests

Additional modifications were made to the facility prior to conducting the production tests. These modifications were:

- End restraints were installed on both ends of the insulation blanket to keep the blanket in the path of the air jet, thereby maximizing debris generation (note that this method of mounting the blanket is not prototypical of BWRs; therefore, debris generation results may not be valid for debris generation models),
- Additional misters were installed to more uniformly wet the structures.
- The Pitot tubes which sustained significant damage in the developmental tests were removed.

Using test procedures developed from experience gained conducting the developmental tests, ten production tests were conducted. The test parameters varied during the tests included the distance between the target insulation blanket and the air jet nozzle, the jet nozzle diameter, and the jet duration time. Debris was collected and bagged by location and type for subsequent drying and weighting which provided the primary data for computing the transport fractions for the CEESI test facility and the capture fractions for the structural components. Test repeatability was shown. Video and still pictures provided visual data for drawing insights into the transport processes.

3.2.3 Data Analyses

The data analysis first focused on accounting for the final distribution of the mass of the original blanket which was weighted prior to each test. The final distribution of mass not recovered from the test was estimated based on observations by the test personnel. (It was not practical to collect much of the very fine debris, such as individual fibers, deposited on the structures and walls. In fact, much of this fine debris was expelled from the test chamber through screens installed at the exits from the test chambers to catch debris.) The debris mass not recovered following the tests was found to dominate experimental error and the estimate of its final location distribution was used to formulate an error analysis. Debris transport and capture fractions were then calculated from the final mass distributions and the capture fractions correlated with the data from the ARL separate effects tests.

3.3. Test Facility Description

The CEESI is located outside Nunn, Colorado approximately 100 miles north of Denver at a converted decommissioned Atlas missile site. The site was converted in 1965 to a commercial air and water calibration facility. The station compressed air facilities can store as much as 11,000 ft^3 of air at 2500 psia. The debris transport tests were conducted in the CEESI Outside Calibration Facility shown in Figure 3-1.

3.3.1 Air Blast Test Chambers

The main test chamber consists of a horizontal large diameter cylinder that was approximately 93 ft in length and 9.4 ft in diameter (inner). A 32-ft long auxiliary chamber of the same diameter was attached with a flanged collar at the exit end of the main chamber in a horizontal "L" configuration. The flow area of the flanged collar (7.2 ft inside diameter) was about 60% of the flow area of the test chambers. A conical diffuser section was attached to the upstream end of the main chamber (behind the air jet nozzle) but this conical section was nearly completely blocked (a small section at the center was blocked by a screen) such that only a small fraction (order of 5-10%) of the air exited the test chamber in the reverse direction. Exhaust air flows exiting the far end of the auxiliary chamber were filtered by a reinforced perforated steel plate (1/8 inch mesh) that covered that opening. Target insulation blankets were mounted on a 12.75 inch outer diameter pipe that extended across the main test chamber at mid height and was positioned directly in front of the air jet nozzle. The target pipe was secured to rails on either side of the test chamber which extended horizontally 30 ft from the jet nozzle. A burst disk mounted upstream of the nozzle in the air supply line ruptured after system pressure of approximately 1000 psig was applied across the disk. Figure 3-2 shows the test chambers drawn to scale.

3.3.2 Structural Test Section

The structural test section contained an assemblage of structural components (e.g., gratings, pipes, and I-beams) designed to simulate a prototypical section of a BWR drywell. A survey was conducted of typical structures that exist in Mark I and Mark II containments and their respective surface areas prior to designing the structural test section. The design generally focused on maintaining the same surface to volume ratios as found in the BWR containments. To the extent practical, the structures were oriented in a manner analogous to the orientations found in the actual plant conditions. A comparison of the CEESI geometry with a Mark I is discussed further in Section 3.4

The structural components of the structural test section are shown schematically in Figure 3-3. All I- and all pipes were 10 inches in diameter. I-beams were oriented with their web into the direction of air flow. Starting from the

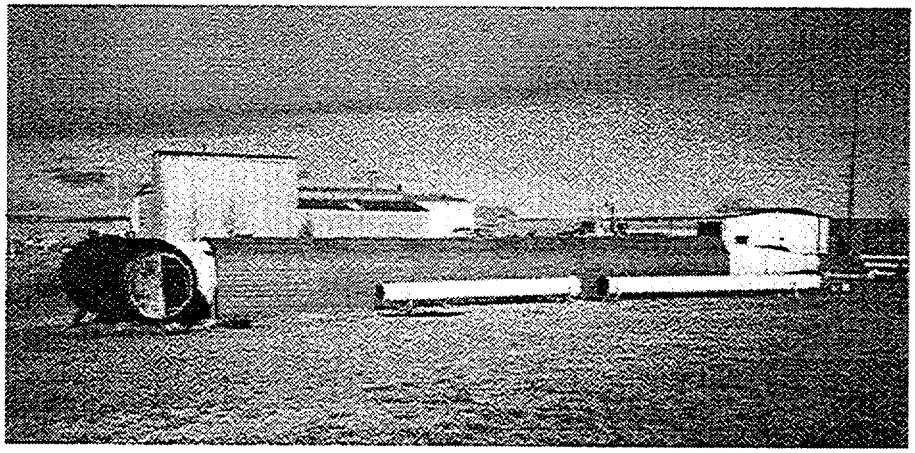

Figure 3-1. CEESI outside calibration facility.

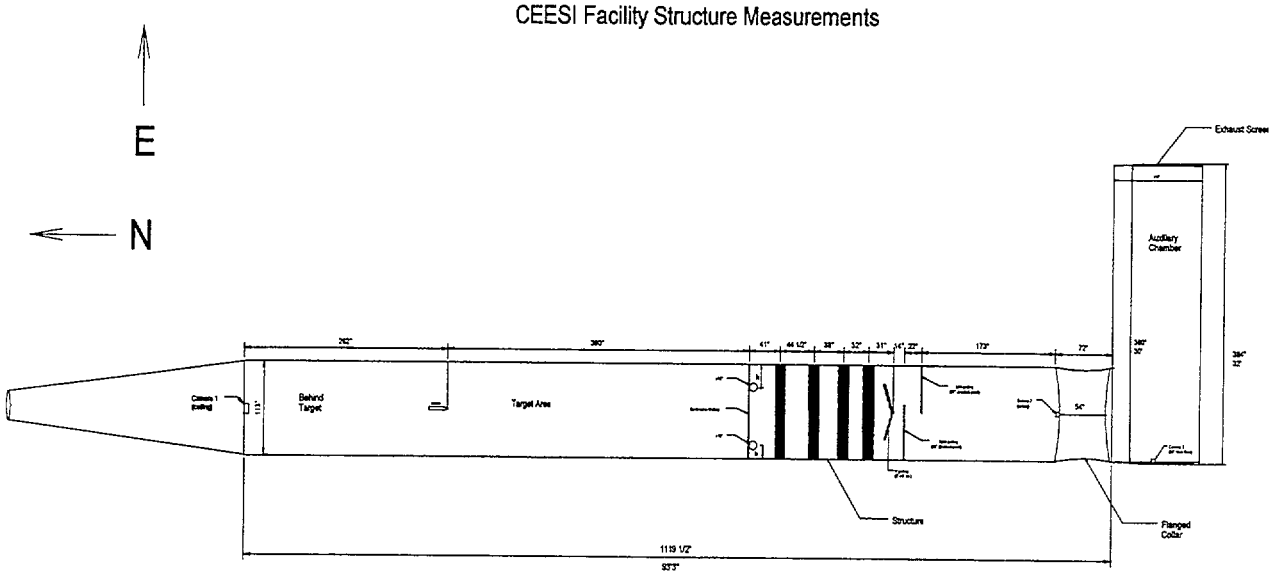

Figure 3-2. CEESI facility structure dimensions.

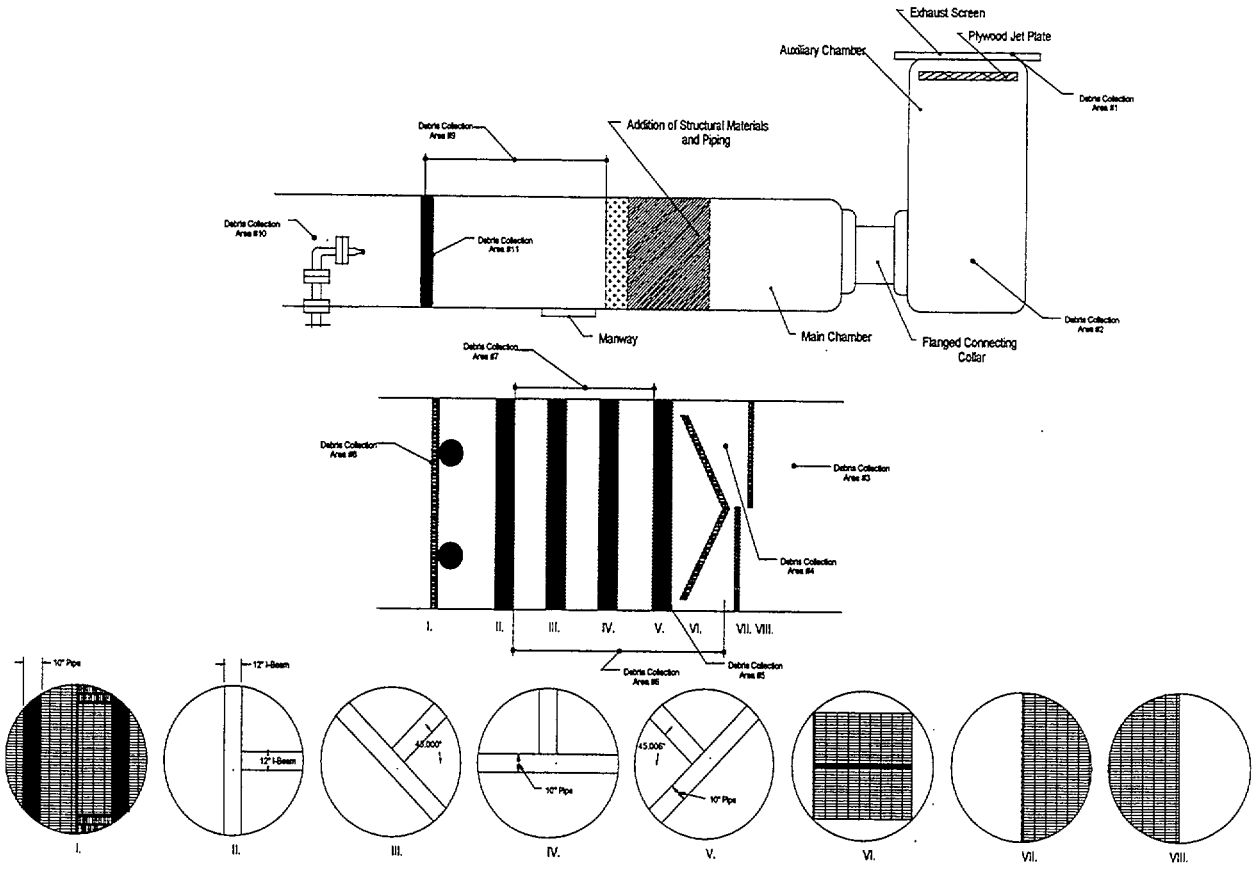

Figure 3-3. Schematic of structural test section.

front (flow entrance) of the structural test section, the test section contains the following structural subassemblies:

- A continuous grating with two vertically oriented pipes directly behind,
- I-beams with a full length beam oriented vertically and a half beam oriented horizontally,
- I-beams with a full length beam oriented 45° from vertical,
- Horizontally oriented pipe with a half I-beam oriented vertically,
- Pipe oriented 45° from vertical,
- V shaped grating,
- Two half-section gratings separated axially by 22 inches, referred as the split grating.

The gratings of the V-grating were at an angle of approximately 56° to the axis of the main test chamber and the V-grating did not obstruct the entire flow, i.e., portions of the air passed over the top, under the bottom, and around the sides without passing through the grating. The V-grating was 5 ft wide at its widest and it obstructed about 57% of the total test chamber flow area. All gratings were manufactured from 1/8-inch steel bars. The dimensions of a 'grating cell', defined by the spacing between the bars was 3.75 inches by 1 inch.

Most of the structural test assembly can be seen in the photo shown in Figure 3-4 taken from just behind the continuous grating. Note that the pipes and I-beams look somewhat like a large pinwheel. A warm water high pressure (150 psi) misting system, constructed from PVC pipe, was installed in the structural test section to wet the structural assemblies.

3.3.3 Test Instrumentation

Test instrumentation for the CEESI debris transport tests consisted of pressure sensors with transducers in the air jet supply line to monitor nozzle air flow, Pitot tubes with transducers in the approach to the structural test section to measure flow velocities, and video cameras to record the motion of debris particles. Locations of the instrumentation are shown Figure 3-5. Other non-instrumentation data consisted of still pictures taken before and after each test and the collection of debris by location and classification from both test chambers.

Nozzle Air Flow. The pressure history of the jet nozzle was measured and recorded for each test by pressure sensors with transducers in the air jet supply line. The actual jet duration time for each test was determined from this pressure history. A sample pressure trace is shown in Section 3.5.

Pitot Tubes. Pitot tubes connected to transducers were mounted in the approach to the structural test section to measure flow velocities. The axial and radial locations of each Pitot tube are shown in Figure 3-5. Two of the Pitot tubes were located axially in front of the other six tubes which were arranged in the same axial plane. The Pitot tubes were only used in the developmental tests. Since the tubes sustained substantial damage during the developmental tests and the test flow velocities were adequately characteristic during these tests, the tubes were removed prior to the production tests.

Video Cameras. Video cameras were mounted in the test chambers to record the motion of debris particles as the particles moved through the chambers. Only one camera was installed for the developmental tests and it was located behind the jet nozzle looking past the target mount and downrange towards the structural test section. Two additional cameras were mounted for the production tests. The first of these was mounted at the far end of the main test chamber looking back towards the structural test section so it could record the motion of debris exiting the split grating. The second of these additional cameras was mounted in the auxiliary test chamber near the joining flange collar looking towards the exhaust screen at the far end so it could record the motion of debris as the debris passes through the 90° bend upon entering the auxiliary test chamber.

3.4 Scaling Considerations

The CEESI experiments were designed to focus primarily on capture of steam-borne debris on various drywell structures following a postulated double-ended guillotine break in a main steam line in the mid region of the drywell. The rationale for that selection and the supporting calculations are documented in Ref. 3-5. This section discusses how the experimental parameters used in CEESI experiments scale to the conditions expected to exist in the BWR drywell following a LOCA. The controlling parameters are: working fluid, flow velocity and flow patterns, debris size/characteristics, debris wetness, drywell surface wetness and structures/obstacles followed by how they are simulated in the CEESI tests.

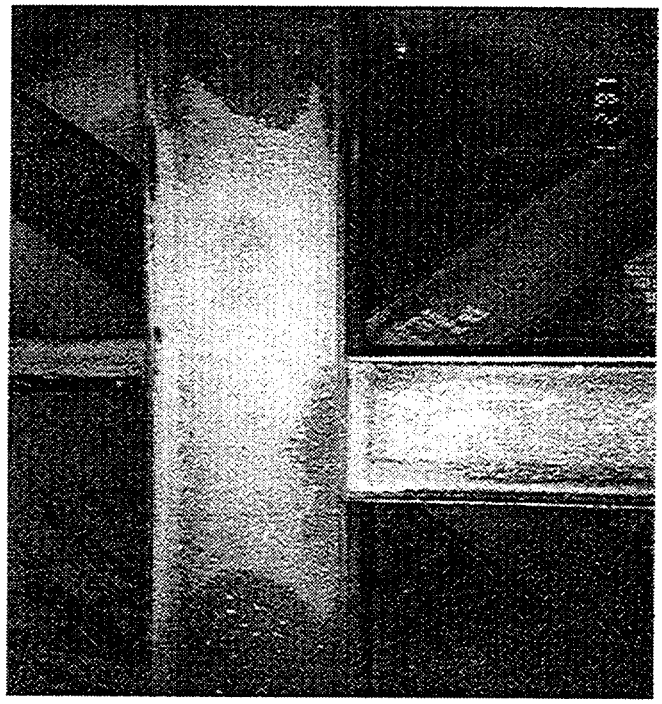

Figure 3-4. Frontal view of a structural test section.

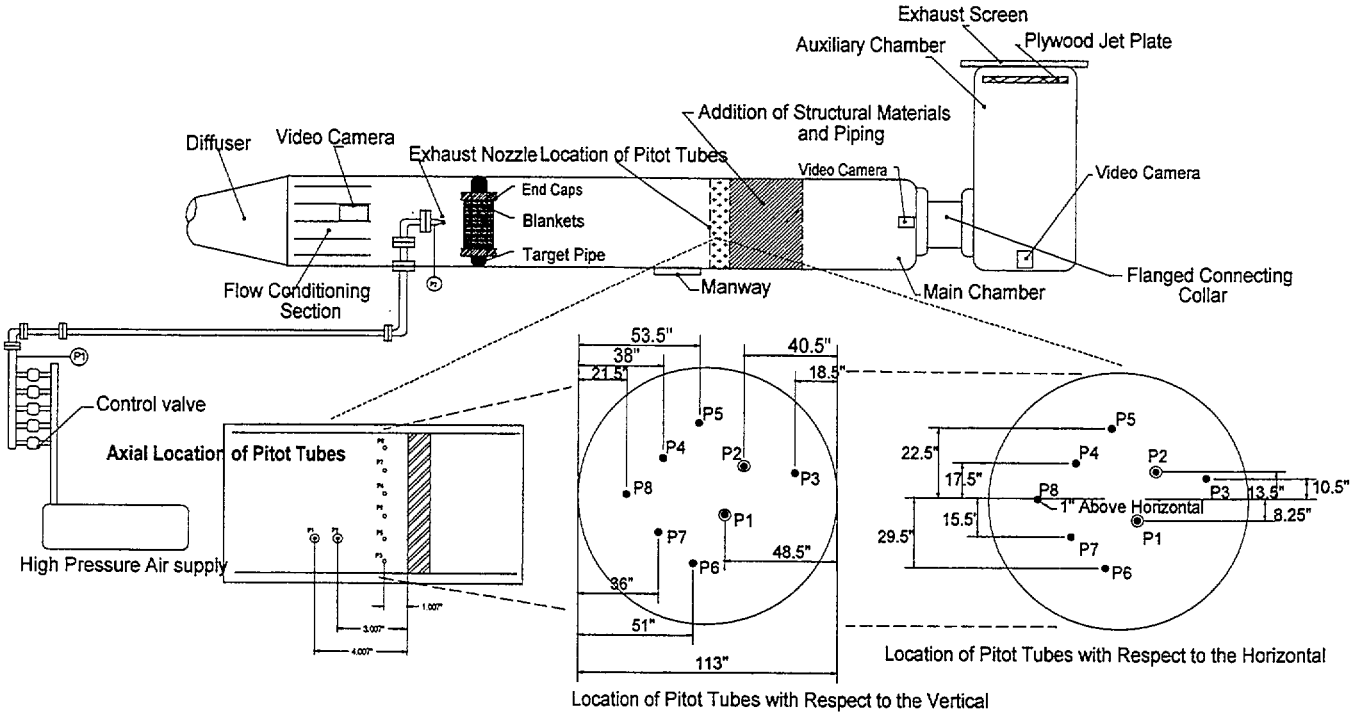

Figure 3-5. CEESI debris transport instrumentation.

Finally, the effect of expected distortions on the experimental results was noted.

Working Fluid Choice: In the bulk of a BWR drywell following a MSLB, the debris would be entrained and transported by steam at a temperature of 260 °F and a pressure of 40 psia(Ref. 3-5). Past calculations have shown that fine water droplets (1-10 microns in diameter) are suspended in a steam continuum (void fraction ≈1.0) at low equilibrium qualities (≈0.1).

In CEESI experiments air (typically 50°F at stagnation condition and 14 psia) was chosen as the working fluid. This known deviation from prototypical conditions could have the following macro- and micro- scale effects:

1. Usage of air instead of condensing steam (or mist flow) eliminates possibility of debris capture by diffusiophoresis. For the debris size of interest, the capture driven by diffusiophoresis (capture velocity ≈0.01 m/s) is negligible compared to inertial capture (Stokes number >> 1) [Ref. 3.5]

2. Expansion of air from its stagnation conditions will result in overcooling in the jet pathway. Past calculations suggest that the resulting temperature can be as low as 5°F, corresponding to a stagnation temperature of 50 °F. If proper precautions are not taken, water may freeze and eliminate surface wetness which is vital for capture[1]. To avoid this possibility, the drywell interior was pre-heated before every test to up to 75 °F. Also warm water (> 100 °F @ 150 psia) was injected into the flow stream to wet the structures. A simple heat balance was conducted to ensure that freezing would not occur. Visual inspection after conclusion of each test revealed no evidence of freezing. The debris can be clearly seen to be attached to structures by a thin water film.

3. Stokes number (Stk) is inversely proportional to the gas media kinematic viscosity, therefore usage of colder air instead of steam results in lower Stokes numbers. At the range of Stk being examined (i.e., 2.5-6.5), this effect on Stk is negligible.

It is difficult to exactly quantify the impact of each of these effects on the capture efficiency measured from these tests. Qualitatively, however, it is clear that these effects possess the potential to lower capture efficiency and thus maximize transportability of debris. No corrections were made to account for this known deviation from prototypicality.

Flow velocity and flow patterns: A series of computational fluid dynamics (CFD) calculations were performed using commercially available CFD codes to draw inferences regarding steam flow patterns that exist in the drywell following a postulated large break LOCA (Refs. 3-5, 3-9, and 3-10). The scope of these calculations varied from 1-D scoping calculations that estimated cross-sectional area averaged fluid velocities assuming plug flow to refined CFD calculations on jet deflection by structural elements. Based on these calculations it was concluded that steam flow velocities in the close proximity of the break tend to be near-sonic or super sonic. The extent of this region depends on the break orientation and the structural congestion close to the break. Sufficiently far from the break (L/D > 10) the jets will dissipate into pressure-driven flows with velocities in the range of 30-50 ft/s, with an average of about 45 ft/s. In the drywell floor region these velocities may be even lower, close to 30 ft/s. The bulk flow can be approximated as being parallel to the drywell walls, where as the localized flow patterns differ considerably within the containment depending on the pipe break location, and structural arrangements. CEESI experiments were designed to measure capture efficiency at velocities that are typical of lower parts of the containment where bulk flow velocities are typically less than 45 ft/s.

To simulate these flow conditions in CEESI experiments, efforts were made to ensure that nozzle size and flow would be sufficient to induce bulk flow $\geq$ 45 ft/s, and that flow as it is entering the piping region of the test section would be nearly axial. Selected calculations were used to design the test section. In addition, the test section was instrumented to confirm that actual flow in the test section is according to the calculations. In the first calculation a 1-D choked-flow model was employed to determine the flow rate through the nozzle at the exit plane. These calculations suggested that a 3.75-inch diameter nozzle (nominally 4 inch nozzle) would be required to establish desired bulk flow velocity of 45 ft/s (corresponding mass flow through the nozzle is about 300 lbm/s). On the other hand, a 3-inch diameter nozzle would be sufficient to establish a flow velocity of 30 ft/s. The mass balance on the high pressure storage tank[2] was used to confirm that

[1] Debris are held on structures by water surface tension as demonstrated by the fact that dry debris do not stick to surfaces (see Section 2).

[2] The storage tank pressure was measured before and after each test. The mass balance was then used to estimate the mass of air discharged.

the actual bulk flow through the test section is equal to or greater than the flow rate predicted by the 1-D model.

During the design process, a CFD calculation was run to examine flow fields that would result from a 4-inch diameter (at the stagnation point) jet on the target pipe. Examples of these CFD calculations are presented in Figures 3-6 and 3-7. Figure 3-6 shows the flows near the jet nozzle as velocity vectors overlaid onto the fluid temperatures (variations in color). The simulated jet is in the lower left corner and the simulated target pipe is shown at mid level. Figure 3-7 shows the flows and temperatures further downstream in the region of the structural test section. The flow pattern, of course, changed with the axial position of the target but the flow patterns through the structural test section remained relatively uniform. The actual flow patterns may differ slightly from the CFD code predictions, because of the underlying modeling assumptions. For example, space behind the nozzle was not modeled to minimize the calculational nodes. Similarly, the first grating was assumed to be a baffle plate with a non-linear pressure drop coefficient of 5 and the presence of various structures in the piping region was ignored. More refined CFD analyses were determined to be cost-prohibitive.

To map actual flow patterns, the experiments relied on two sets of measurements. The test section was instrumented with fast-responding Pitot-tubes to monitor axial velocities of flows entering the structural test section. A total of three tests were run with the sole purpose of mapping out the flow patterns. No effort was made to map out flow patterns within the piping regions. These measurements exhibited some dependence of flow velocity on the radial and angular position with respect to the center-line (see Section 3.5.2.3). In addition, the test section was equipped with three video cameras which were used to monitor movement of small debris. The debris pieces (especially the small debris) served as tracers illuminating three-dimensional flow patterns. These video pictures indicated that bulk flow moved consistently in the forward direction (with respect to the nozzle exit plane), but that there exists a 3-D movement of the flow. Flow patterns within the structural test section appeared to be simple; no eddies were discovered. A strong eddy was noted to exist behind the nozzle, which was capable of entraining a fraction of the debris and trapping the debris behind the jet. The data reduction procedures corrected the test results for the debris deposited behind the jet.

Based on these analyses and measurements, it was concluded that at a nozzle diameter of 3.75-inch, bulk flow velocity in the test section would vary between 38 and 60 ft/s, depending on the radial location and axial plane. These velocities are typical of expected flow velocities in the majority of drywells. A comparison of present experimental results with the results of the separate effects tests[3] indicates that presence of three-dimensional flow patterns has little effect on the debris capture.

Debris Size and Debris Characteristics Debris generation experiments conducted by past experimenters have shown that generated fibrous debris would range in size from individual fibers to partially destroyed blankets. Transportable debris can be adequately categorized with three general size groups: small, medium and large. The small pieces are best described as loosely attached fibers with no structure left over from the original blanket. The medium pieces tend to possess some of the original blanket structure at the middle, but appears beaten-up on the outside. The large pieces on the other hand are torn pieces of the original blanket. Their composition is likely to vary with the location and orientation of the target pipe with respect to the nozzle.

The CEESI experimental facility was best suited for producing such a wide range of debris and simultaneously introducing them into the flow stream in a prototypical manner. The following sections provide a pictorial description of the actual debris generated and used in the present experiments. Visual inspection of these debris suggests that debris used in the CEESI tests are consistent with photographs and videos published by past investigators.

Debris Wetness The debris generation experiments have also shown that steam generated debris are nearly dry (with some moisture on the outside). Two bench-top experiments were conducted as part of this study, to confirm that debris subjected to steam remain mostly dry. In the first experiment, a steam jet from industrial steam boiler (150 psi) was used to generate small pieces from an intact blanket. Visual inspection of the pieces suggested that the outer surface gets wet. In the second experiment,

[3] In the separate effects tests diffusers were used to straighten the flow and ensure that flow closely resembles plug flow as confirmed by tracer visualization of the flow fields.

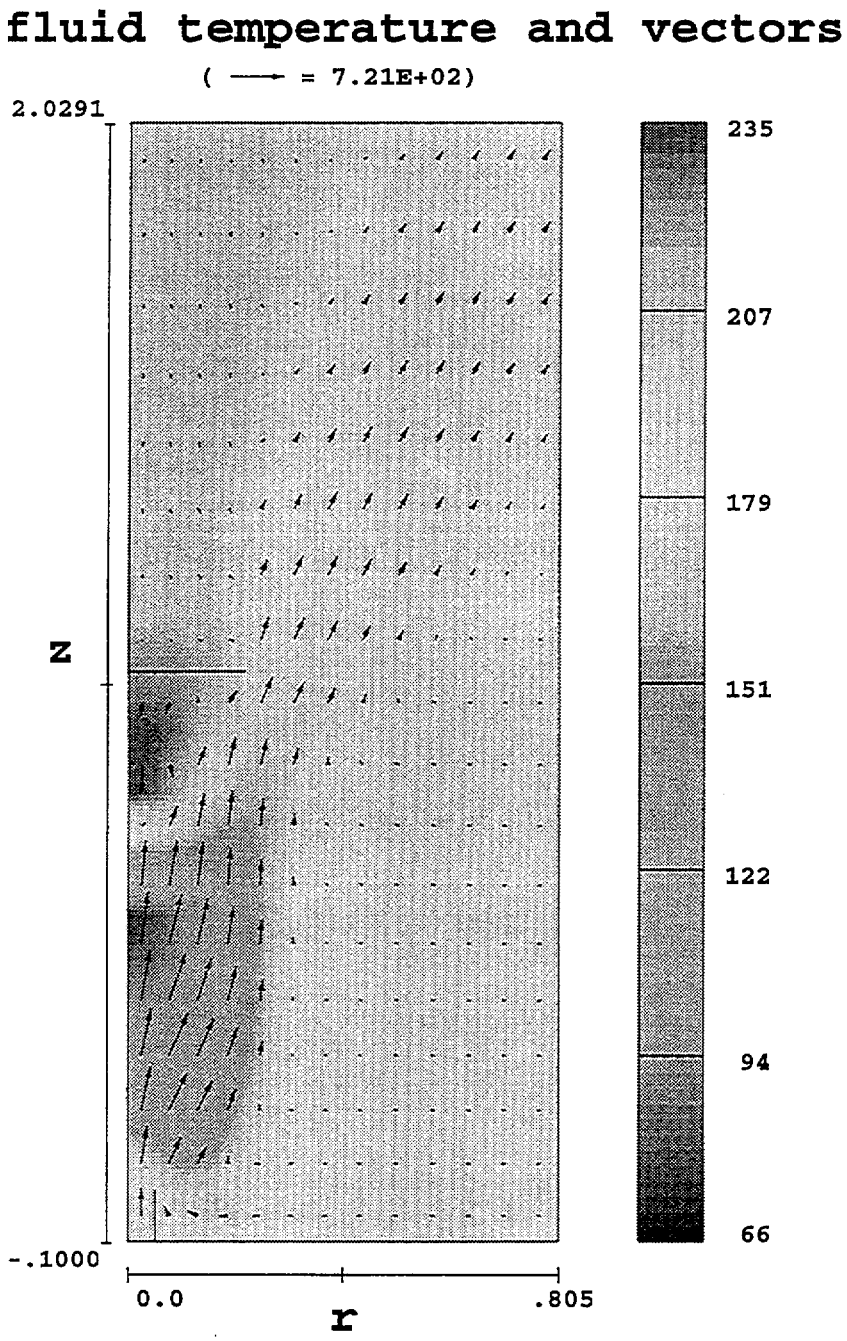

Figure 3-6. Typical CFD calculated flow patterns near jet nozzle and target.

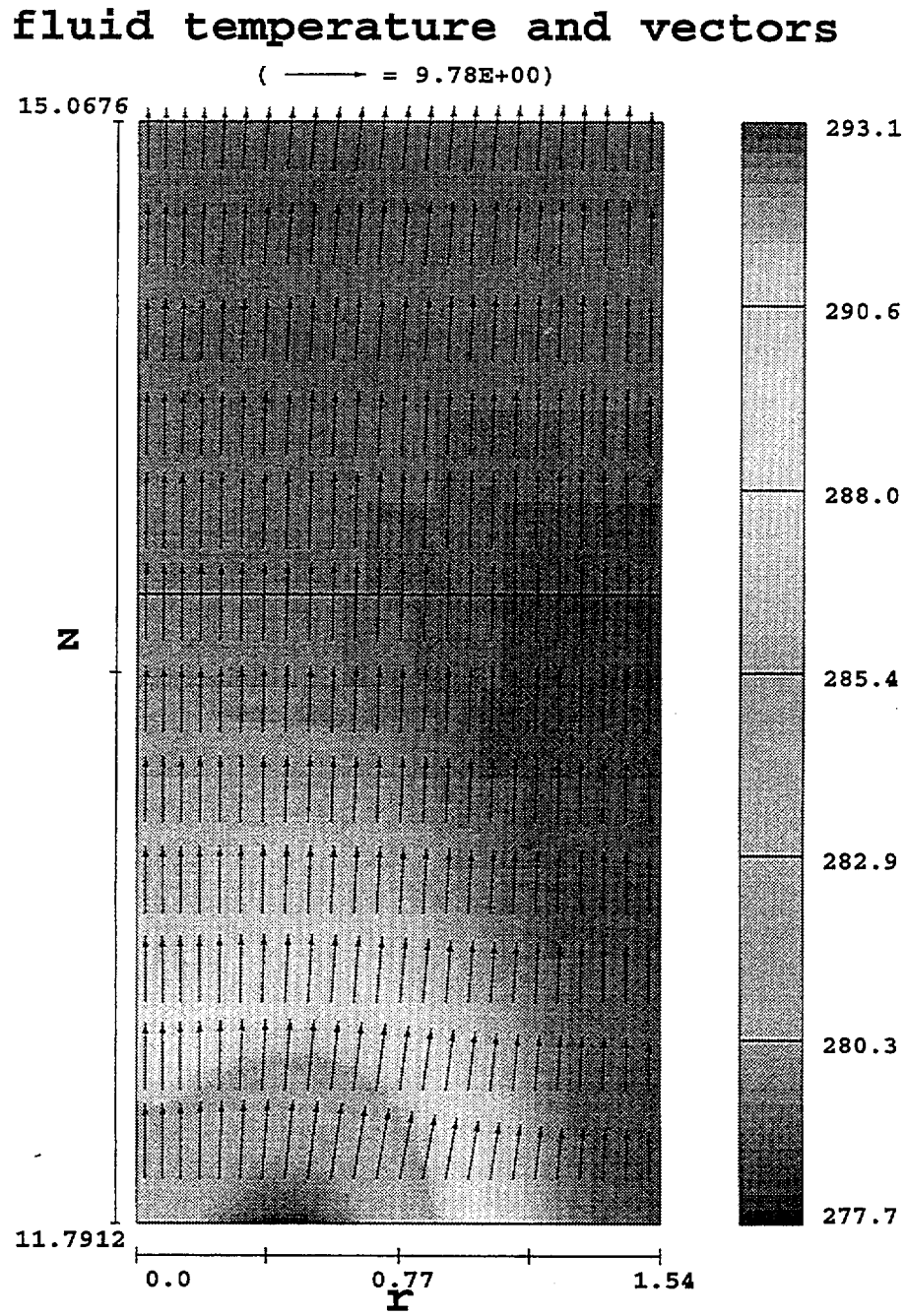

Figure 3-7. Typical CFD calculated flow patterns in structural test section.

previously destroyed blanket pieces were exposed continually to steam flow with suspended water droplets. After a minute of exposure, the debris mass increased by no more than 10%, indicating negligible wetting.

No efforts were made to simulate debris wetness. This is a known deviation from the prototypical conditions. Its effect is likely to minimize debris capture on various structures, and thus maximize debris transport.

Structural Surface Wetness Structural surfaces would be wet as a result of: a) deposition of fine water droplets produced during isentropic expansion of steam jets in the containment and b) condensation of steam. Actual water layer thickness on a given structure most likely varies with time. Past scoping calculations and MELCOR calculations suggest that steam condensation alone can produce water layer thickness as high as 200 microns with in 1 second. The scoping calculations also suggest that water droplets produced by isentropic expansion would be about 10-50 microns in diameter and would possess sufficiently large stokes number to impact various structures located in the bulk flow. Together, it is very likely that all structural surfaces would be wet, with thickness sufficient to drain (or be re-entrained by steam flow) within the first two seconds.

Procedures for wetting structures located in the CEESI facility were developed based on several exploratory tests in which fine misters positioned at different locations were used over selected intervals. Sprays were added as needed to ensure that all structures were evenly wetted. Typically sprays were run several minutes before each test to ensure that a liquid layer builds up to sufficient thickness to drain under gravity. After approximately 5 minutes of spraying, the liquid film on the structures attained a steady state. Rough measurements[4] of liquid layer thickness suggest that it is a strong function of the structural orientation and structural geometry. For example on the horizontal section of a I-beam the layer thickness is typically about 0.5 mm, on the other hand layer thickness on the vertical surface of the I-beam is much less ($\approx$ 0.1 mm). It is important to note that observed deposition profile exhibited little or no dependence on the initial layer thickness. For example, on an I-beam, the majority of the deposition occurred on the vertical surface which was perpendicular to the bulk flow direction, but is lowest where film is thicker.

[4] Choice of not using accurate water film thickness is based on insights gained from ARL experiments which suggested that for layer thickness higher than 100 μm debris capture is only weakly dependent on the surface wetness.

Geometric Scaling A comprehensive survey of drywell structures (Ref. 3-5) was undertaken to identify types of structures present in a drywell and the levels of congestion. Typical piping runs were found to vary between 6-inch and 28-inch, while the I-beams varied from 6" wide to 12" wide. The surface area for each structural class are shown in Table 3-1. This table did not include structures that are judged to be plant specific or those that vary widely from plant to plant. As evident from this table, the average surface to volume ratio of the structures in the drywell is about 1 ft^2/ft^3, although it varies from 1.3 ft^2/ft^3 in the lower regions of the drywell to 0.4 ft^2/ft^3 in the upper part of the neck. All the structural elements with a characteristic diameter larger than 12"are laid-out vertical or horizontal (e.g., steam lines and grating I-beams) and together they contribute to about 0.6 ft^2/ft^3. The remaining structures (conduits and instrument tubes) were designed to fit the space and contribute up to a surface to volume ratio of 0.4 ft^2

Pictures of the drywell at different elevations, together with Table 3-1, were used to design the CEESI test geometrical configuration. The intent was to initially assemble the major structures up to a congestion level of 0.66 ft^2/ft^3 over 25-ft long test section. If considerable capture is observed, then increase the congestion to 1.3 by adding miscellaneous structures to study its impact on capture efficiency. Initial structures consisted of 12" diameter pipes arranged perpendicular or parallel to the flow direction and 12" wide I-beams with webs facing the flow. In addition, actual size gratings employed in the plant as floor gratings were also used in the CEESI facility. As little capture was noted during the developmental tests that no additional structures were added prior to the production tests.

The congestion levels employed in these tests was approximately the same as the congestion expected in the regions between the first and second gratings. Measured capture efficiency is therefore typical of that estimated in the mid-region of the drywell. Usage of this capture efficiency for the area below the lowest grating would maximize potential for transport (which is conservative). The scaling of the CEESI facility to a Mark I drywell is summarized in Table 3-2.

Geometrical Orientation: The CFD calculations indicated that primary flow direction in the Mark I and II containments would be vertical. The orientation chosen in

Table 3 -1. Typical BWR drywell surface areas.

	Mark I		Mark II	
Type of structure	**Area (ft^2)**	**Fraction of total**	**Area (ft^2)**	**Fraction of total**
Containment structures	38,600	0.260	43,420	0.229
Pipes and conduits	66,290	0.448	66,290	0.350
Valves and equipment	8,510	0.057	8,510	0.045
Gratings	18,330	0.124	54,990	0.290
Ductwork	9,850	0.067	9,850	0.052
Miscellaneous	6,500	0.044	6,500	0.034
Total	148,100	1.000	189,500	1.000

Table 3-2. Summary of CEESI facility scaling to Mark I drywell.

Parameter	**Parameter value**		**Scale**
	BWR Mark I	**CEESI**	
Nominal MSL break size	22 inch	4 inch	5.5 to 1
Lower grating cross-sectional area	2,000 ft^2	70 ft^2	29 to 1
Predicted bulk flow velocity at grating	<50 ft/sec	<50 ft/sec	1 to 1
Containment volume upstream of final grating	130,000 ft^3	4,200 ft^3	30 to 1
Containment volume upstream of downcomers	170,000 ft^3	7,700 ft^3	22 to 1
Post-blowdown atmosphere turnover time	4 seconds	2 seconds	2 to 1
Surface-to-volume ratios* Pipes and I-beams Gratings Walls and miscellaneous	 0.45 0.12 0.43	 0.47 0.13 0.40	 1 to 1 1 to 1 1 to 1
*Over a 10-ft long section			

the CEESI experiments is horizontal. This deviation raised the following concerns:

1. As debris transports from the target to the structures, it may separate from the flow and stratify towards the lower regions of the test section. Such stratification would skew the final results. Theoretically it is known to occur if the gravitational settling velocity of the debris class is equal to or higher than the bulk flow velocity and the flow turbulent velocity. For the present conditions of interest, the gravitational settling velocity for the debris was measured to range between 0.75 - 5 ft/s (small to large) while the bulk flow velocity is in excess of 45 ft/s and estimated turbulence velocity is in excess of 7 ft/s. Corresponding to such conditions, gravitational settling is expected to be minimal. An experiment was conducted at ARL to confirm these calculations, where debris varying in size from small to medium was injected into the flow and was captured down stream using a mesh screen. At a bulk velocity of 30 ft/s, debris were uniformly distributed across the flow cross-section, confirming that no stratification is expected for flow velocities larger than 30 ft/s.

2. Inertial impaction potential may vary as a result of gravity vector orientation. Typically this effect is evaluated by the ratio of Stokes number to Froude number (which translates into a ratio of gravitational settling velocity to flow velocity). If the ratio is much smaller than unity, the flow is commonly believed to be dominated by inertial forces and its direction on particle deposition is negligible. For the present experiment, this ratio varies between 0.03 and 0.15 depending on the debris size.

Based on these analyses it was concluded that this noted deviation has negligible effect on the measured capture cross-sections.

3.5 Developmental Tests

Seven developmental tests were conducted to determine adequacy of the experimental design to achieve the test objectives and to develop optimal test procedures to get the most out of the production tests to follow. The bulk flow velocities entering the structural test section were measured and compared with velocity predicted by design analyses.

Experience was gained in prewetting structural surfaces prior to initiating the test and in collecting and classifying debris. Debris generation and transport within the CEESI facility were examined.

3.5.1 Test Matrix for the Developmental Tests

The test parameters varied included the nozzle diameter, the jet duration length, the distance between the jet nozzle and the target insulation blanket, the blanket manufacture, the method of restraining the blankets, and the method of wetting the structures. The test conditions for each of the seven developmental tests are shown in Table 3-3.

The first three tests focused on mapping test chamber flow velocities and the last four tests focused on characterizing the debris generation and transport. Target insulation blankets were not installed on instrumentation tests I-1, and I-2 so that debris would not interfere with the instrumentation (the target pipe mount was however in place in front of the jet to disperse the jet flow). Because the flow velocities were reasonably well mapped during the first two tests, the decision was made during testing to install a target insulation blanket on the third instrumentation test.

All developmental tests used the nominal 4 inch nozzle except Test W-1 which used the nominal 3 inch nozzle (actual diameters were slightly smaller than nominal diameters). The focus was on the 4-inch nozzle because this nozzle provided higher test chamber bulk flow velocities (more prototypical) than the 3 inch nozzle. Data collected during the production tests using the 3 inch nozzle provided debris transport data at an alternative bulk flow velocity. The jet duration time, i.e., the length of time air was supplied to the nozzle, of 5 seconds was adequate for the instrumentation tests but was found inadequate for complete debris transport.

The distance between the jet nozzle and the insulation blanket was varied because it affected the level of destruction of the blanket and consequently the quantity of debris generated. The distances shown in Table 3-3 were measured from the nozzle to the front face of the blanket. This distance is also expressed in the multiple of the nominal jet diameter, i.e., L/D, to accommodate debris destruction models based on this ratio.

Table 3-3. Test Matrix for the developmental tests.

Test		Nozzle diameter	Air Jet duration	Target position		Blanket description			Structure wetness
No.	ID	(inch)	(second)	Distance (inch)	L/D	Make	Length (ft)	Restraints	
Instrumentation tests									
1	I-1	4	5	56	14	None	N/A	N/A	Dry
2	I-2	4	5	40	10	None	N/A	N/A	Dry
3	I-3	4	5	40	10	Transco	3	None	Partial
Debris characterization tests									
4	W-1	3	5	36	12	Transco	3	SS Bands (3)	Wet
5	W-2	4	12	48	12	PCI	1.5	SS Bands (2)	Wet
6	W-3	4	12	48	12	Transco	3	SS Bands (3)	Wet
7	W-4	4	12	100	25	Transco	3	SS Bands (3)	Partial

The insulation blankets used were manufactured by was provided by Performance Contracting, Inc. (PCI). The Transco blankets were 3 ft in length compared to 1.5 ft for the PCI blanket. Stainless steel bands (either 2 or 3) were placed around the blanket to hold the blanket in place but the blankets were not encapsulated by a metal jacket.

Surfaces in the structural test section were wetted for the debris characterization tests because surface wetness is both prototypical and has been shown to strongly influence debris capture. In Tests W-1, W-2, and W-3, the structures were sprayed using the installed misting system prior the initiating each test. In Tests I-3 and W-4, the misting system was not activated but the surfaces were prewet with a water hose prior to the test. The hosing method of wetting surfaces was found to leave the surface only partially wet because the water tended to drain off of the surfaces before the tests could be conducted.

3.5.2 Flow Velocity Mapping

The development tests were instrumented with Pitot tubes connected to transducers to monitor and map flow distributions before the flow entered the congested test section. The locations of the Pitot tubes were shown in Figure 3-5.

3.5.2.1 Nozzle Discharge

The air discharge was monitored and recorded, as discussed in Section 3.3, by pressure sensors equipped with transducers in the jet air jet supply. One sensor was located in the air supply tank and the second sensor was located upstream of the nozzle. A typical nozzle pressure history is shown in Figure 3-8.

The jet duration time specified for each test was approximated with a countdown by the facility operators at CEESI and the actual jet duration time verified for each test from the recorded pressure once the supply valve was closed. The actual jet duration time shown in Figure 3-8 was about 12.5 seconds where the test specification called for 12 seconds but the jet air flow continued until about 14 seconds.

3.5.2.2 Pitot Tube Performance

The Pitot tubes/transducers used were not designed to measure initial shock flow but quasi-steady flow following the flow shock that follows the rupture of the rupture disk. The response time of the Pitot tube/transducers to changes in flow velocity was about 0.05 to 0.1 seconds. The response time for the data acquisition system was.

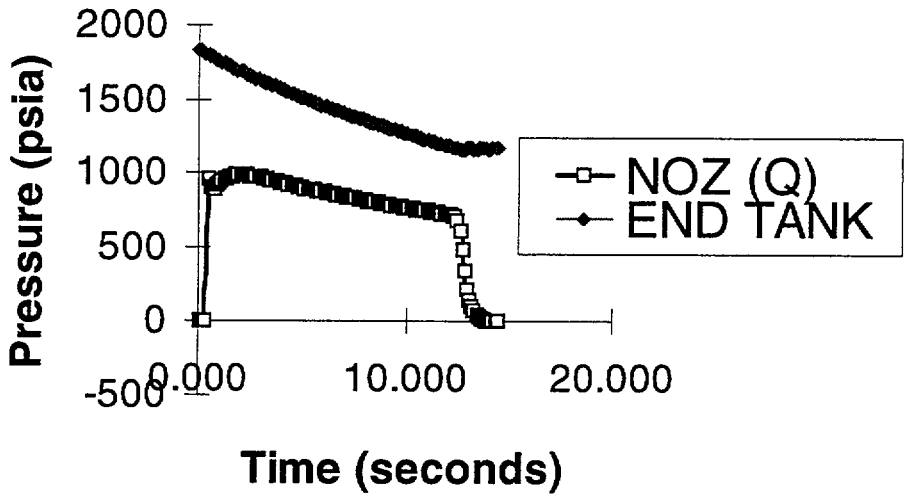

Figure 3-8. Typical nozzle pressure history.

0.05 seconds. The Pitot tubes were not protected from the impact of insulation debris, and were therefore susceptible to plugging

The data acquisition had a total of 16 channels available for data collection and each Pitot tube required two channels, therefore Pitot tubes were mounted in eight locations designated as P1, P2, P3, P4, P5, P6, P7, and P8, as shown in Figure 3-5. No data , however, is available for Pitot tube P3. The measurement ranges for the Pitot tubes are listed in Table 3-4.

Processing the Pitot tube data was accomplished by smoothing the fluctuations with a moving average technique, as illustrated by the typical Pitot tube response shown in Figure 3-9 for Pitot tube P6 during Test I-2. The moving average technique simply projected the next value based on the average of the preceding 25 values. A singular value representing a characteristic velocity was then estimated for each valid Pitot tube response.

Many of the Pitot tube responses were invalidated either due to the response being out-of-range for that instrument or due to an erratic response. Each Pitot tube response was reviewed to ensure that the response was within the measurement range of the instrument. Figure 3-10 shows that the response of Pitot tube P1 during Test I-1 ranged between 5 and 15 ft/sec whereas the instrument range was 67 to 133 ft/sec, therefore, this data was out-of-range and not considered valid (this Pitot tube was subsequently replaced with a lower ranged tube). Other Pitot tubes responses were invalidated when their responses became erratic due to obstructions of insulation debris or to water intrusion into its transducer, such as, the response shown in Figure 3-11.

3.5.2.3 Characteristic Bulk Flow Velocities

The bulk flow velocities measured for the 4 inch jet nozzle ranged from about 35 to 60 ft/sec. Only two valid velocity measurements were obtained for the nominal 3 inch nozzle (Test W-1) and these velocities were 28 and 30 ft/sec. The measured flow velocities are tabulated in Table 3-5. The transducers for Pitot tubes P4, P5, and P8 performed poorly following the first test, Test I-1, most likely due to water intrusion into the transducer.

As shown in Figure 3-12, the measured bulk flow velocities compared favorable with the velocities predicted from the one-dimensional jet expansion calculations that were modeled assuming isentropic flow through a nozzle. The predicted flow velocities were about 30 and 45 ft/sec for the 3 and 4 inch nozzles, respectively.

Table 3-4. Pitot tubes/transducer ranges of performance.

Pitot tube location	Transducer rating (In-H2O)	Minimum flow velocity (ft/sec)	Maximum flow velocity (ft/sec)
P1*	0 to 5.0 0 to 2.5	67 47	133 105
P2	0 to 2.5	47	105
P4	0 to 1.0	30	67
P5	0 to 1.0	30	67
P6	0 to 1.0	30	67
P7	0 to 1.0	30	67
P8	0 to 2.5	47	105

Tube ranging to 5.0 in-H_2O was replaced with lower range tube after Test I-1. The upper range after Test I-1 was 2.5-H_2O.

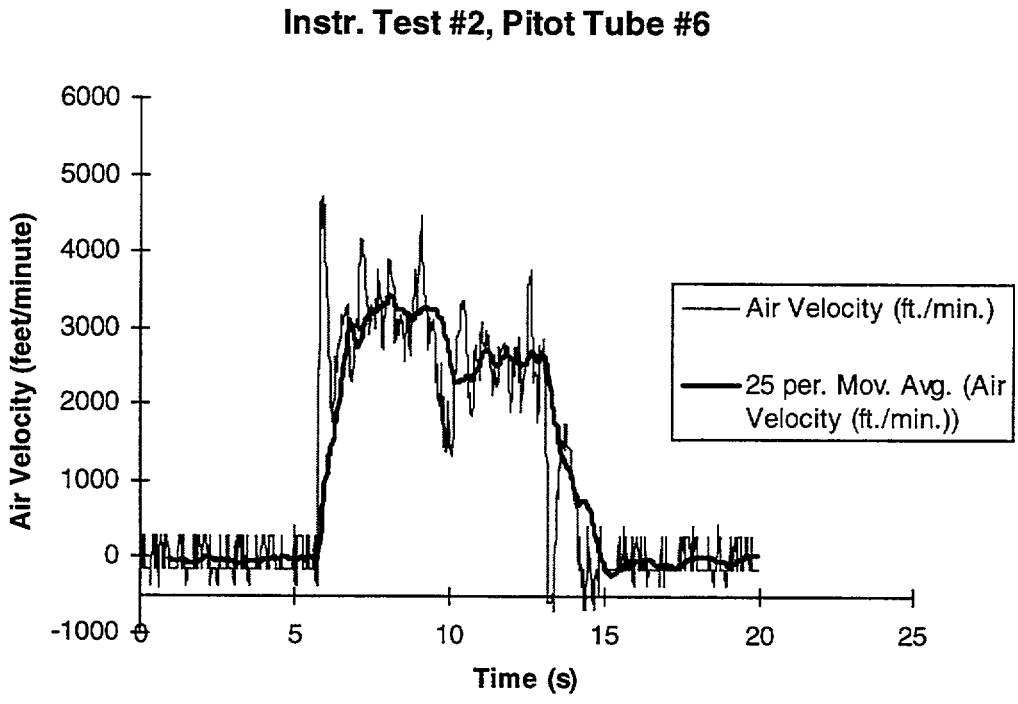

Figure 3-9. Typical pitot tube response.

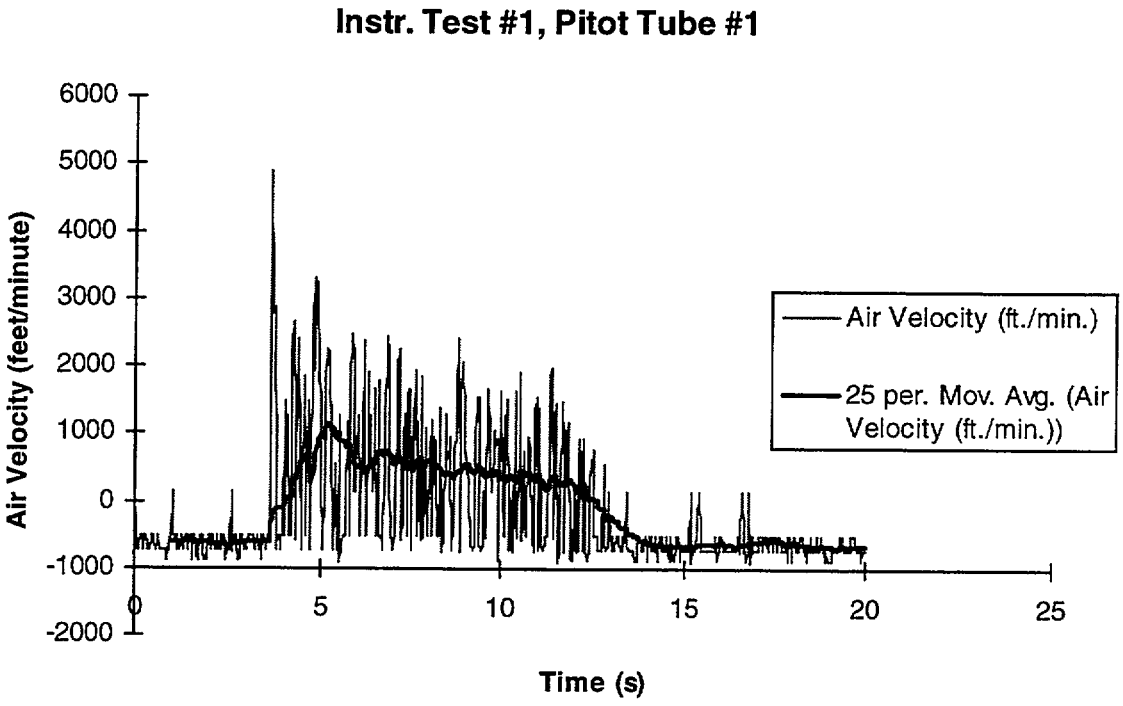

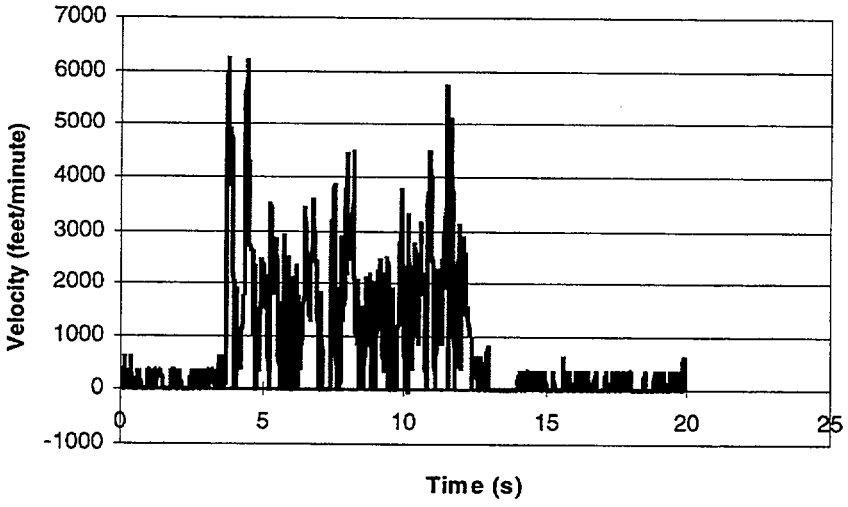

Figure 3-10. Out-of-range pitot tube response.

Figure 3-11. Plugged pitot tube response..

Table 3-5: Measured characteristic bulk flow velocities.

Test ID	Flow velocity at pitot tube location Pn						
	P1 (ft/sec)	P2 (ft/sec)	P4 (ft/sec)	P5 (ft/sec)	P6 (ft/sec)	P7 (ft/sec)	P8 (ft/sec)
I-1	Invalid	37	45	52	47	42	57
I-2	38	43	Invalid	Invalid	45	40	Invalid
I-3	37	0	Invalid	Invalid	42	40	Invalid
W-1	Invalid	Invalid	Invalid	Invalid	28	30	Invalid
W-2	37	42	Invalid	Invalid	Invalid	Invalid	Invalid
W-3	37	41	Invalid	Invalid	42	40	Invalid
W-4	Invalid	Invalid	Invalid	Invalid	Invalid	Invalid	Invalid

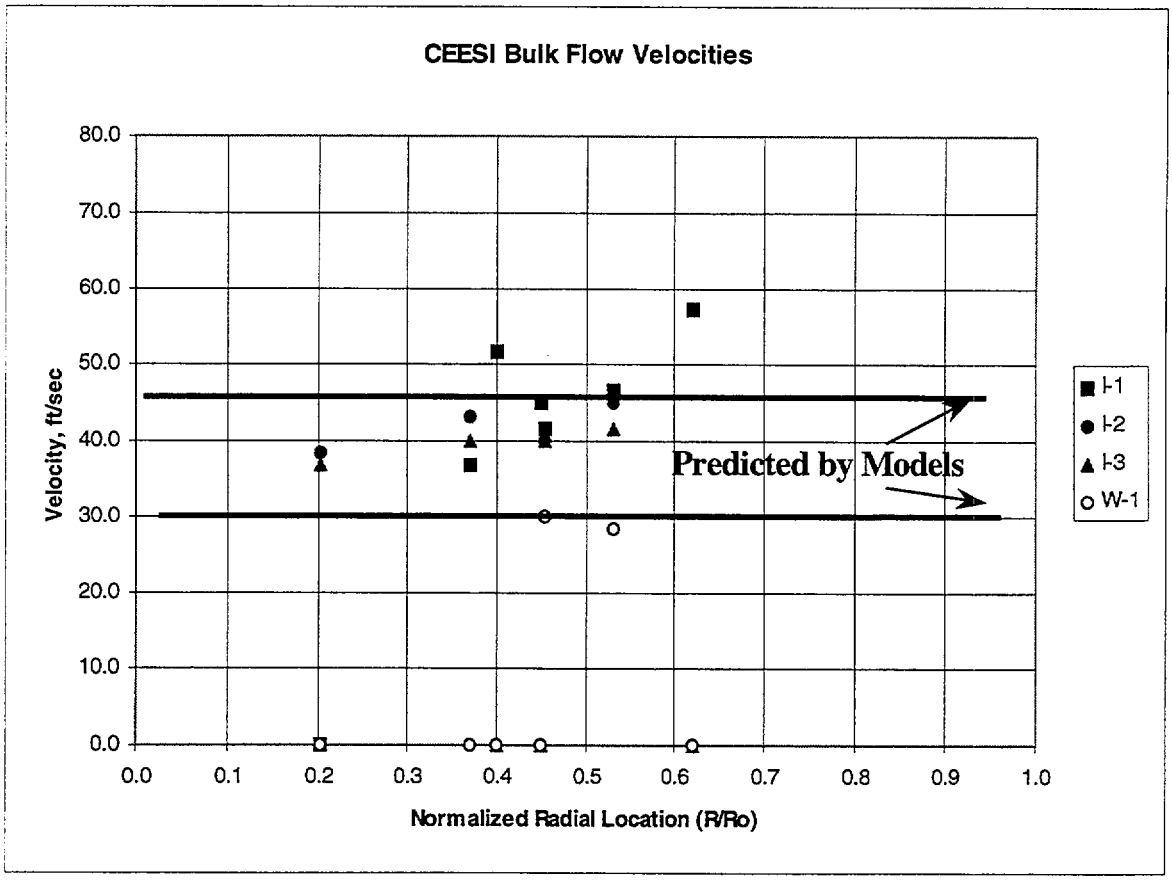

Figure 3-12. Comparison of measured and predicted bulk flow velocities.

3.5.2.4 Adequacy of Flow Fields Relative to Debris Transport Objectives

The jet nozzles (i.e., 3 and 4 inch nominal diameters) selected for these tests appeared adequate to complete the objectives of these tests but the faster flows of the 4-inch nozzle was deem more appropriate. Therefore, most of the production tests employed the 4-inch nozzle.

Flow velocity measurements illustrated that the focused jet flow was sufficiently dispersed or disrupted by the target mount to achieve a reasonably uniform flow through the structural test section. A review of the video cameras footage showed extremely turbulent mixing of debris in the target region of the test chamber. Still photos of the structures showing the captured debris further support a relatively uniform mixing of the debris.

A small portion of the air flow, less than 5% of the total flow, exited the test chamber through a small screened opening behind the jet. This reverse air flow and its associated debris transported were factored into the debris transport analyses.

3.5.3 Initial Debris Generation and Transport Characteristics

3.5.3.1 Debris Generation

Four developmental tests were conducted using Transco blankets consisted of fiberglass insulation encased in a tough canvas bag designed to wrap around the pipe. Each Transco blanket was 3 ft long and approximately 3 inches thick. The blankets were held in place by canvas straps and on most tests were further supported by stainless steel bands. The blanket was arranged so that seams did not face directly into the air jet. One test, Test W-2 was conducted with a 1.5 ft long PCI blanket but only an insignificant amount of debris was generated because the short blanket was ripped from the pipe mount relatively intact. In the other tests, the blankets remained more than 50% intact indicating the need for a modification to the blanket mount to enhance debris generation in the production tests to meet the test objective of predicting debris capture under relatively high loading conditions.

Four of the seven developmental tests provided useful debris transport and capture data and those results are presented in Section 3.7.

3.5.3.2 Jet Duration

Minimizing air usage was critical to keeping tests costs within budget, but to obtain valid debris transport results, the air jet must flow long enough for the debris generation process to complete and the resulting debris to either deposit on a structure or pass through the test chamber. Determining the time required to flush the system was one objective of the developmental tests. Post test observations of debris deposits, Tests I-3 and W-1, where the jet duration time was only 5 seconds indicated that 5 seconds was not enough time for complete debris transport. The other tests that used 12 seconds of air appeared adequate. It was determined that the production tests would use at least 10 seconds for 4 inch nozzle tests and 12 seconds for 3 inch nozzle tests. Note that the flushing time for a 3 inch nozzle test was longer than for a 4 inch nozzle test because the flows were slower. This issue was further evaluated in the production tests.

3.5.3.3 Surface Wetting

Two methods for prewetting the surfaces of the test structures prior to the activating the air jet and subsequently destroying the blanket were tested. One method was to simply spray the structures with a water hose until the surfaces were thoroughly wet and the other was to spray the surfaces using the PCV pipe misters installed inside the test chamber. The hosing method was found inadequate because the water tended to drain from the surfaces before the test could be conducted whereas the misting system was operated until the test was completed. The misting system was operated long (approximately 10 minutes) enough to form a draining water layer. Draining water formed small pools on the chamber floor prior to flowing out through small drain holes. Structure wetness was verified by the test operators upon reentry into the chamber following the test.

3.5.4 Facility Modification and Test Procedure Development

Assessing the data from the developmental tests indicated a need for some addition but relatively minor modifications to the CEESI facility. The following modifications were made prior to performing the production tests:

1. The special end supports were installed on the target mount pipe to prevent the blanket from moving axially along the pipe and out of the path of the jet flow. Holding the insulation target in place longer enhanced the destruction of the blanket, thereby increasing the mass of debris available for transport through the structural test section.
2. The spray misting system was enhanced to more uniformly wet the structures in the structural test section.
3. To accommodate the extreme winter conditions at the facility, heaters were purchased to heat the test chamber interior to a temperature >70 F to prevent the extreme exterior cold from affecting test results,
4. A second and a third video camera were installed to film debris transport at two alternate locations.

Experience gained with these tests was applied to developing the operating procedures for the production tests.

3.6. Production Tests

Ten production tests were conducted to produce data for the calculation of insulation debris transport and capture fractions. This section describes the tests conducted, test procedures, data collection procedures, photographic results, and the subsequent drying and weighting procedures. The data reduction and tests results are discussed in Section 3.7.

3.6.1 Test Matrix for the Production Tests

The test parameters varied included the nozzle diameter, the jet duration length, whether or not the surfaces were wet, and the distance between the jet nozzle. The test conditions for each of the ten production tests are shown in Table 3-6.

These tests focused on the 4 inch nominal jet nozzle because of the faster bulk flow velocities resulting from the larger nozzle. Two tests, L1 and L2, were conducted .with the 3 inch nozzle to test for differences in debris capture characteristics associated with the slower flow velocities.

The tests specifications called for an air blast duration time of 10 seconds for the 4 inch nozzle tests, except for Test H2 which was specified as 15 seconds, and 12 duration times listed in Table 3-6, however tended to be seconds for the 3 inch nozzle tests. The actual recorded somewhat longer the test specifications. Based on post-test observations, the air jet duration times were in all tests deemed long enough to flush the airborne debris from the test chambers.

The structures in the structural test section were wet by the spray misting system in all tests, except Test H7 which was conducted dry. Test H7 was conducted dry to illustrate the pronounced influence that surface moisture had on debris capture.

The distance of the target from the jet (i.e., the distance from the nozzle to the front face of the blanket) was varied to ensure at least one test with maximum possible debris generation and to vary the density of debris passing through the structural test section. Tests conducted with an L/D in the neighborhood of 30 were found to completely or nearly completely totally destroy the blanket restrained as it was in these tests.

Test H1R was designed to repeat test H1 as closely as possible to show test repeatability. As it turned out, Tests H1, H1R, H2, and H3 were all close enough in test conditions to demonstrate repeatability (shown in Section 3-7).

3.6.2 Description of Target Insulation Blankets

All of the target insulation blankets used in the production tests were manufactured by Transco specifically for these tests. Transco blankets consisted of fiberglass insulation encased in a tough canvas bag designed to wrap around a pipe. Each Transco blanket was 3 ft long and approximately 3 inches thick. The blankets were held in place by canvas straps. The blankets were further supported by 3 stainless steel bands and 2 end supports to prevent axial movement along the pipe mount. The Transco blankets each had 2 seams, i.e., each blanket was formed from 2 half sections, which were arranged so that the seams were at the top and at the bottom and did not directly face the nozzle. The target blanket for Test H1R as mounted for testing is shown in Figure 3-13.

3.6.3 Testing Procedures

The following test procedure was followed as closely as practical for all of the production tests.

Table 3-6. Test matrix for the production tests.

Test		Nozzle diameter	Air jet duration	Structure wetness	Target position	
No.	ID				Distance	L/D
		(inch)	(second)		(inch)	
1	H1	4	13	Wet	120	30
2	H1R	4	13	Wet	120	30
3	H2	4	15	Wet	120	30
4	H3	4	14	Wet	80	20
5	H4	4	13	Wet	160	40
6	H5	4	14	Wet	200	50
7	H6	4	14	Wet	40	10
8	H7	4	16	Wet	120	30
9	L1	3	17	Wet	80	27
10	L2	3	24	Wet	84	28

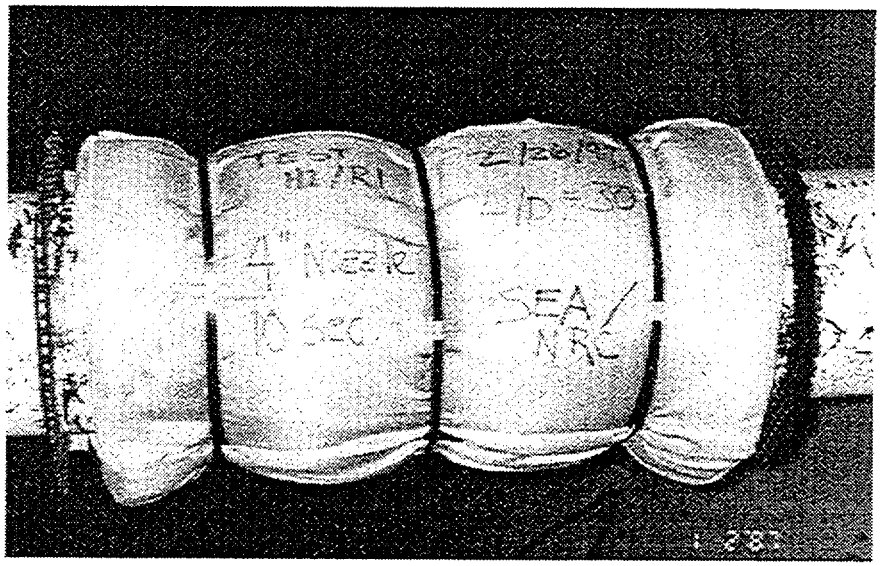

Figure 3-13. Target blanket installation.

1. Record test parameters.
2. Clean test chamber of debris and unneeded equipment.
3. Warm test chamber using propane heaters as needed.
4. Weigh and mount insulation blanket on target mount.
5. Record test chamber interior temperature.
6. Setup and activate all three video cameras and check lighting.
7. Clear chambers of personnel and secure screen door.
8. Open wooden cover plate on the blocked-off diffuser end of the main test chamber.
9. Turn on misters and spray structures for approximately 10 minutes.
10. Open the air supply and pressurize air jet rupture disk.
11. Turn off air supply to jet nozzle after specified air jet duration.
12. Turn off misters immediately afterwards to avoid washing captured debris off of the structures.
13. Close the cover to the diffuser section.
14. Wait 2 minutes before entering test chambers.
15. T urn off video cameras.
16. Take still pictures of test chamber interior showing blanket destruction and debris capture.
17. Collect debris per debris collection procedures.
18. Record observations and deviations from standard test procedures.
19. Obtain test pressure history from CEESI data acquisition system.

3.6.4 Data Collection Procedures

Debris transport data consisted of collecting as much of the insulation debris as reasonably practical and photographing the interior structures and spaces. A portion of the debris in each test was not recovered, referred to herein as non-recoverable debris (NR). The majority of the NR debris included fine debris blown out of the test chambers through the exhaust screens and fine debris deposited on walls and structures that was simply too small to collect from a practical consideration.

3.6.4.1 Debris Collection Locations

Determining debris transport and capture fractions required knowing where the debris resided immediately following completion of the test, therefore debris was collected from discrete sections of the test chambers or from specific structures. Twelve specific locations were predetermined to accomplish this task. Debris collected at these locations was bagged separately by its location and by its classification that is described in the next section. The 12 locations were:

1. On the screen door at the far end of the auxiliary test chamber where the exhaust air exited from the chamber.
2. The remainder of the auxiliary chamber.
3. The section of the main chamber between the split grating and the collar joining the main and auxiliary chambers.
4. On the split gratings.
5. On the V-grating.
6. The section of the main chamber between the continuous grating (first grating) and the split
7. The structural components of the structural test assembly.
8. The continuous grating.
9. The main chamber between the target mount and the continuous grating.
10. The main chamber behind the target mount including the inside surface of the panel blocking flow through the diffuser section.
11. The target mount itself.
12. Behind the panel blocking the diffuser section including a small amount sometimes found on the concrete pad outside of the test chamber.

3.6.4.2 Debris Classifications

Insulation debris consisted of pieces of bare fiberglass insulation of various sizes, pieces of shredded canvas, agglomerated pieces containing both insulation and canvas, and large sections of the canvas cover that remained relatively intact and sometimes contained substantial quantities of insulation. The bare insulation pieces were divided into 3 general size groups, i.e., large, medium, and small. Their characteristics are provided in Table 3-7. It was reasonably assumed that all of the NR debris was small debris since virtually all the large and medium debris was collectable.

In the collection process, debris was bagged by seven classifications at each location. These seven classifications were:

A. Canvassed insulation consisting of large sections of canvas covers encapsulating insulation (protected insulation).
B. Insulation attached to Class A debris but extruding from the canvas (unprotected insulation).
C. Large pieces of exposed insulation.
D. Medium pieces of exposed insulation.

Table 3-7. Insulation debris sizes.

Debris classification	Relative size	Description
Large	> hand size	Large pieces were too large to pass through a grating and therefore were all located either upstream of the continuous grating or behind the target mount.
Medium	> grating cell but < hand size	Medium pieces sometimes were forced through a grating, although they were generally larger than a grating cell.
Small	< grating cell	Small pieces would generally pass through a grating cell unless the piece was to inertially impact on a grating bar. Small debris included fine particles such as individual fibers that could also pass through the catch screen of the exhaust flow.

E. Small pieces of exposed insulation.
F. Pieces of shredded canvas without insulation.
G. Agglomerated debris consisting of a tangled mix of canvas and insulation.

The target blankets during the production tests were generally completely or nearly completely destroyed by the air blast and the destruction was similar from one test to another. Usually one relatively large section of canvas was found on the floor near the target or hanging on the continuous grating and this section of canvas sometimes contained substantial insulation, up to 45% (Test H5) of the total. Other times this canvas section was empty. Insulation found inside of the canvas would be trapped by any grating and would then be expected to be protected from subsequent erosion by washdown flows in a BWR drywell. This insulation was classified as Class A upon collection. However, any insulation attached to this large section of canvas but hanging out of the canvas would not be protected from washdown erosion but would still be trapped by any grating. This insulation was collected separately and classified as Class B but as it turned out, there was very little Class B debris (< 3%).

All debris transporting to the far end of the test chamber, i.e., exhaust screen, was small debris. The large pieces were stopped by the continuous (first) grating encountered. The medium sized debris making it through the continuous grating was usually stopped by the next grating encountered but none of the medium was found at the exhaust screen. Only a relatively small quantities of medium debris were generated and the quantities were not sufficient to evaluate debris capture fractions.

The debris collection process was rather thorough in order to anticipate any type of debris generated and its subsequent transport. However as it turned out, the debris transport in the CEESI tests was focused almost entirely upon the transport of small pieces of debris.

Several photographs were taken of debris samples during the process of drying and weighing the collected debris. A typical piece of small debris might measure 3 inch in length and 1 inch in diameter and its density likely significantly reduced from its originally density. A sample of small debris is shown in Figure 3-14.

Medium and large debris, as shown in Figure 3-15 and 3-16, respectively, generally had the appearance of intact insulation. The original insulation was formed in layers and these layers tended to separate during the destruction process. Large and medium debris tended to still show this layered structure.

Figure 3-17 shows a sample of the agglomerated debris. This sample consisted mostly of a wad of canvas strings with small bits of entangled insulation.

The large, medium, small, and agglomerate samples shown in Figure 3-14 through 3-17 are compared in Figure 3-18 so that their relative sizes can be put into prospective. The samples were, moving clockwise from the upper left corner, large, small, agglomerate, and medium.

To help visualize the destructive process of the air blast, a sampling of canvas shreds is shown in Figure 3-19. The metal piece in the photo was the blankets identification tag.

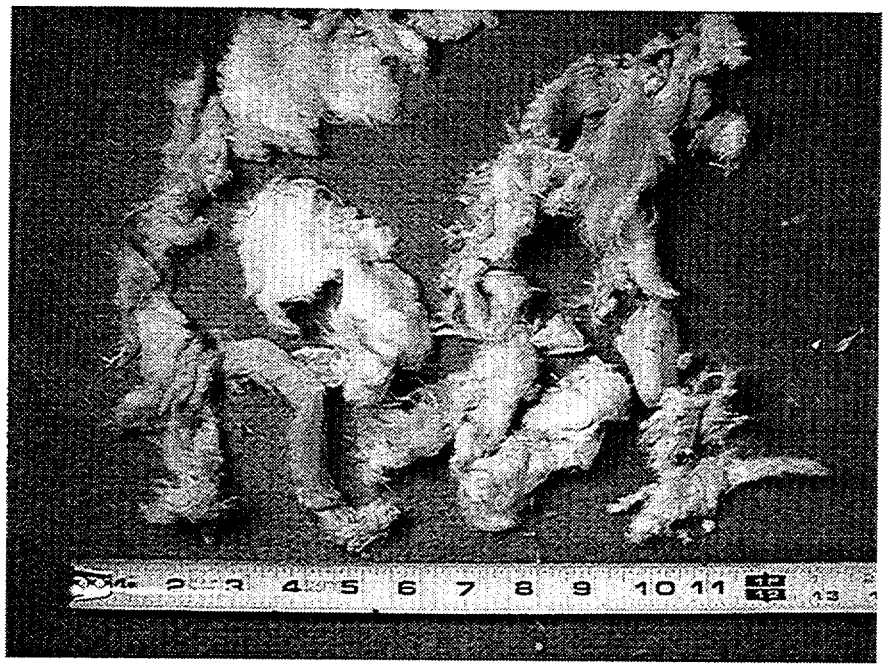

Figure 3-14. Sampling of small pieces of debris.

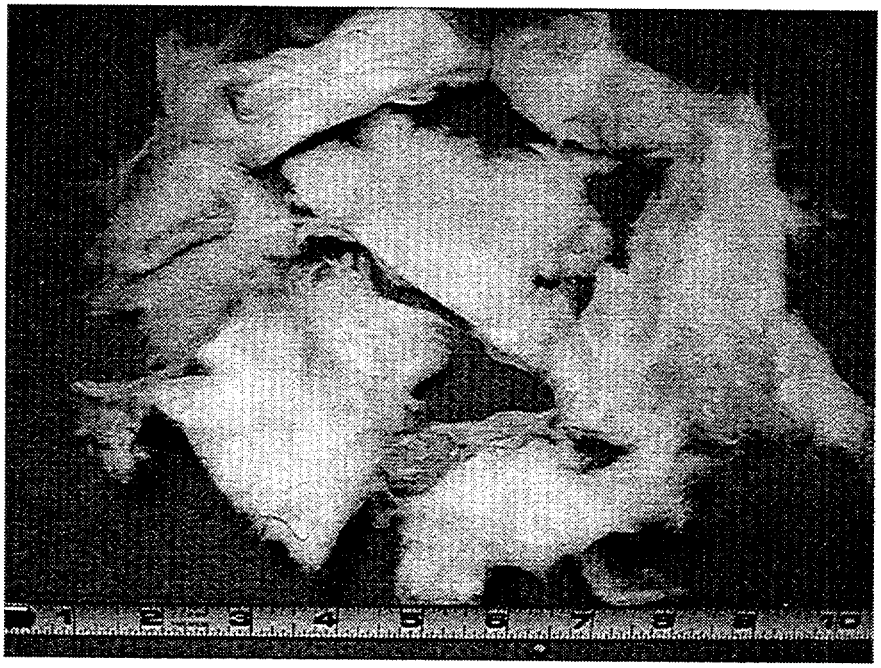

Figure 3-15. Sampling of medium pieces of debris.

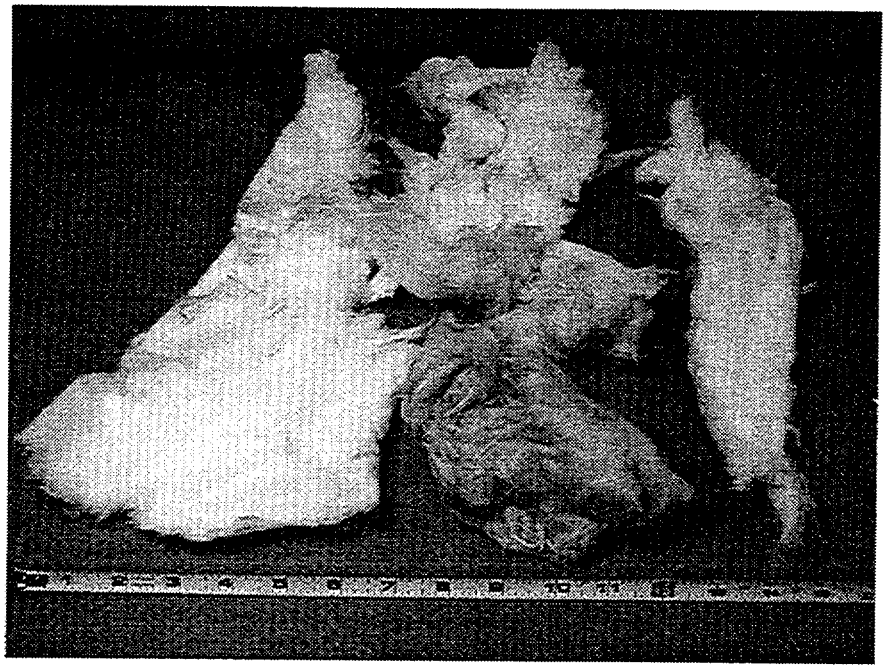

Figure 3-16. Sampling of large pieces of debris.

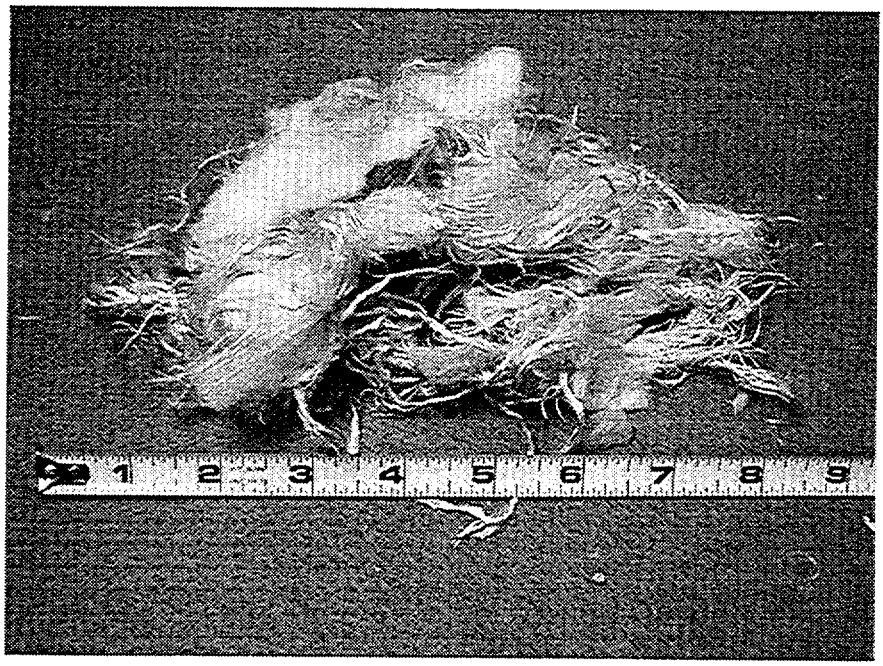

Figure 3-17. Sample of agglomerate debris.

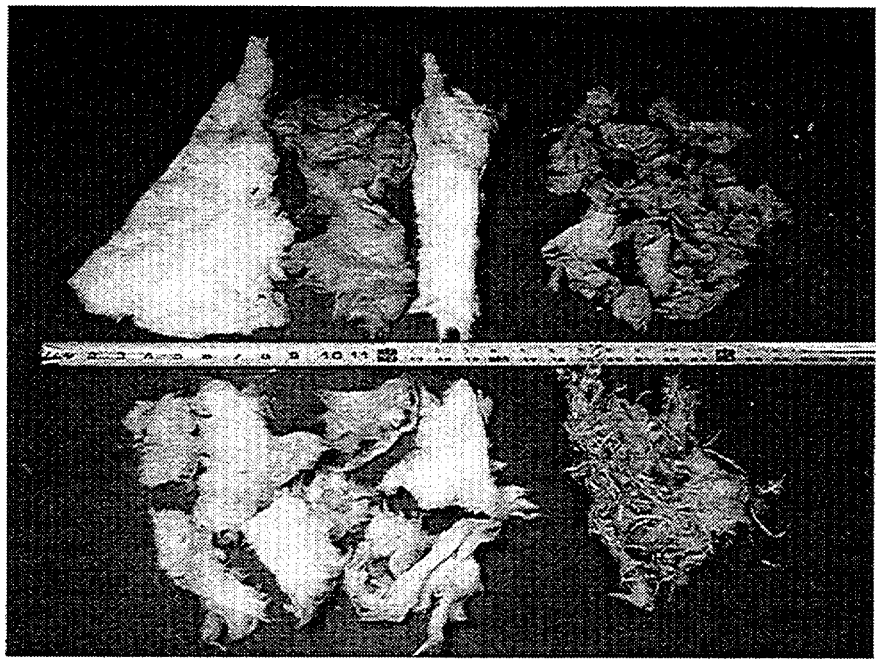

Figure 3-18. Comparison of debris samples.

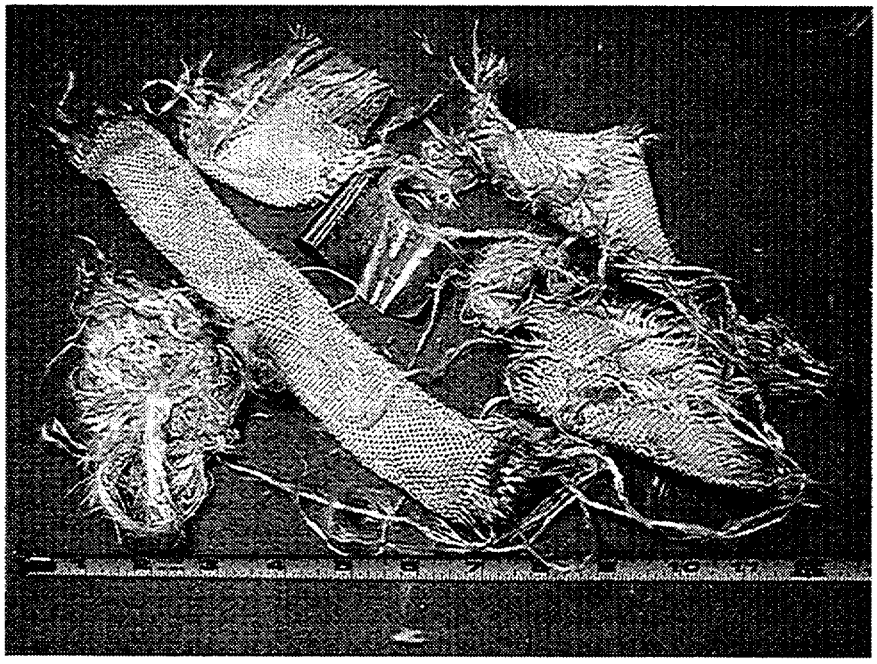

Figure 3-19. Sampling of shredded canvas debris.

3.6.4.3 Photographic Data

Upon reentering the test chamber following each test, the test engineer photographed features of the test for later analysis. These visual experimental results helped greatly in understanding and documenting the debris transport process. A sampling of the photos are presented here.

Figure 3-20 shows the front side of the continuous grating following Test H6. The target in Test H6 was placed relatively close to the nozzle (L/D of 10) and the large section of blanket shown hanging from the continuous grating held about 42% of the total insulation. Also seen in this figure is a section of the PCV misting system (upper left) and the two vertical pipes located directly behind the continuous grating.

The dominant debris deposition process was inertial deposition which is clearly shown in Figures 3-21 through 3-23. In Figure 3-21, which shows a portion of the split grating following Test H1R, fine debris is seen captured somewhat uniformly on the front surfaces of the bars. Figure 3-22 shows a larger portion of the split grating following Test H2. Larger pieces of small debris looking somewhat like "cotton balls" are shown. All of this debris was small enough to pass through the grating, which this size of debris did when it did not impact the bars. Note that there is no medium or large debris present in these pictures. Figure 3-23 shows similar deposition on the V-grating.

The deposition shown in the preceding three photos was deposition onto wet gratings. Test H7 was conducted dry to specifically illustrate the effect of wetness on debris capture. A portion of the split grating for Test H7 is shown in Figure 3-24. Only a few small "cotton ball sized" pieces were captured by the grating. Note the total lack of fines that were shown so clearly for deposition of a wet grating in the preceding photos.

Dry surface behavior was also evident in Figure 3-20 that showed the continuous grating following Test H6. As it turned out, the misting system did not wet the continuous grating as planned, most likely because a slight draft in the test chamber after the diffuser cover was opened caused the mist to drift downrange from the target. However, a side benefit of the drifting mist was the wetting of the auxiliary chamber wall where the flow makes its 90° bend.

A view within the auxiliary tank that includes the wall impacted by the bending flow is shown in Figure 3-25. As shown in the figure, substantial small debris was inertially captured at the bend. Nearly all of the debris collection in the auxiliary tank, except for the debris on the exhaust screen, was found at the bend.

Although surface wetness had a profound affect on the ability of a surface to capture debris, quantifying the wetness of the surfaces was not practical for these tests. The tests have clearly shown that wet surfaces tend to hold onto debris while dry surfaces do not. The tests also indicate that partial wetness, somewhere between wet and dry, will capture with an effectiveness somewhere between wet and dry capture effectiveness and this is demonstrated in results presented in Section 3-7. A brief attempt was made to photograph surface wetness to roughly quantify the wetness of these tests. The best of those photos is shown in Figure 3-26. The water film on a horizontal I-beam was compared to the thickness of a coin (quarter). This film appears to be about 0.5 mm (500 microns) thick. The film thickness on the vertical I-beam surfaces was obviously considerable thinner than on the horizontal surface. A general observation regarding surface wetness was that even a thin film, such as formed on the vertical surfaces of the grating bars, was sufficient to capture significant quantities of fine debris.

A view of the auxiliary tank exhaust screen from the inside following Test H1R is shown in Figure 3-27. The pattern of debris deposits on the screen from filtering the exhaust air flow shows the debris preferentially deposited on the outer portion of the screen probably was the result of the flow structure after the flow made the 90° bend. The video cameras indicated a spiral type of motion down the auxiliary tank.

A view of panel blocking of diffuser section behind nozzle following Test H7 is seen in Figure 3-28. The blocking panel was constructed of plywood with a narrow screen section in the middle. The photo shows some small debris that was filtered from air escaping the test chamber through the diffuser section. A small amount of air also escaped through the narrow gap between the panel and the test chamber walls resulting in a small quantity of debris behind the panel in some tests.

3.6.4.4 Video Cameras

Video footage was taken of each test by each of three video cameras. This footage was of limited value but some debris transport trends were observed. These trends are discussed here.

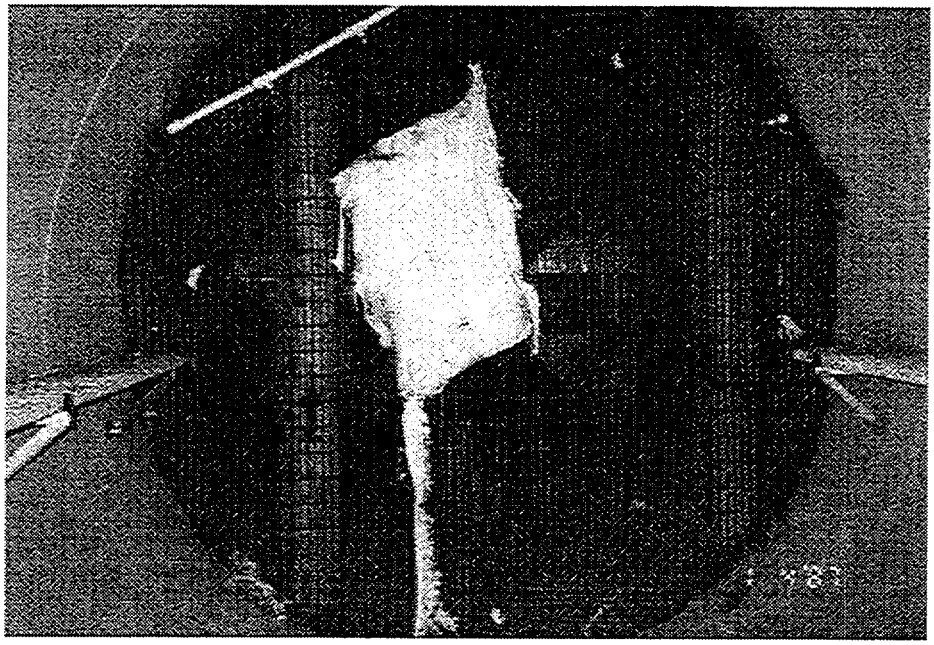

Figure 3-20. Large section of canvas on continuous grating (Test H6).

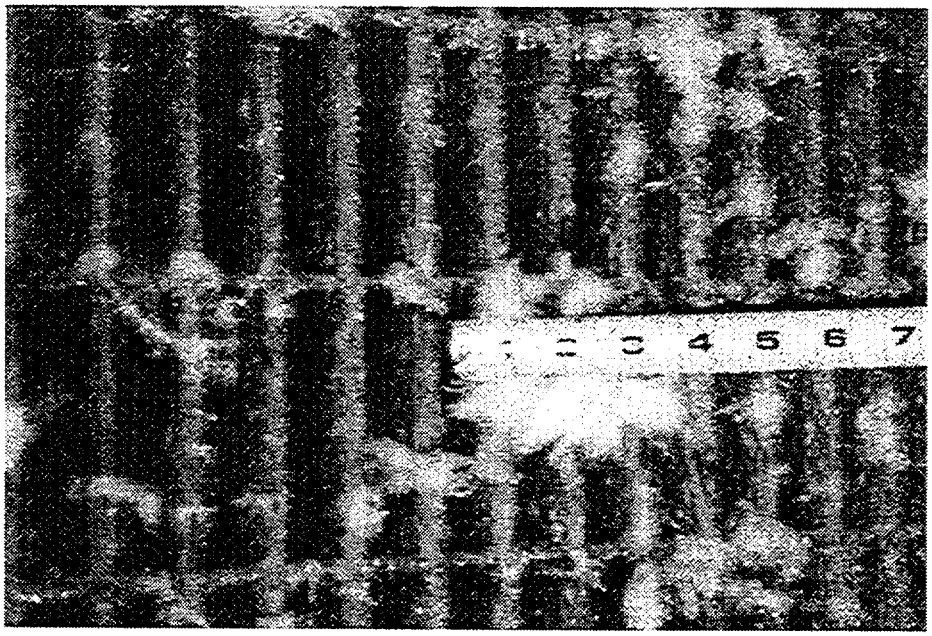

Figure 3-21. Typical debris deposition on split grating (Test H1R).

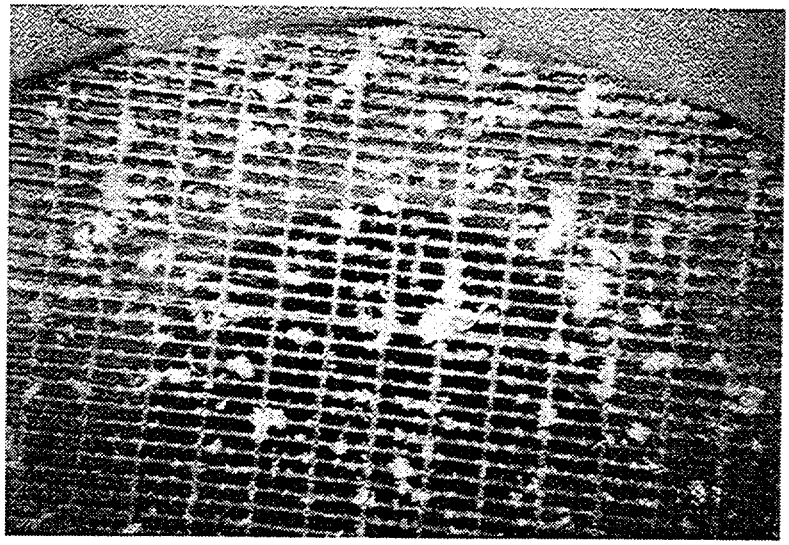

Figure 3-22. Typical debris deposition on split grating (Test H2).

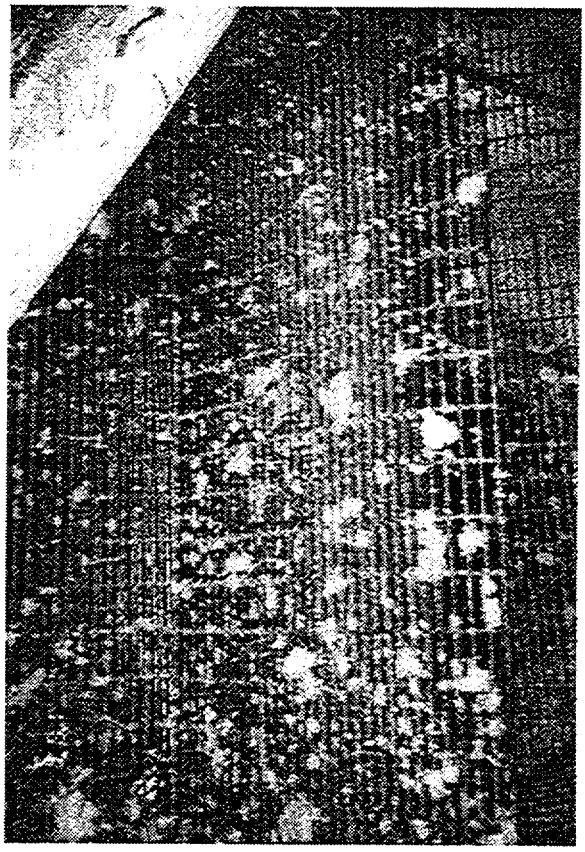

Figure 3-23. Typical debris deposition on V-grating (Test H2).

Figure 3-24. Debris deposition on a dry split grating (Test H7).

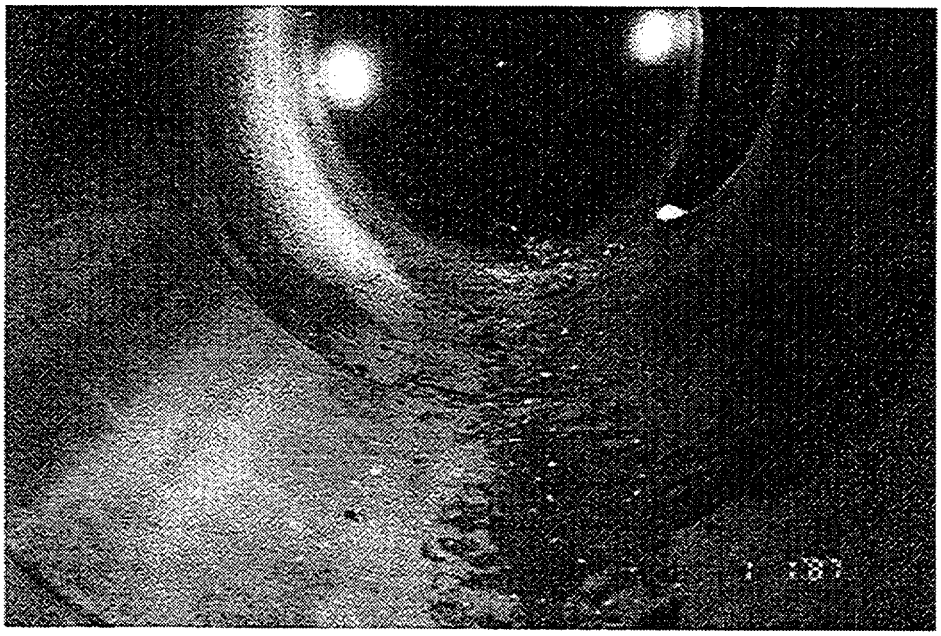

Figure 3-25. Deposition in auxiliary tank at bend (TestH2).

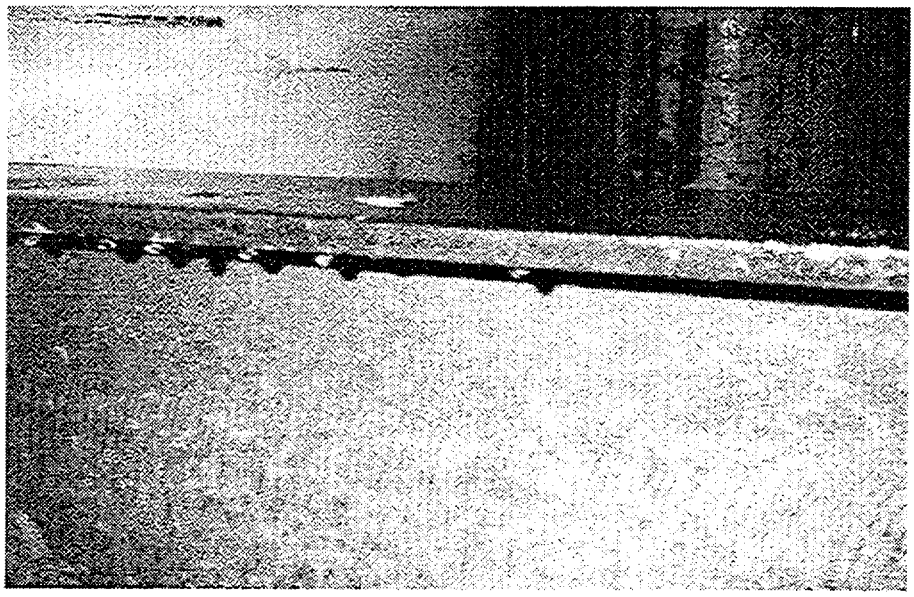

Figure 3-26. Water film on horizontal I-beam (Test H1).

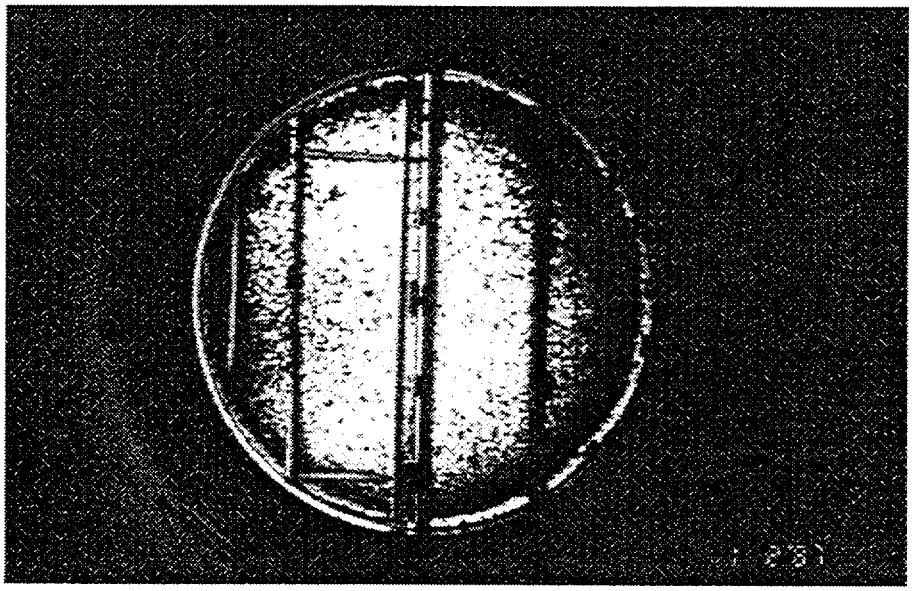

Figure 3-27. View of exhaust screen in auxiliary tank (Test H1R).

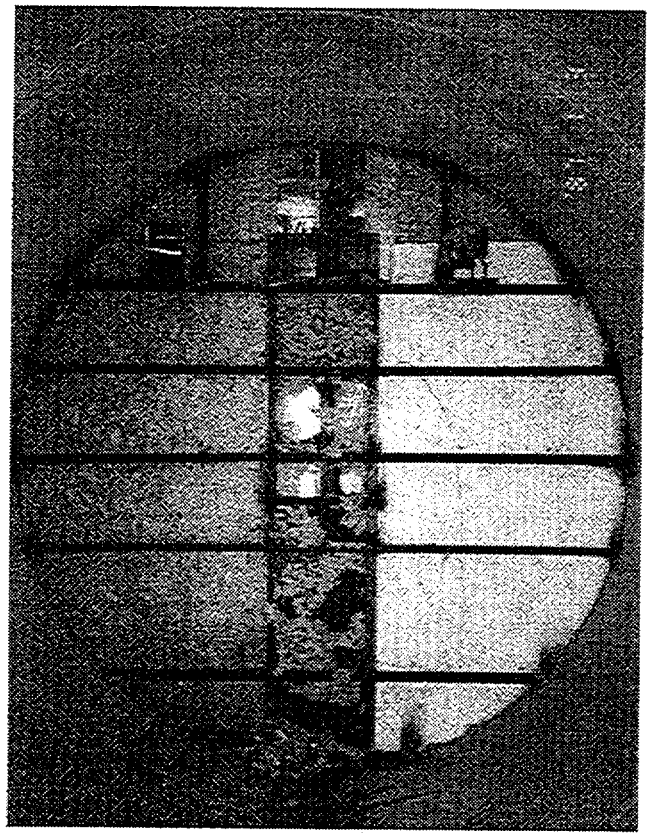

Figure 3-28. View of panel blocking of diffuser section behind nozzle (Test H7).

Video Camera 1 The first camera was mounted behind the jet nozzle facing downrange past the target to the structural test section. It was intended that this camera film the destruction off the target blanket but field of view so quickly filled with whirling debris that little could be seen. This camera observed very turbulent debris transport that showed some spiral flow behavior across its field of view.

Video Camera 2 The second camera was mounted at the far end of the main test chamber facing uprange toward the structural test section. This camera filmed small debris after the debris passed through the split grating on its way to the auxiliary tank. The debris looked similar to large snowflakes coming at the windshield of a moving car.

Video Camera 3 The third camera was mounted in the entrance end auxiliary test chamber facing the exhaust screen. This camera filmed the debris as it made the 90° bend turn upon entering the auxiliary tank. This debris was generally propelled towards the opposite auxiliary tank wall where the non-deposited debris tended to curl upwards in the beginning of a spiral flow pattern as the debris was then propelled towards the exhaust screen. Prior to the onset of the jet flow, the mist from the PCV spray system could be seen drifting into the auxiliary tank where it wetted the opposite wall where deposition was observed. Note that a spray system was not installed in the auxiliary chamber.

3.6.5 Drying and Weighing Debris

The insulation and canvas debris collected following each test and was placed in plastic bags and labeled with the test identification, collection location, and debris classification. The processing of all this debris starting with verifying that bags had been properly classified.

Most of the debris absorbed water from the surfaces or from the floors of the test chambers.

The moisture levels of the debris ranged from dry to extremely wet and the debris had to be dried before weighing. A variety of methods were tried including

wringing excess water from the debris, heating the debris in an oven, and simply spreading the debris out on tablesand allowing the moisture to evaporate. The oven worked best but it could only accommodate a small quantity of debris at a time. The best procedure seem to be to wring out the excess moisture, spread the debris and allow it dry in a heated room for a few days, and then finishing the process by placing debris that had not dried sufficiently in the oven. The debris was dried until any remaining moisture would not significantly impact the test results.

Prior to weighing the debris, the canvas was separated from the insulation. The canvas for each test was weighed collectively rather than by location. Each bag of insulation was weighed separately and recorded. As a quality assurance measure, the debris for the entire test (contained in one large trash bag) was weighed and recorded, plastic bags included. Then, the weights of the individual bags were summed along with a reasonable estimate for the plastic bags and then compared to the total weight. The weighing process continued until all mass was accounted within an error margin of less than 2%.

The test results now consisted of tables of debris masses arranged by collection location and debris classification. These tables were then used to calculate debris transport and capture fractions which is the subject of Section 3-7.

3.7 Debris Transport and Capture Test Results

Debris transport and capture in these tests conducted at CEESI focused on the small debris which consisted of debris generally smaller than the cell size of a grating (see Section 3.6.4.2 for debris size classifications). Relatively intact sections of blanket, large sections of canvas, and large pieces of insulation were always stopped by the first grating encountered. Although a substantial fraction of the medium debris, which was generally larger than a grating cell size, was forced through the first grating encountered and then stopped by a subsequent grating, there was not enough of the medium debris generated to justify calculating debris transport data. All debris found at the exhaust screen was small debris. Therefore, this section focused on small debris transport.

Small debris was found to readily transport at the CEESI test flow velocities which were designed to be prototypical of the bulk of the BWR drywell following a MSLB. Significant gravitational settling was not observed, i.e., flow turbulence kept debris churning until completion of the air blast, even in the more quiescent places such as end space in the auxiliary tank (opposite the exhaust end). The dominant debris capture mechanism was clearly inertial deposition which was strongly influenced by surface wetness.

Debris transport fractions and debris capture fractions were computed from the collected debris weight tables.

3.7.1 Definitions of Debris Transport and Capture Fractions

The transport fraction as applied to the CEESI tests defined the fraction of debris entering the congested structural test section that subsequently transported to the exhaust screen at the end of the auxiliary test chamber. Note the structural test section was design to simulate the structural congestion of a portion of a BWR drywell. The transport fractions presented herein were calculated using the following equations.

$$F_t = \frac{M_{screen} + M_{exhaust}}{M_{cont}} \qquad (3\text{-}1)$$

where

F_t
=
the transport fraction
M_{screen}
=
the mass deposited on the exhaust screen of the auxiliary tank
$M_{exhaust}$
=
the mass passing through the exhaust to the outside
M_{cont}
=
the mass approaching the continuous grating

$$F_c = \frac{M_{str}}{M_{str} + M_{bypass}} \qquad (3\text{-}2)$$

where

F_c = the capture fraction
M_{str} = the mass deposited on the structure
M_{bypass} = the mass passing by or through the structure.

Debris transport and capture fractions presented herein were plotted as a function of debris loading. Debris loading as used herein is defined as the total time-integrated one-dimensional mass flux of debris approaching a particular structure. This included both debris captured by that structure as well as debris bypassing that structure. The units used herein are lbm per 100 f^2 of test chamber cross sectional area.

3.7.2 Data Reduction Procedure

Starting with the tables of debris masses correlated by collection location and debris classification, the debris transport and capture fractions were calculated using the following data reduction procedure

- The initial mass of the canvas cover was estimated and subtracted from the initial weight of the blanket (blankets was weighed prior to testing) to obtain an estimate of the initial insulation mass.
- Total mass of non-recovered debris was calculated as the difference between initial insulation mass and the total mass of debris recovered.
- A best estimate distribution for the final location of the non-recovered mass was estimated (see next section).
- The estimate of non-recovered mass was added to the recovered mass to obtain a complete mass balance.
- The transport and capture fractions were calculated per the above equations.

The error analysis, discussed in Section 3.7.4, shows that the distribution of the non-recovered mass dominated the overall experimental error. The distribution of the non-recovered then became the corner stone of the error analysis.

The computations were programmed into an EXCEL spreadsheet to facilitate the data reduction procedure.

3.7.3 Estimate of Non-Recovered Mass Distribution

A distribution showing where the non-recovered debris mass was likely to have been was estimated based on the observations of the test engineer. These observations included:

- All non-recovered mass safely assumed to be small debris.
- Substantial debris was lost from test chambers
  - Substantial amount of fine debris seen passing through auxiliary tank exhaust screen (documented in video footage).
  - Substantial amount of fine debris seen passing through auxiliary tank exhaust screen (documented in video footage).
  - Small quantities of debris collected in diffuser section and behind blockage panel and some even collected on concrete pad outside diffuser nozzle entrance.
  - Test chambers had a number of small orifices such as the floor drain holes where some debris could have been lost.
  - In Test H7, a cover plate blocking a man hole on top of the auxiliary tank was blown off allowing considerable debris to be blown out.
- Substantial debris was deposited within the test chamber but was not collected, primarily because it was too small.

-
Post-test washdown of the test chambers showed accumulation of fines in the washdown flows.
-
Considerably more of the washdown fines were found in the main tank than in the auxiliary tank.
-
Washdown fines in the main tank were found predominantly near the structural assemblies.
-
Washdown fines in the auxiliary chamber were found predominantly near the exhaust screen.

These general observations were compiled using the logic chart shown in Figure 3-29 to form a plausible best estimate distribution of where the non-recovered mass resided. The first decision in the logic chart was the fraction of the non-recovered mass that was retained within the test chambers. Observation suggested that half or a little more than half remained in the chambers. The best estimate engineering judgment was that 60% remained within the chambers leaving 40% to be expelled.

Of the expelled debris, 20% was judged to leave through the blocked off diffuser section behind the nozzle. An estimate of flow resistances suggested that only about 5% of the air flow went in this direction but this air would

have had a higher density of debris since it was closer to the target. Therefore, 20% was deemed a reasonable estimate. The next logic question in the chart was how much of the non-recoverable mass was deposited in the main chamber. Observations suggested that the dominant amount was in the main chamber and the engineering judgment was 75% in the main chamber leaving 25% for the auxiliary tank.

Most of the debris mass in the washdown flow was found near the structural test section and likely consisted of fine debris actually captured by the structures but too fine to collect. Sixty percent of this debris was distributed among the structural components based on their relative efficiency of capturing debris and the other 40% was applied to the chamber itself with half placed before the test section and half after the test section. In the auxiliary tank, more of the washdown debris was found near the exhaust screen, therefore, based on engineering judgment it was assumed that two-thirds of the debris was fine debris washed off of the screen.

These engineering judgments resulted in the plausible best estimate shown at the right in Figure 3-29. It was recognized that this process was not very exact but it provided a reasonable method of proceeding. Best estimate debris transport fractions and capture fractions could then be calculated. The uncertainty of the method provided the basis for the error analysis which put error bars on the reported data herein.

3.7.4 Estimate of Canvas Cover Weight

Each insulation blanket was weighed prior to mounting the blanket in the test chamber. Because the insulation was sewn into the canvas cover, it was not possible to weight just the insulation. Therefore, the weight of the canvas cover including its attaching hooks, bands, and name tag had to be estimated. The blanket manufactures, Transco, were consulted and they indicated that weight would vary slightly from blanket to blanket but that the weight was likely a few ounces over 5 lbm for each blanket. Upon destruction by the air blast, some lost of canvas mass in the form of fine debris was expected. The total weight of canvas debris recovered after each test approached 5 lbm. Subsequently, a nominal weight of 5 lbm was assumed for the total weight of the canvas cover including its attachments for each test. Any data reduction error introduced into the results from using this assumption was deemed minimal. Note that approximately 37% of the total blanket weight was in the canvas cover.

3.7.5 Error Analysis

The error analysis consisted of identifying the sources of error associated with conducting the CEESI tests, determining which sources dominated the experimental error, and then quantifying the dominant sources.

3.7.5.1 Source of Experimental Error

The sources of experimental error, i.e., means by which an error could have been introduced into the experimental data, can be grouped into three categories. These categories are the conditions of the tests, the collection of the insulation debris, and the post-test processing of the debris.

3.7.5.1.1 Test Conditions

Any departure from specified test conditions had the potential of affecting the results of the experiment. Departures from specified test conditions noted during the experiment included:

- Non-uniformity in the insulation blankets,
- Uniformity in surface wetness,
- Integrity of the test chamber, and
- Air temperature.

The destruction of the target blanket likely varied somewhat from blanket to blanket. For example, the blanket in Test H1R was completely destroyed in that no insulation remained within the canvas cover, whereas in Test H1 about 22% of the insulation remained in a large section of the canvas. Test H1R was intended to repeat Test H1, i.e., identical test specifications. Minor variations existed in the construction of the blankets, as evidenced by the variation in their weights which ranged from 13 to 14 lbm (13.5 " 4%). The impact of blanket non-uniformity was a variation in the quantity of debris generated and as will be demonstrated in the presentation of the results did not significantly affect the debris transport and capture fractions.

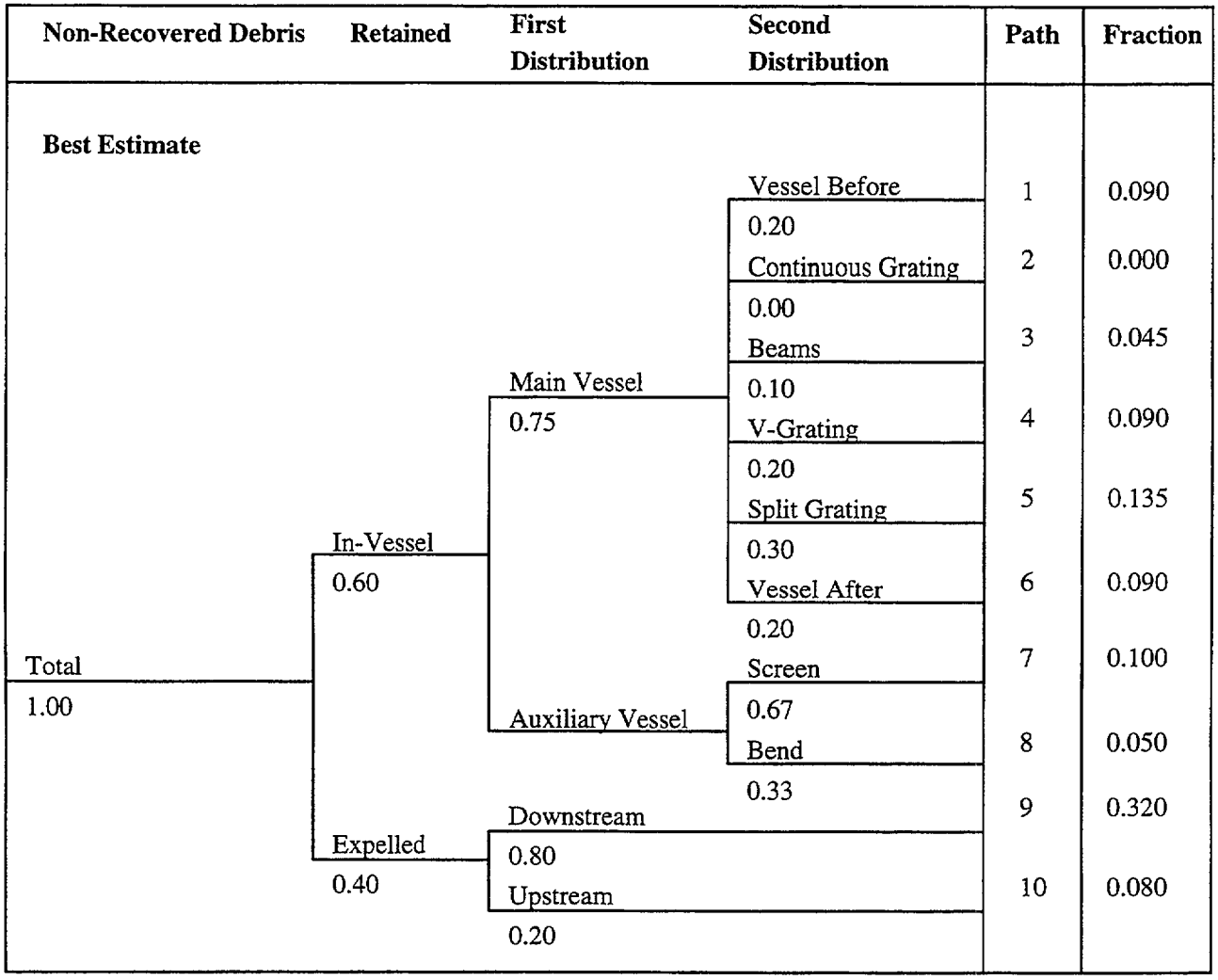

Figure 3-29. Distribution of non-recovered insulation mass.

Since surface wetness had a dominant influence on the ability of a structure to hold onto captured debris, non-uniformity in surface wetness was expected to affect the debris capture results. Two methods of wetting the structures was tested during the developmental tests, i.e., spraying the structures with a water hose prior to initiating the test and misting the structures for about 10 minutes prior to and during the test. The hose spraying method was rejected because the water tended to drain from the structures letting the surfaces dry before tests could be conducted leaving the surface only partial wet. The mist from the misting system, used during the production tests, was found to drift downrange leaving the continuous grating (first grating) relatively dry. Further, the misting time varied from test to test because the time required to setup and conduct the air burst varied. The tests show that surface wetness tends to reach an asymptote where additional wetness does not increase the effectiveness of the structure to capture debris. The major impact of these variations in surface wetness was 1) the continuous grating behaved like a dry structure and two of the developmental tests shows capture results somewhere between wet and dry behavior. It is likely that some variation in the capture results can be attributed to variation in surface wetness.

The integrity of the test chamber was compromised in one test, Test H7, when a hatch cover was blown out causing a substantial loss of insulation debris. Since Test H7 was conducted dry, considerably more debris collected on the exhaust screen at the end of the auxiliary tank than collected during the other tests. This greater mass of debris caused a larger back pressure in the auxiliary tank which over pressurized the hatch. This problem, of

course, only affected Test H7 and did so by increasing the uncertainty in its capture fractions.

The test chamber were preheated with propane heaters to about 70 °F prior to conducting each test. However, due to sometimes extreme winter conditions, the chamber air temperatures could not be controlled with a high degree accuracy. The primary concern was to prevent freezing of water sprayed onto the structures which would certainly have invalidated the data. Freezing was definitely prevented and the fluctuations in air temperature that did occur were not expected to significantly affect the quality of the data.

3.7.5.1.2 Debris Collection

Incomplete or inaccurate collection of the insulation debris was a primary source of experimental error in the CEESI tests. Insulation debris was widely dispersed throughout the test chambers from one end to the other. Collection problems included:

- Debris lost from the test chambers,
- Debris relocation prior to collection,
- Incomplete debris collection within the test chambers, and
- Bagging errors.

Substantial debris was lost from the test chambers through the exhaust screens in the form of very fine debris and this debris certainly could not be retrieved once blown out into the open environment beyond the screens. This fine particle debris, as observed and recorded with a video camera, appeared as an opaque brown cloud extending 10 to 20 ft from the exhaust screen and lasting several seconds.

Captured debris may have relocated following a test before it could be collected. In particular, debris could have fallen off of a structure where it was captured so that it was collected as floor debris which of course would reduce the resulting capture fraction for that structure. Personnel were instructed to exercise all care practical to not facilitate relocation of debris and it is believed that little actual relocation occurred.

It was not feasible to collect all of the really fine debris such as the individual fibers that was found coating wet surfaces. Even the task of collecting all of the smaller pieces was a formidable one. Visual observations during the post-test washdown of the test chamber indicated that a substantial amount of fine debris was deposited on the interior surfaces.

The possibility that a bag of debris was mislabeled was minimized by checking the inventory during post-test processing with the inventory taken immediately following the test and further checking the inventory with known locations where debris should have been taken. Further, the contents of the bags were check to ensure that the debris was categorized correctly. Experimental error of this type was minimized.

3.7.5.1.3 Post-Test Processing of Debris

Following completion of the tests, the debris was dried and weighted by location and classification. Possible post-test debris processing errors included:

- Incomplete separation of canvas and insulation,
- Incomplete drying of the debris, and
- Inaccurate weighing.

Insulation debris and canvas debris were usually intermixed and intertwined. While large pieces of canvas debris were easily separated from the insulation, much of the canvas debris consisted of individual threads of canvas and it was not practical to separate all the threads from the insulation. Conversely, canvas pieces usually had small bits of insulation adhering to them. Incomplete separate of debris was not deemed to have a significant impact on the transport results.

Any moisture left in the debris upon weighing, minor dampness, would introduce error into the test results. The drying process was continued until any remaining moisture was deemed unimportant.

Debris weighing errors were minimized by performing a mass balance, i.e., the weight of all of the debris from one test was compared to the total of the weights of individual bags (including the plastic bags). This process continued until these two weights were within 2% (usually less) of each other. Therefore, errors associated with debris weighing were not considered to be a primary source of experimental error.

3.7.5.2 Bounding Experimental Error

Debris collection errors were found to dominate over the post-test processing errors. Variations in test conditions were not amenable to bounding the magnitude of the error but were reflected in the data scatter. The post-test

processing errors were estimated to be on the order of 1 to 2%. Thus, the mass of debris not recovered during the debris collection process dominated the overall errors (order of 15 to 25%) associated with the experimental results. Therefore, the error analysis focused on the non-recovered mass.

The method described in Section 3.7.3 was used to bound the experimental error associated with the non-recovered mass. The logic chart illustrating this method, shown in Figure 3-29, was also employed in the error analysis. The dominant uncertainty in the non-recoverable mass distribution logic chart was the fraction of non-recovered mass lost from the test chambers. The more non-recovered mass that was lost through the exhaust screen at the end of the auxiliary tank, the smaller would be the calculated debris capture fractions. Conversely, the more mass retained within the test chambers, particularly if the mass was on the structures, then the larger the calculated capture fractions.

Using the logic chart and taking the fraction of debris expelled from one extreme to the other extreme (all or nothing) would certainly bound the error associated with the non-recovered mass. However, the extreme conditions of zero and one were deemed excessive because substantial mass was known to be expelled and substantial mass was known to be retained. The error bounds shown in the result plots in the next section were determined by assuming first that 90% of the non-recovered mass was lost from the system to obtain one bound and then assuming 10% to get the other bound. These bound are likely overly conservative in estimating the errors associated with the non-recovered mass and therefore should reasonably compensate for not considering all of the other smaller sources of error.

The error bounds were expanded for two tests where special debris collection problems were encountered. In Test H7, as previously noted, a hatch cover was blown off thereby greatly increasing the lost of debris mass from the test chamber (approximately 53% of the total insulation mass). For Test H7, the logic chart was modified to add an addition path for debris to leave the test chambers and it was assumed that 70% of the expelled mass left through the blown hatch.

During post-test processing of Test L1, it was apparent that all of the debris from the preceding test, Test H6, had not been collected because the total quantity of Test L1 debris exceeded its initial insulation mass. The data from Test L1 was salvaged by comparing its masses with those of other tests to determine likely locations containing extra mass, and then adjusting the mass table accordingly to obtain best estimate results. Engineering judgment was used to expand the error bounds for Test L1 sufficiently to ensure that the bounds enclosed the true experimental result. The end result was larger error bounds for Tests H6 and L1.

3.7.6 Test Results

Generated debris was classified in three size groups, small, medium, and large. Only the small debris was amenable to the development of debris capture fractions and therefore will be discussed first. The medium and large sized debris are then briefly discussed.

3.7.6.1 Transport of Small Sized Debris

Small insulation debris consisted of insulation smaller than the approximate size of a typical grating cell. This debris included fine particles such as individual fibers but did not include small pieces of insulation attached to canvas that effectively transported as medium or large debris. The small debris test results for the CEESI debris transport tests are shown in the following series of figures.

Overall Transport in CEESI Facility The overall transport of debris in the CEESI test chamber is shown in Figure 3-30 as the fraction of the small debris entering the structural test section at the continuous grating that subsequently transported through the structural test section into the auxiliary tank and onto the exhaust screen. These transport fractions are shown as a function of the debris loading entering the structural test section, i.e., the time-integrated mass flux of debris impacting the continuous grating in units of lbm per 100 ft^2 of chamber cross-sectional area (the cross-sectional area of the chambers was 69.6 ft^2).

A transport fraction is shown in Figure 3-30 for each of the tests where significant debris was generated. Tests using the 4 inch nozzle are shown with a circular point and those with using the 3 inch nozzle with a square point. Tests where the structural surfaces were wet are shown as solid points, whereas dry and only partially wet tests are shown as non-solid points. The points are shown with the error bounds discussed above indicated as error bars. Since Test H7 was conducted dry, its transport fraction was nearly one (shown in the upper right hand corner). Tests I3 and W4, shown as the two non-solid circles in the upper left corner, were conducted with the structures only partially wet because these tests were wet using the water hose method which proved inadequate. The

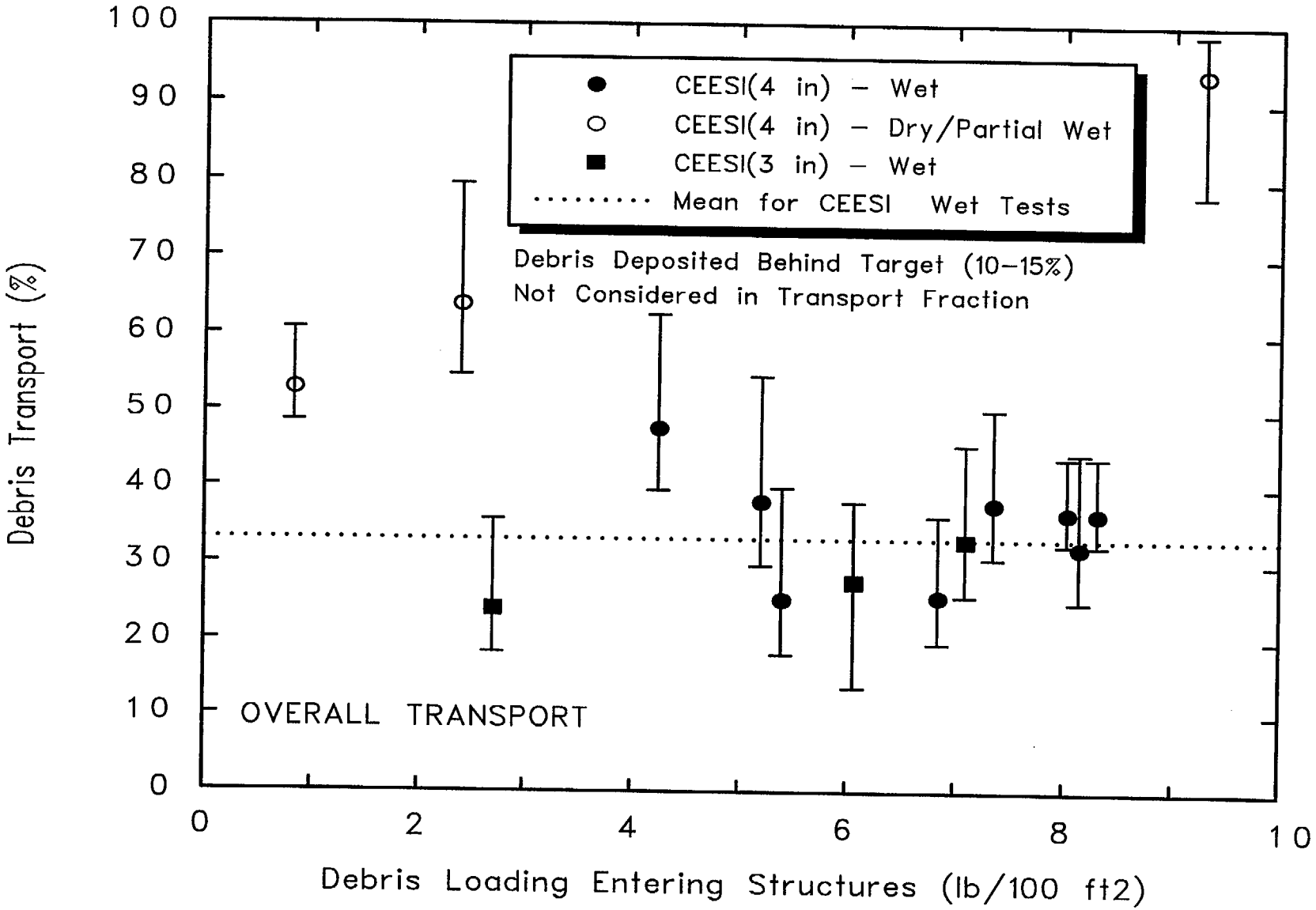

Figure 3-30. Overall transport of small debris through test facility.

developmental tests, shown as the four left most data points had lower debris loadings because the target blankets were not adequately restrained to maximize debris generation. The effect of surface wetting on debris transport is clearly shown in Figure 3-30, i.e., wet structures capture debris while dry do not and partially wet surfaces perform somewhere in between wet and dry behavior. The mean value of all the wet tests was 33%. Note that the transport does not appear to be a function of the debris loading, at least for the loading ranges studied. The error margins tended to be smaller for the tests with higher debris loadings because there was more debris mass generated and the fraction of debris not recovered tended to be lower.

I-Beam and Pipe Structures The fraction of debris captured while passing through the I-beam and pipe assemblies is shown in Figure 3-31 as a function of the debris entering these assemblies. The mean value for the wet tests was 9.3%. The CEESI results for debris capture by I-beams and pipes were compared to the results from the ARL separate effects tests. Adjusted test data for eight ARL separate effects tests are also shown in Figure 3-31. The ARL data applicable to this comparison was reproduced in Table 3-8.

The ARL data was adjusted because the ARL capture fractions applied to individual beams or pipes, whereas, the CEESI capture fractions applied to the combines structural assemblies. The cross-section areas of the beams and pipes, as viewed by the approaching debris, expressed in the fraction of the test chamber cross-sectional area were approximately 50% for the I-beams and 20% for the pipes.

Little debris was observed captured on the pipes in CEESI and the ARL capture fraction for a 12 inch pipe (note that CEESI pipes were 10 inch in diameter) in a 50 ft/sec air flow was only 4%. With 20% of the test chamber cross-sectional areas obstructed by pipes which capture 4% of debris traveling within this 20% area, then only about 1% (0.2 X 0.04 = 0.008) of the debris passing through the structural test section would be expected to be captured by the pipes.

Since the I-beams obstructed 50% of the test chamber area, the ARL capture fraction for I-beams was adapted to CEESI by simply dividing the ARL number by 2. The total expected capture fraction for the combined CEESI structural test section based on the ARL data was one-half the ARL number for I-beams plus 1% to account for pipes. The ARL capture fractions adapted to the CEESI structures are shown in Table 3-9 as well as being plotted in Figure 3-31.

The ARL data in Figure 3-31 was focused at one relatively light debris loading at about 1.4 lbm/100ft^2 which was an artifact of the limitations of that experiment. Thus, this figure clearly demonstrates one of the primary objectives of the CEESI tests, i.e., to obtains debris capture data at higher debris loadings more prototypical of accident conditions postulated for a BWR drywell. Postulated BWR debris loadings could extend to even higher levels than the CEESI experiment. The quantities of debris under study in NUREG/CR-6224 peaked at about 111 ft^3, which would correspond to a CEESI debris loading of about 11 lbm/100ft^2 if uniformly distributed over a 2500 ft^2 drywell grating. Therefore, the CEESI debris loading agreed well with the debris generation quantities understudy in NUREG/CR-6224. Research performed after the NUREG/CR-6224 study by the BWR Owners Group contains much more conservative debris generation quantities which could result in debris loadings several times the maximum loading generated in the CEESI tests. Although the I-beam capture fractions shown in Figure 3-31 do not indicate a dependency upon debris loading, care should be taken in extrapolating beyond the CEESI debris loadings.

In Figure 3-31, the range in the ARL capture fractions generally encompasses the CEESI data. The variation in the ARL capture fractions was due primarily to variations in wetting (10 or 30 seconds of sprays) and debris size (either 2-to-4 or 2-to-6). Larger debris captured better than small debris and wetter surfaces captured better than dryer surfaces. The wetness was not quantified in either experiment but was deemed based on visual observation to be generally comparable. The CEESI debris size distribution from the air blast destruction of a blanket was generally broader than the ARL debris which was artificially created. All in all, the capture results for the two experiments are in good agreement.

Gratings The fractions of debris captured while passing through a grating are shown in Figures 3-32 and 3-33 for the V-grating and the split grating, respectively. The debris loadings in these figures are the mass flux of debris impacting that particular structure. The mean values for the wet tests were 28% and 24%, respectively. The results for the two gratings are very similar in terms of their debris capture per unit surface area as shown in the figures. The V-grating, however, only obstructed 57% of the entire cross-section of the test chamber which was factored into Figure 3-32.

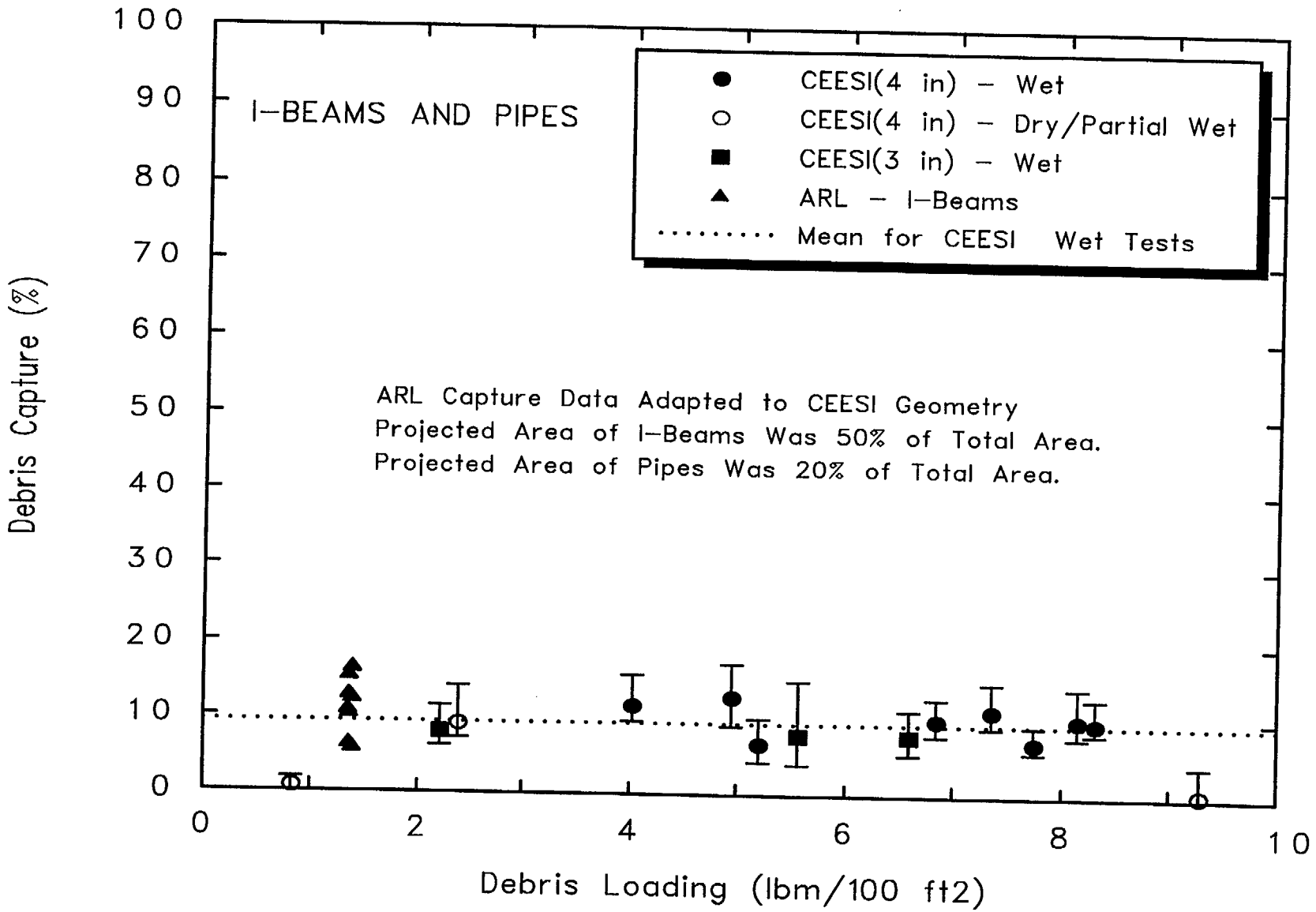

Figure 3-31. Capture of small debris by I-beams and pipes.

Table 3-8. Comparable ARL I-beam and pipe debris capture data.

Test ID	Prewet time (sec)	Flow velocity (ft/sec)	Debris size	Debris loading on structure (lbm/100ft^2)	ARL capture fraction (%)
Pipes (12 inch)					
3	10	50	2 to 4	1.38	4
19	10	25	2 to 4	1.38	5
I-beams (10 inch)					
8	10	50	2 to 4	1.38	23
9	30	50	2 to 4	1.38	31
12*	10	50	2 to 4	1.35	11
16*	10	50	2 to 4	1.35	24
17*	30	50	2 to 4	1.34	20
18*	30	50	2 to 4	1.35	29
21	10	25	2 to 4	1.38	10
22*	30	50	2 to 4	1.35	19
*I-beam in a combination arrangement					

Table 3-9. Modified ARL I-beam/pipe debris capture data.

Test ID	Indiviual I-beam capture fraction (%)	Capture fraction modified to CEESI geometry (%)
8	23	12
9	31	16
14	11	6
16	24	13
17	20	11
18	29	15
21	10	6
22	19	10

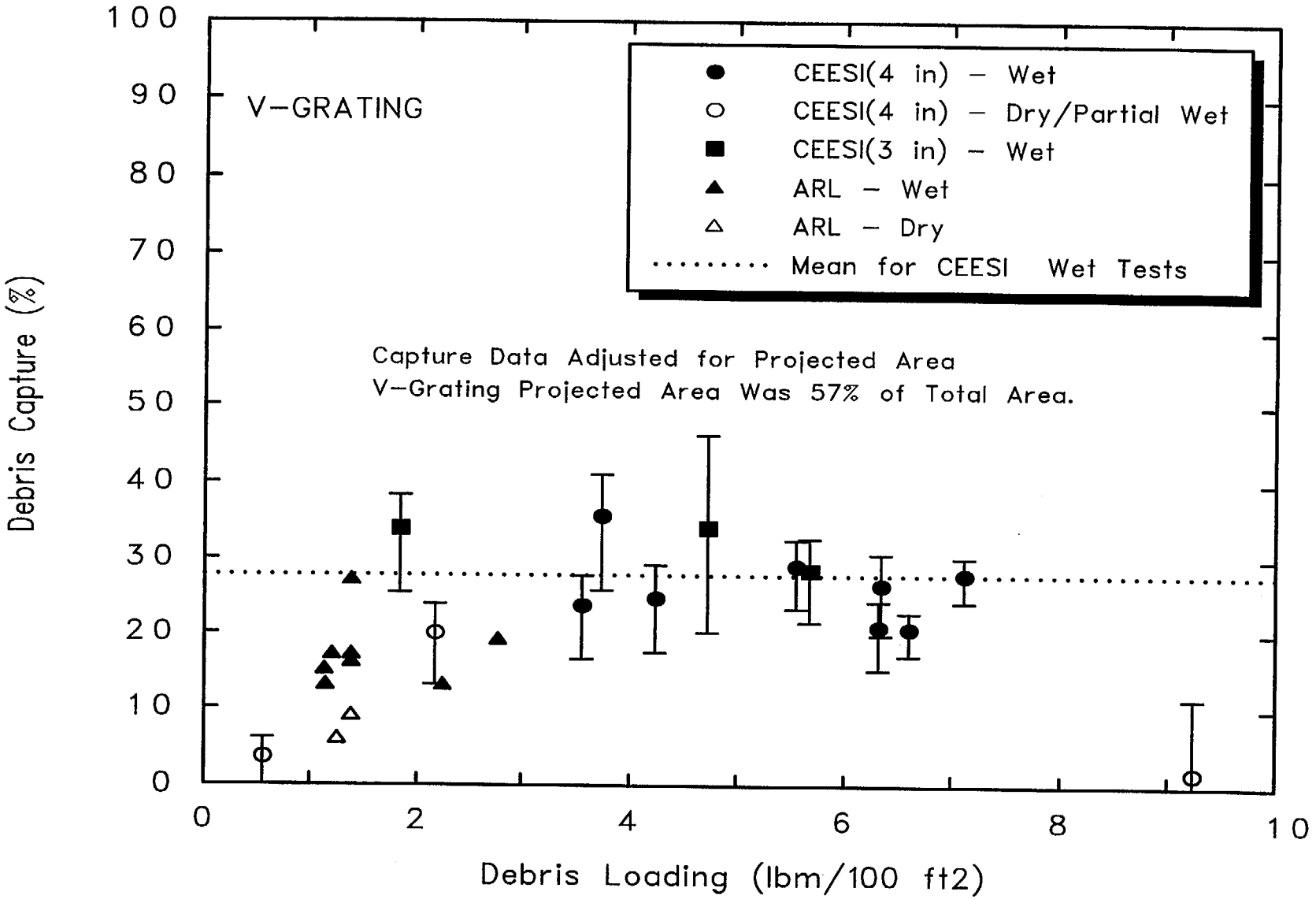

Figure 3-32. Capture of small debris by V-grating.

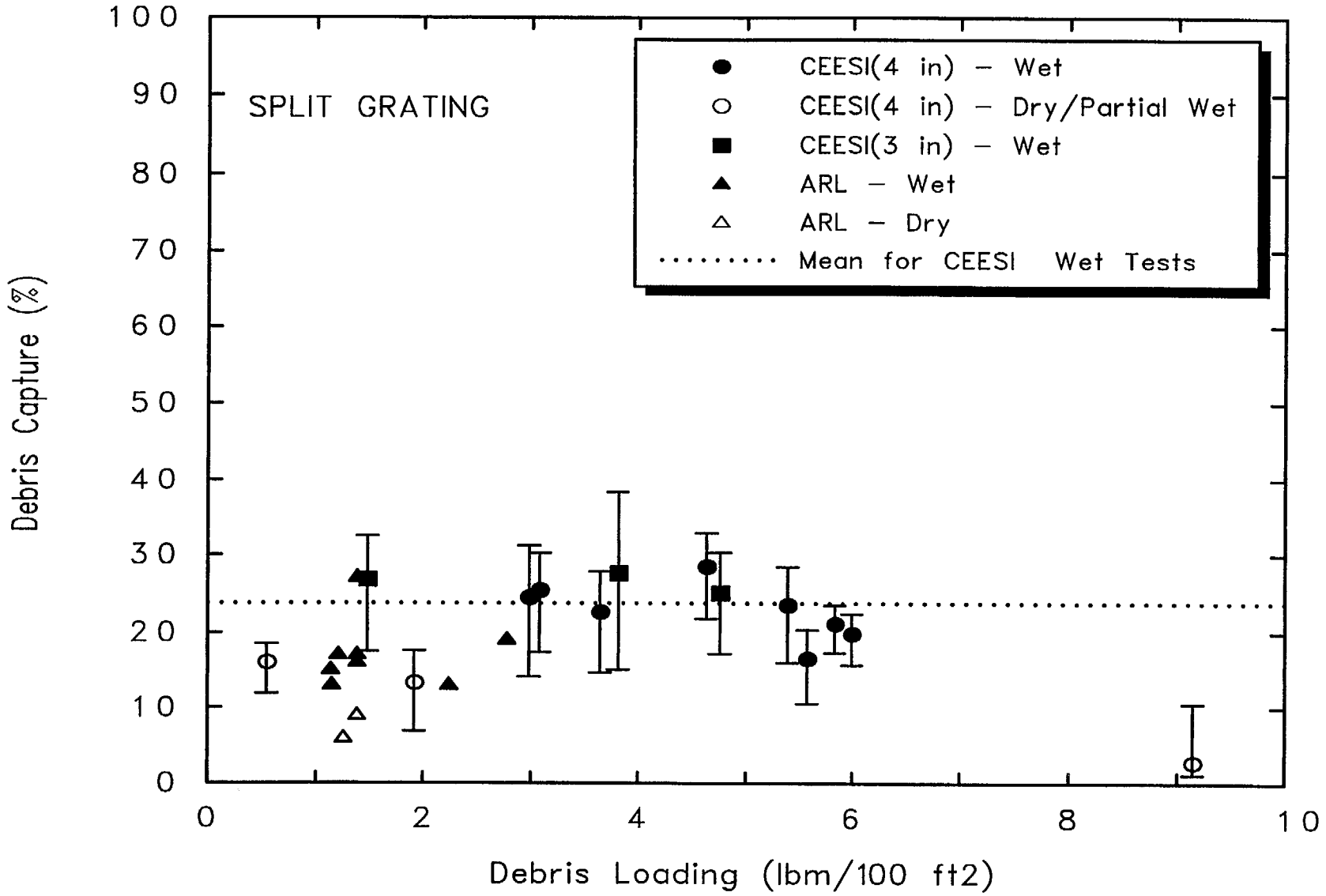

Figure 3-33. Capture of small debris by split grating.

Again, the CEESI test data was compared with applicable ARL separate effects test data, as shown in Figures 3-32 and 3-33. The ARL data applicable to this comparison was reproduced in Table 3-10. While certainly comparable, the ARL data tended to be somewhat lower than the CEESI data. The highest ARL capture fraction of 27% was for a test with larger debris (2-to-6) and with the longer 30 second wetting time. One significant difference between the CEESI and ARL debris was that the CEESI debris included a considerable mount of fine particles, whereas the ARL debris did not. The importance of capture of these fine particles by gratings is clearly shown in Figure 3-21, which shows a consistent layer of fine debris on the front surfaces of the grating. The relatively effective capture of this fine debris in the CEESI tests was likely responsible for the somewhat higher capture fractions seen in the CEESI tests.

The first grating that the debris encountered was the grating referred to as the continuous grating. It was intended that this grating provide debris capture data at a relatively higher debris loading since it was the first grating encountered. However, as it turned out, this grating remained dry or nearly dry due to an air draft moving downrange that caused the water mist to bypass wetting the continuous grating. Therefore, little debris was actually captured by the continuous grating. The debris capture results for this grating, shown in Figure 3-34, are presented to further show the contrast between debris capture by a wet grating (V-grating or split grating) and a dry grating. In Figure 3-34, virtually no small debris was captured on the continuous grating in many of the tests. These data points are shown as non-solid circles at the bottom of the plot. Other tests showed a small amount of small debris capture but substantially less than found on the V and split gratings. This was likely due to some moisture on the continuous grating but much less than complete wetness. Note the complete lack of fine debris capture in Figure 3-20.

Bends in the Flow Path When the blast air flow entered the auxiliary test chamber from the main chamber, the flow had to make a 90° bend where the chamber wall had been wetted by mist drifting with the slight air draft through the chambers. A substantial amount of debris was deposited at this bend and this deposition expressed as a capture fraction is shown in Figure 3-35 as a function of the debris passing through the collar to the auxiliary chamber in term of mass flux based on the cross-sectional area of the chambers, not the collar. The mean value for the wet tests was 17%. Note that the cross-sectional area of the collar was about 60% of the main chamber area and that the mean capture fraction based on the collar cross-sectional area would be about 28%.

Test Repeatability One measure of the quality of any experimental result is whether or not the test result could be repeated. As it turned out, four of the CEESI tests were very similar. Test H1R was intended to be a repeat of Test H1. The test conditions for these tests are repeated in Table 3-11. The blankets in Tests H1R, H2, and H3 were considered completely destroyed, i.e., 100% of insulation turned into debris. Test H1 was considered about 78% destroyed since 22% of its insulation remained within the canvas cover. The transport and capture of small debris for these four tests are compared in Figure 3-36. The data clearly illustrates test repeatability.

3.7.6.2 Transport of Large and Medium Sized Debris

The majority of the debris generated in the CEESI tests (not including insulation still encased in canvas) was classified as small debris, however, each test had some large and medium sized debris. Typically, a few percent of the insulation was classified as large debris and a few percent as medium debris. Some general statements can be made regarding the transport of large and medium debris but there was not sufficient quantities of the debris to determine capture fractions for the structures.

The large debris (i.e., debris somewhat loosely sized as larger than a hand) was found stopped by the first grating encountered. No large debris was found beyond the continuous grating in any of the tests implying a grating capture fraction of one. The large debris was all contained in the section of the main chamber bounded by the panel blocking off the diffuser section behind the jet nozzle and the continuous grating. Within this space, the large debris generally churned with the highly turbulent flows until the air blast ceased. Following the air blast, the large debris was recovered from both in front of the jet and behind the jet with no clear preference as to which way. In Test H1R, for example, 94% of the large debris was found behind the jet but in Test H2, 93% was found in from of the jet. In conclusion, the large debris appeared to easily transport with the depressurization flows and relatively thoroughly mix due to the turbulence but was readily contained by a grating.

Some medium debris (i.e., debris somewhat loosely sized as smaller than a hand but larger than the cell of a grating) was forced through the cells of the continuous grating, however, there was not a statistically sufficient quantity of

Table 3-10. Comparable ARL capture data for gratings.

Test ID*	Prewet time	Flow velocity	Debris size	Debris loading on structure	ARL capture fracture
	(sec)	(ft/sec)		(lbm/100ft^2)	(%)
4	10	50	2 to 4	1.13	15
5	10	50	2 to 4	1.20	17
12	10	50	2 to 4	1.38	16
13	30	50	2 to 4	1.38	27
23-1 23-2	10	50	2 to 4	1.38 1.14	17 13
24-1 24-2	10	50	2 to 4	2.76 2.23	19 13
26-1 26-2	Dry	50	2 to 4	1.38 1.25	9 6
*Tests 23, 24, and 226 each had two gratings.					

Integrated Effects

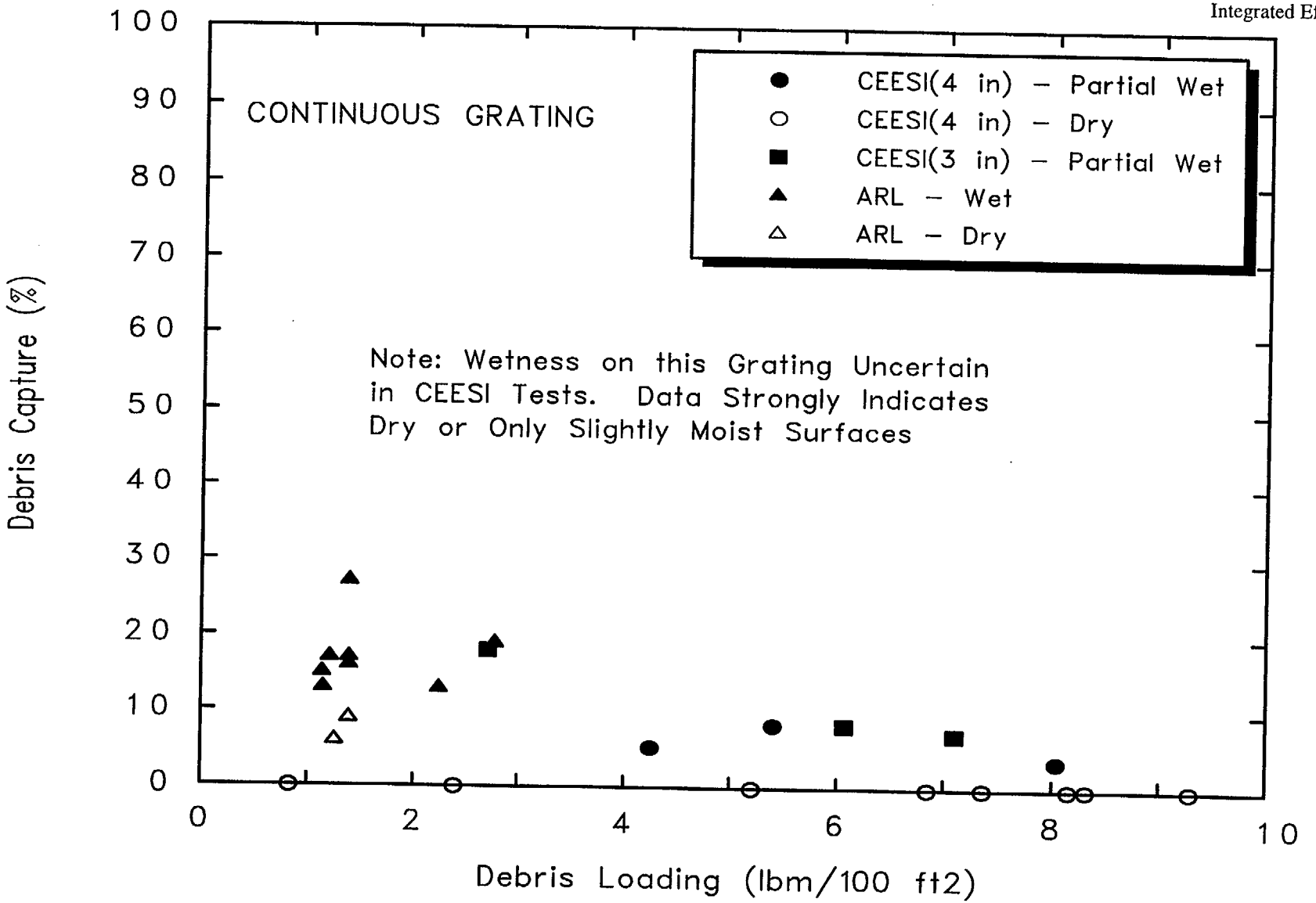

Figure 3-34. Capture of small debris by continuous grating

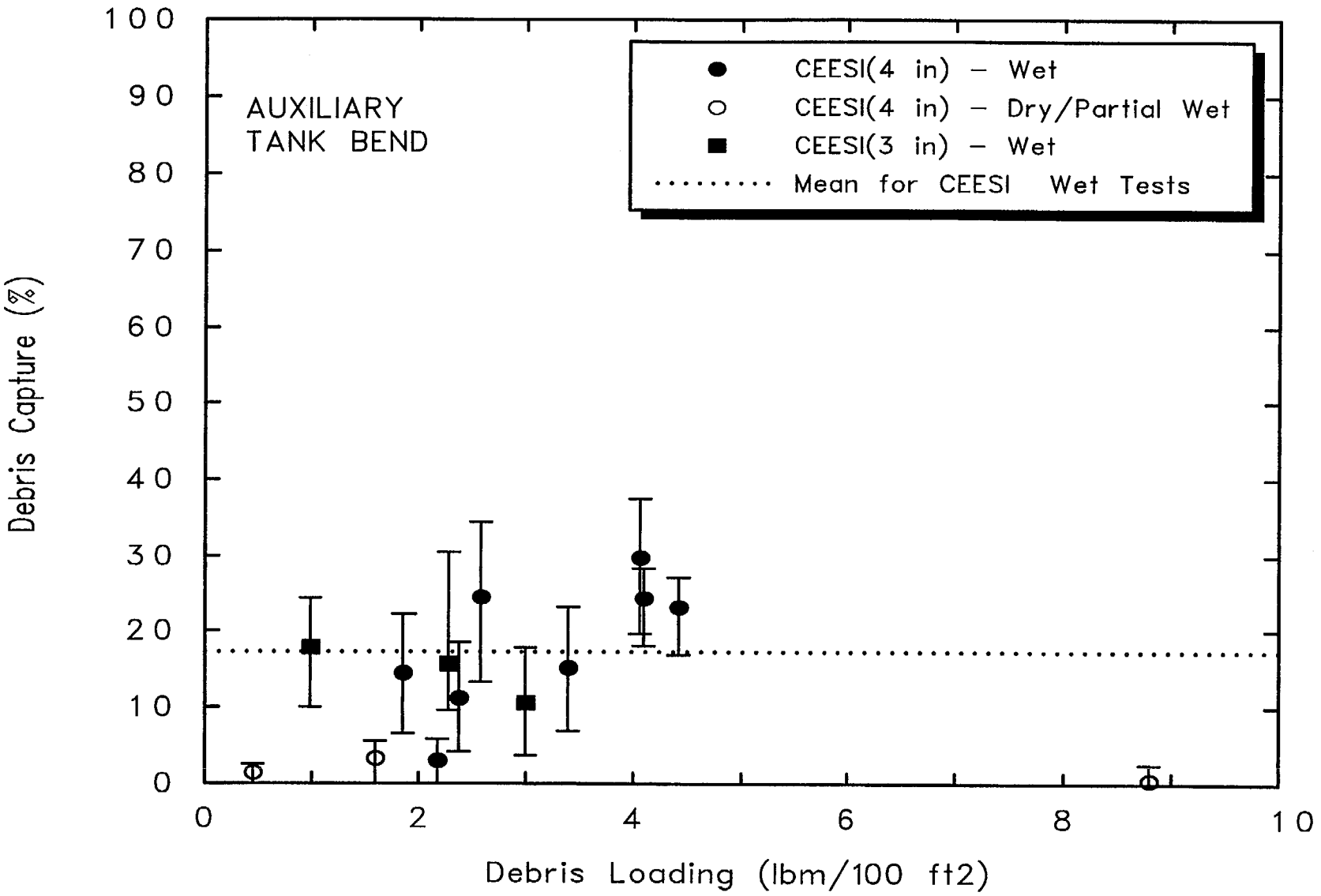

Figure 3-35. Capture of small debris by auxiliary tank bend.

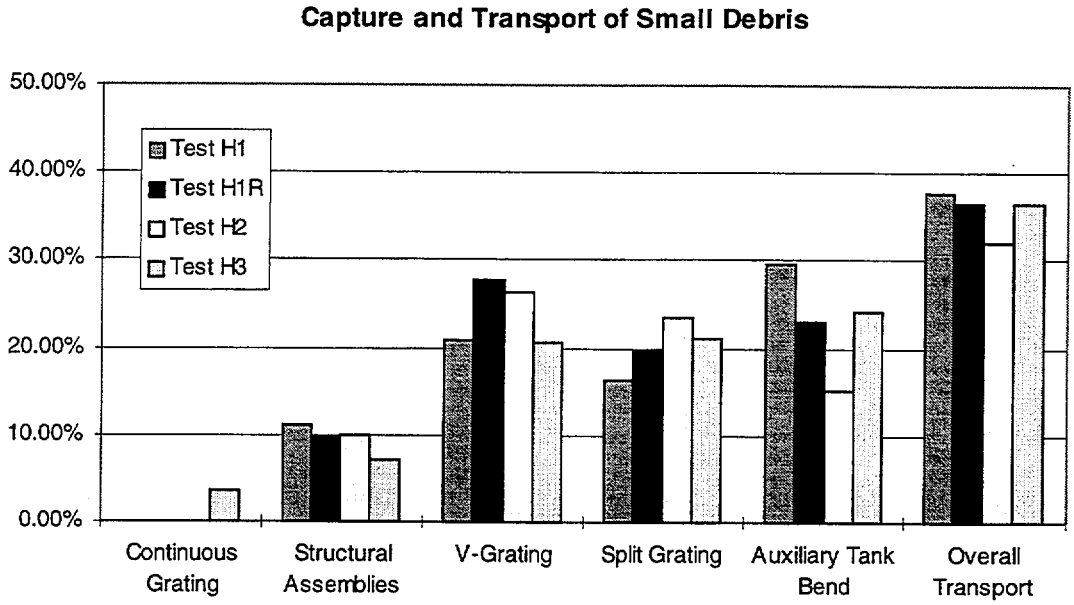

Figure 3-36. Demonstration of CEESI test repeatability.

Table 3-11. Test Matrix for the repeatability tests.

Test		Nozzle diameter	Air jet duration	Structure wetness	Target position	
No	ID				Distance	L/D
		(inch)	(sec)		(inch)	
1	H1	4	13	Wet	120	30
2	H1R	4	13	Wet	120	30
3	H2	4	15	Wet	120	30
4	H3	4	14	Wet	80	20

the medium debris. The total quantity of debris generated was only a few tenths of a pound. When capture fractions were calculated using the method employed for the small debris, the capture fraction for the continuous grating varied from zero to 50% and for subsequent gratings, the capture fraction varied from near zero to 100%. In general, medium sized pieces of debris forced through the first grating were stopped by the second grating encountered. I-beams and pipes did not appear to capture any medium sized debris. No medium debris transported to the exhaust screen and in only one test, Test H7 conducted dry, was any medium debris collected in the auxiliary tank. Therefore, there was no data produced regarding the capture of medium debris at a bend in the flow. In conclusion, medium debris mixes well in flow turbulence and readily transport in open spaces, but will be heavily captured by gratings.

3.8 References

3-1 "Parametric Study of the Potential for BWR ECCS Strainer Blockage Due to LOCA Generated Debris," G. Zigler, J. Brideau, D. V. Rao, C. Shaffer, F. Souto, and W. Thomas, NUREG/CR-6224 Science and Engineering Associates, Inc., SEA93-554-06-A:1, October 1995.

3-2 "Potential Plugging of Emergency Core Cooling Suction Strainers by Debris in Boiling Water Reactors," NRC Bulletin 96-03.

3-3. "Water Sources for Long-Term Recirculation Cooling Following a Loss-of-Coolant-Accident," Regulatory Guide 1.82, Revision 2 May 1996.

3-4. "BWR Drywell Debris Transport Phenomena Identification and Ranking Tables (PIRT)," Gary E. Wilson, Brent Boyack, Mark Leonard, Ken Williams, and Lothar Wolf, Letter Report to USNRC, Initial Issue, June 28, 1996.

3-5. "Drywell Debris Transport Study," D. V. Rao, F. Sciacca, C. Shaffer, F. Souto, and G. Zigler, Draft Phase 1 Letter Report to the NRC, SEA 96-3105-010-A:2, September 27, 1996.

3-6. "MELCOR 1.8.0: A Computer Code for Nuclear Reactor Severe Accident Source Term and Risk Assessment Analyses," R. M. Summers, R. K. Cole, Jr., E. A. Boucheron, M.K. Carmel, S. E. Dingman, and J. E. Kelly, NUREG/CR-5531, SAND90-0364, SNL, January 1991.

3-7. "Experimental Evaluation of Internal Debris Capture on BWR Drywell Structures Following a LOCA,"" P. S. Stacy, M. Padmanabhan, and G. E. Hecker, 85-97/M787F, April 1997.

3-8. "BWR Drywell Debris Transport PIRT Review of SEA Experimental Plan," Gary E. Wilson, Brent Boyack, Mark Leonard, Ken Williams, and Lothar Wolf, Letter Report to USNRC, Initial Issue, November 15, 1996.

3-9. "Simulation of BWR Drywell Flow Behavior in Response to a Recirculation-Line LOCA Using a Computational Fluid Dynamics (CFD) Code," Ken Williams, Flow Simulation Services, Inc., Letter Report to USNRC, FSS Report RX-96-05, November 1996

3-10. "Drywell Transport Study Supplemental Report: Analytical Studies," D. V. Rao and C. Shaffer, NUREG/CR-6369, Supplement, Science and Engineering Associates, Inc., SEA 97-3105-A:16, September 1997.

4. Separate Effects Test Program to Evaluate Washdown of Insulation Debris by ECCS Flow

4.1 Introduction

4.1.1 Background

As discussed in the previous sections, the floor gratings employed in the BWR drywells provide the largest potential for capture and retention of insulation pieces as they are being transported during blowdown. Nearly all the debris pieces that are considerably larger than the floor-grating clearance (4"x1.5") are likely to be captured by the grating and a significant fraction of the pieces smaller than 4"x1.5" would be captured by the grating. Therefore, it can be postulated that at the end of blowdown the floor gratings would accumulate considerable quantities of insulation debris. For some plants, the volume of debris trapped on the gratings at the end of blowdown may be as high as 400 ft^3. This insulation debris would then be subjected to water flows that can result from break overflow (primarily in the case of a recirculation line break) or containment sprays turned on to cool the drywell atmosphere. A fraction of the debris may be washed down to the drywell floor as a result of exposure to water flow. Presently very limited experimental data is available to quantify the transport fraction associated with this phase of the accident, which has the potential to be a dominant contributor, especially considering that large quantities of debris are exposed to continuous water flow for extended periods of time.

Two tests were conducted by the BWROG (TR25 and TR31) to study the potential for erosion and/or transport of large and small insulation debris by washdown [Ref. 4-1]. In these tests, a large piece of insulation (6"x3"x2") was placed on a full-scale grating at the start of the test. The piece was initially subjected to blowdown flow (for a period of 15 seconds) which consisted of steam in case of TR25 and a two-phase mixture in case of TR31. Erosion of less than 2% was observed in case of steam blowdown, while close to 20% of the piece was eroded by the mixture. The left over piece was then subjected to water flow that varied with time, increasing from an initial value of 1 GPM/ft^2 to 12 GPM/ft^2. In TR25 the piece was exposed to water flow for a total of 30 minutes, while in TR31 it was subjected to water flow for 75 minutes. Based on these two tests, the BWROG concluded that:

- Most of the small debris (< grating size) would be washed down with very small quantities of water flow irrespective of where they were located originally, and
- About 20% of the large piece will be eroded and transported to the drywell floor in the form of small clumps [Ref. 4.1]. Washdown reaches an asymptotic behavior with erosion leveling off after about 15 minutes of continuous exposure to water.

These results were then used by BWROG to develop guidance related to a drywell debris transport fraction Their conclusions were not based on a defensible rationale given that: a) the duration of testing and test flow rates are not typical of those expected in BWRs following a LOCA (e.g., tests were conducted using a maximum of 60 GPM flow spread evenly over 5 ft^2 of grating), and b) the conclusions were drawn based on two tests in which several variables were simultaneously varied in a non-prototypical manner; their data did not appear to support their conclusions (e.g., in TR31 less than 10% of NUKON brick appeared to have been eroded by water flow in contrast to 25% recommended by BWROG). Finally, the BWROG tests did not provide any insights into the type and size of pieces generated by erosion and their transportability.

To overcome this lack of data, SEA conducted a series of tests under sponsorship of the NRC.

4.1.2 Objectives and Scope

The primary objective of SEA testing was to obtain experimental data that could be used to estimate what fraction of insulation initially captured by floor gratings would be eroded and transported by water flow during the washdown phase. The secondary objective was to confirm the conclusions stated by BWROG and their usage in developing the guidance presented in Reference 4.1. Tests were conducted with water at room temperature using insulation pieces generated by air-jet from aged Thermal Wrap™ insulation blankets. Both debris sizes and water flow rates were varied to simulate washdown of small debris by containment sprays as well as erosion and transport of large debris by break flow.

4.2 Test Facility

4.2.1 Test Setup

The tests were performed at the SEA Santa Fe facility. Figure 4-1 is a photograph of the test set up and Figure 4-2 is a schematic of the test facility. A 400 gallon

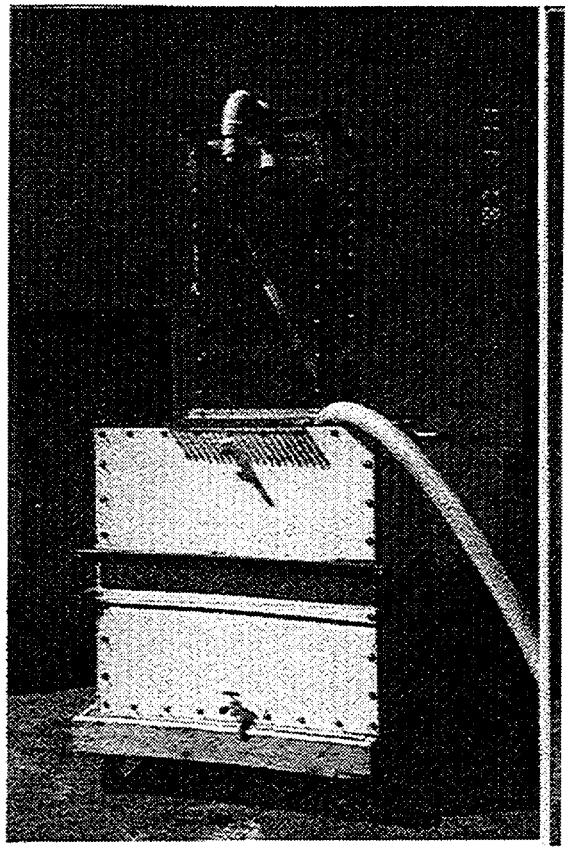

Figure 4-1. Photograph of the washdown experimental set-up. Experiments were conducted at SEA-Santa Fe.

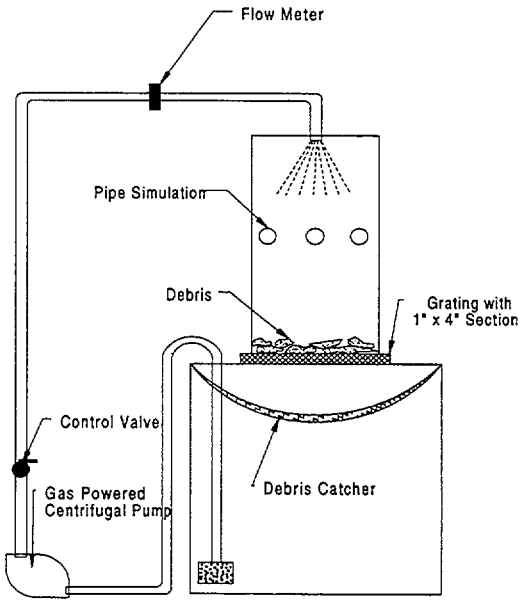

Figure 4-2. Schematic representation of the washdown test setup.

tank was used as the water reservoir for recirculation purposes. To avoid recirculating debris pieces along with the flow, two filters were placed in the tank. The first filter, a debris catcher, was positioned right below the test section to trap large pieces. The second filter was fitted to the pump section to filter out finer debris.

Aluminum grating with dimensions identical to those of the steel grating in BWR drywells was placed across the top of the tank. The test section, 2-ft x 2-ft in cross-section and 5-ft long, was placed on top of the grating. The entire section was fabricated using 0.50" thick clear polycarbonate, which allowed visual observation of the tests. Three 2-in. diameter plexiglass pipes were used across the inside of the box to simulate pipes in the actual reactor containment and break-up the jet in a prototypical fashion.

A 250 GPM centrifugal pump was used to inject water into the test section through a 4" diameter PVC pipe. In tests simulating break flow, the water was allowed to flow directly from the PVC outlet. In tests simulating spray-induced washdown, a removable spray head (2-ft x 2-ft in cross-section with a hole size of 1/8") was attached to PVC outlet. The desired flow rates were achieved by properly throttling the control valve located downstream of the pump. Calibrated flow meters were used to monitor the flow. Two different flow meters had to be used due to the large difference in flow rate requirements between break flow and spray flow.

Water from the pump outlet was allowed to fall under gravity to impact the mock-up pipes which broke the jet and spread the water flow across the test section fairly uniformly. The cascading flow was then allowed to impinge on the debris layer placed on the grating at the start of each test. Under gravity, the water was allowed to washdown to the bottom of the test section and then into the storage tank.

4.2.2 Debris Materials

The insulation material used was heat treated Thermal Wrap™, which is a low density fiber glass marketed by Transco Products, Inc. (TPI). Four sizes of debris were used in the tests. These sizes were selected to represent a wide range of debris sizes expected to be generated following a LOCA. The CEESI air blast test results were used to select the debris size and characteristics, as described below.

Fine (F):
Finely destroyed insulation pieces that can be best characterized as loosely attached individual fibers less than an inch long. Typically such fines were found attached to wet surfaces, such as pipes and grating. These debris were obtained directly from blast-jet experiments conducted previously by SEA (see Section 3). These materials were used in two tests (C-2 and C-4).

Small (S):
The Insulation debris of a light, loose, and well-aerated texture with an average density lower than 0.25 lbm/ft^3 usually consisting of loose clusters of individual fibers. Typically these pieces were about 1.5" in size and possessed little of the original structure or the chemical binding. In CEESI tests, they were found to have been attached to the wet gratings. These debris were obtained directly from blast-jet experiments conducted previously by SEA (see Section 3). These debris were mainly used in spray tests.

Medium-J (M-J):
Insulation debris pre-torn from the blanket by an air-jet impingement. These pieces keep some of the original structures in the inner regions, while they look torn-down or loose on the outside. Typically these pieces are about 6"x4" in dimension. In CEESI tests they were found to have been attached to the wet or dry gratings. These debris were obtained directly from blast-jet experiments conducted previously by SEA (see Section 3). Very few pieces that can be characterized as M-J were obtained from SEA testing. As a result only two tests were conducted using this type of debris.

Medium-O (M-O):
Same geometric as above, but the pieces were produced by cutting the intact insulation into small pieces. These pieces were primarily used in break flow tests as a substitute to jet generated debris, because only limited quantity of jet generated debris were available for testing. These pieces possess same density as as-fabricated blankets.

Large (L):
The SEA Air-Jet tests have clearly demonstrated that large pieces produced from jet impingement tend to retain most of their original structure. As a result, large cut-out pieces of as-manufactured blanket were used. These blanket pieces ranged in size from 10"x 10" to 18" x 18" depending on the availability of insulation.

4.3 Test Plan and Test Procedure

4.3.1 Text Matrix

Table 4-1 presents the test matrix. The testing proceeded in two steps: a) confirmatory tests and b) erosion tests. The confirmatory tests consisted of five tests designed to confirm some of the observations reported by BWROG [Ref. 4.1]. Then 21 erosion tests were conducted to quantify erosion as a function of flow rate and debris size. Selection of test parameters varied in these tests is based on the rationale described below.

Table 4-1. Experimental uncertainties.

Experimental parameter	Measurement unit	Estimated uncertainty
Flow Rate (Break Flow)	GPM	±10%
Flow Spray Flow)	GPM	±15%
Insulation Mass	gm	±3 gms
Moisture in Dried Insulation	gm	May have contributed toward lowered estimates of erosion rate by up to 10%.
Duration of Exposure	min	+1 min

1. Flow rate into the test section. A control valve located downstream of the pump was used to control the flow rate. A flow meter located downstream of the control valve was used to monitor flow rate; flow meters were calibrated. Two flow rates were selected for experimentation. A flow rate of 175 GPM (or approx. 45 GPM/ft^2-grating) was selected to be representative of break flow. On the other hand, a flow rate of 20 GPM (or approx. 5 GPM/ft^2-grating) sprayed by 1/8" nozzles was used to simulate the containment spray flow. The following rationale was used to derive the flow rates:

Break Flow

- Estimated flow area at the lower grating in a BWR: 2000 ft^2 for Mark I, 4500 ft^2 for Mark II. Assuming that water trickles down to a quarter of the containment, the flow cross-sectional area is 500 ft^2 for a Mark I.
- Estimated ECCS flow rate: 25,000 GPM (±15 % depending on the plant power level). Probably real flow rates would be much lower given that 25000 GPM is the design flow at a head of 150 ft-water. During recirculation, flow would most likely be around 17500 GPM.
- Estimated Flow Rate in a Mark I BWR is 50 GPM/ft^2. Credible Flow Rate = 35 GPM/ft^2.
- Maximum Flow Rate scaled to the test section: 50 gpm/ft^2 x 4 ft^2 = 200 GPM. Credible Flow Rate = 140 GPM..
- Corresponding Velocity: 0.14 ft/s.
- Simulated Flow Rate: 175 GPM.

Spray Flow

- Estimated flow area at the lower grating in a BWR: 2000 ft^2 for Mark I, 4500 ft^2 for Mark II. Containment sprays cover entire containment.
- Estimated spray flow rate: 7500 GPM
- Flowrate in a real BWR is 4.7 GPM/ft^2.
- Flowrate scaled to the test section: 4.7 GPM/ft^2 x 4 ft^2 = 18.75 gpm.
- Corresponding Velocity Velocity: 0.0104 ft/s (Note velocities are very low. Not much erosion possibly)
- Simulated Flow Rate: 20 GPM

2. Debris layer weight (or theoretical thickness) and debris size. Debris was weighed before each test. Also debris was manually cut into desired size pieces (if needed). The test facility can handle pieces as large as 1.5-ft x 1.5-ft. Sizes were as described in Section 4.2.2. Debris layer theoretical thickness were varied from ¼" to 2" which corresponds to mass loading of 5 lb/100-ft^2-grating to 40 lb/100-ft^2-grating. This falls well within the expected volume of insulation trapped on the grating which varies from 50 ft^3 (or 120 lbm) to 400 ft^3 (960 lbm).

3. Duration of Exposure. Duration of exposure was monitored manually. All spray experiments were carried out for 30 minutes, which was estimated to be the maximum credible time sprays would be operated following a LOCA (Emergency Operating Procedures call for operation of sprays for 3 to 4 times following a LOCA, about 10 minutes each time). The break flow experiments were carried out for up to 3 hours, which was estimated to be the maximum credible time for continuous operation of ECCS at full flow. It is very likely that operators will throttle the ECCS within the first hour after LOCA.

4. Mode of water injection (spray vs. break). Tests addressed both spray and break flow induced erosion. No other processes of washdown (e.g., condensate drainage) were studied.

4.3.2 Test Procedure

The following step-by-step test procedure was followed during every test:

- At the beginning of every day, wash and fill the storage tank with water.
- Cut and weigh debris required for test according to the test matrix.
- Select spray or break flow type. If spray is selected, then install spray header.
- Carefully place debris pieces of pre-determined size and weight on the grating.
- Close the valve and turn on the pump, taking suction from the fine-mesh filtered intake.
- Slowly open the valve until desired flow is achieved.
- Let the water flow continue for the duration called for in the test matrix.
- Turn off the pump.
- Collect left-over debris on the grating, oven dry it until it is completely dry.
- Collect the debris on the filter screen under the grate. Also dry and weigh it for the purpose of mass balance.

4.3.3 Experimental Uncertainties

The following uncertainties in the experimental measurements are estimated based on calibration and repeated measurements.

4.4 Test Results

A total of 26 tests were conducted (see Table 4-1). In each test, a pre-determined quantity of insulation debris was placed on the grating and then subjected to spray or break flow for a period of up to 3 hours. At the end of the test, pieces left-over on the grating were collected and dried. Mass eroded and percentage eroded were estimated from the mass difference between the initial and final mass on grating. Table 4-2 presents the results for each test. Figures 4-3 and 4-4 illustrate examples of debris before and after being subjected to washdown in Tests E-1 and E-13, respectively. Figure 4-5 shows eroded pieces trapped on the debris catcher (Test E-1). In Test E-1 medium pieces of debris cut from original blankets were subjected to break flow washdown for a period of 30 minutes. As shown in Figure 4-3, erosion occurred fairly uniformly, thus suggesting that all pieces were subjected to similar water flows irrespective of their location. Even at the end of the test, the original blanket structure is visible in the non-eroded portion, suggesting that the erosion process consists of peeling off layers from the top. Visual observation suggests that erosion occurs continuously with time. Note also that eroded pieces are typically very small and can be best characterized as fines. These pieces tended to remain suspended in the 400-gallon water tank under minimal turbulence conditions.

In Test E-13 Small (S) pieces of CEESI air-blast generated debris were subjected to spray flow for a period of 30 minutes. As shown in Figure 4-4, spray flow washed down most of the loosely attached clumps and clumps that possess some of the original structure survived. Visual observations suggest that the majority of the washdown occurred within the first 15 minutes.

4.4.1 Confirmatory Tests

The objective of the confirmatory tests was to verify the following conclusions stated by the BWROG [Ref. 4.1]:

1. Little or no erosion is possible for insulation pieces covered in canvas when subjected to washdown flow resulting either from break overflow or containment spray.
2. Most of the Small debris pieces will be washed down by water within first 10-15 minutes after which washdown reaches an asymptote.
3. Large pieces will not be forced through the grating even at high flows. They will remain on the grating and may erode with time. Erosion also exhibits an asymptotic behavior.

Test C-1 was designed to address the issue related to erosion of insulation covered in the original canvas cloth in which it is packed. A piece of partially torn Thermal Wrap blanket generated from CEESI Air Blast tests was cut into 10" x 10" x 3" piece and placed in the center of

Table 4-2. Test matrix for SEA washdown experiments.

Test ID	Flow/Test configuration			Insulation debris characteristics			Quantity of insulation	
	Type	Flow (GPM)	Duration (m)	Size category	Size physical	Canvas	Mass (gms)	Theo. Thick (in)
C-1	Break	175	30	M(O)	6" x 4"	Y	196	0.5
C-2	Break	175	30	S+F	1.5" x 1.5"	N	200	0.5
C-3	Spray	20	30	F	<1.5" x 1.5"	N	185	0.5
C-4	Spray	20	30	F	<1.5" x 1.5"	N	184	0.5
C-5	Break	175	30	M(O)	6" x 4" x 1/4"	N	Not Measured	0.5
E-1	Break	175	30	M(O)	6" x 4"	N	196	0.5
E-2	Break	175	30	M(O)	6" x 4"	N	362	1.0
E-3	Break	175	15	L	>10" x 10"	N	360	1.0
E-4	Break	175	180	L	>10" x 10"	N	362	1.0
E-5	Break	175	30	L	>10" x 10"	N	366	1.0
E-6	Break	175	60	L	>10" x 10"	N	370	1.0
E-7	Break	175	30	M(O)	6" x 4"	N	180	0.5
E-8	Break	175	30	<M(O)	6" x 4"	N	194	0.5
E-9	Break	175	30	S(O)	1.5" x 1.5"	N	185	0.5
E-10	Break	175	30	L	>10" x 10"	N	720	2.0
E-11	Spray	20	30	M(J)	6" x 4"	N	184	0.5
E-12	Spray	20	30	S(J)	1.5" x 1.5"	N	364	1.0
E-13	Spray	20	30	S(J)	1.5" x 1.5"	N	96	0.25
E-14	Spray	20	30	S(J)	1.5" x 1.5"	N	187	0.5
E-15	Spray	20	30	L	>10" x 10"	N	368	1.0
E-16	Spray	20	30	<M(O)	6" x 4"	N	186	0.5
E-17	Spray	20	30	S(J)	1.5" x 1.5"	N	368	1.0
E-18	Spray	20	60	M(O)	6" x 4"	N	187	0.5
E-19	Spray	20	30	S(J)	1.5" x 1.5"	N	715	2.0
E-20	Break	175	120	L	>10" X 10"	N	362	1.0
E-21	Break	175	30	M(J)	6" x 4"	N	720	2.0

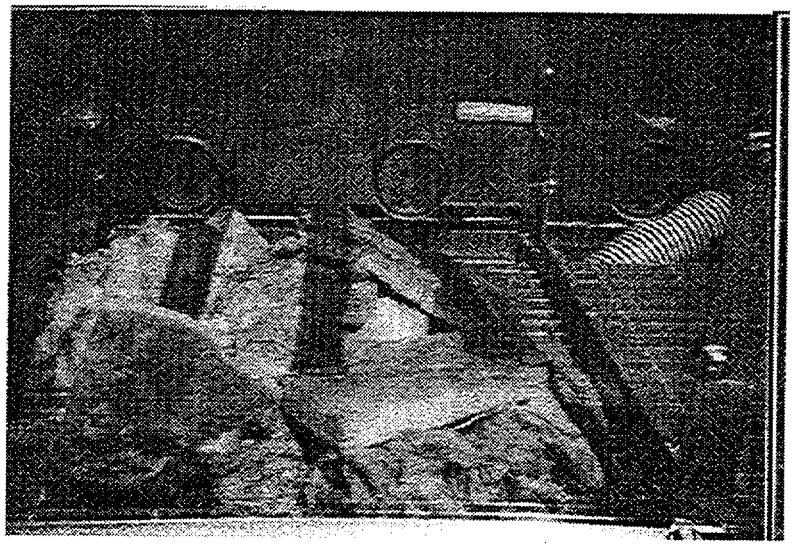

A. Before exposure to break flow.

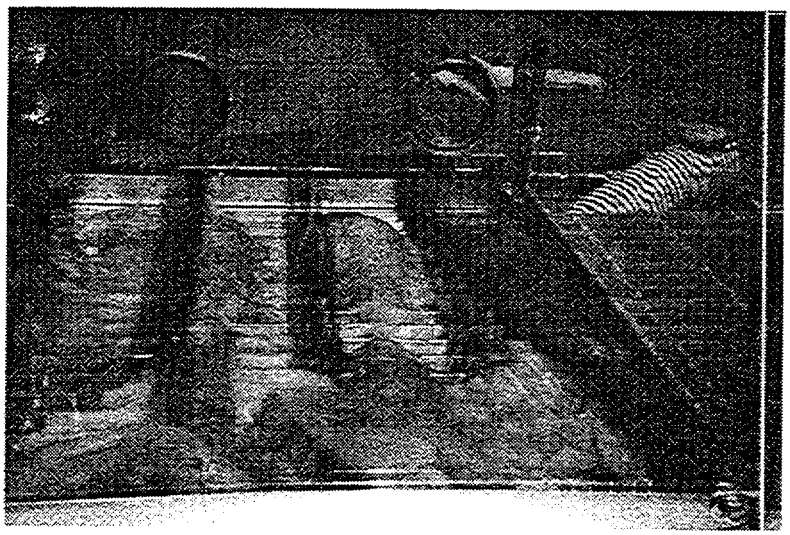

B. After exposure to break flow.

Figure 4-3. Erosion of medium size debris manually cut from original blankets by break flow (test 1).

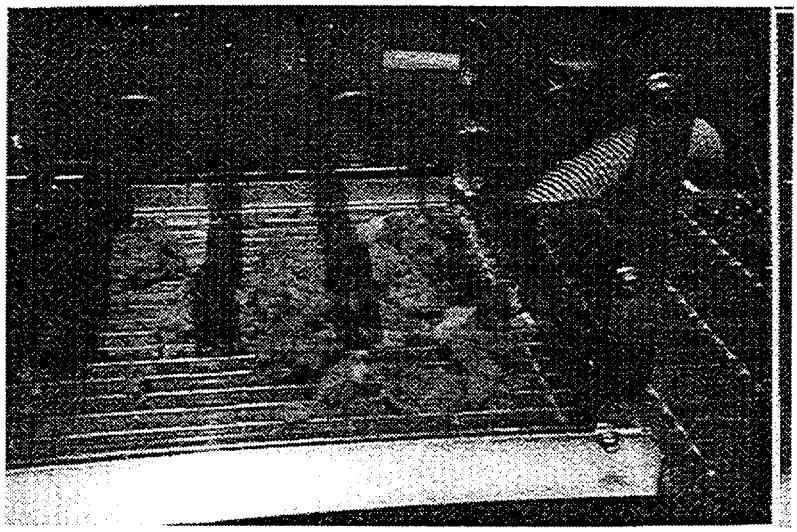

A. Before exposure to spray flow.

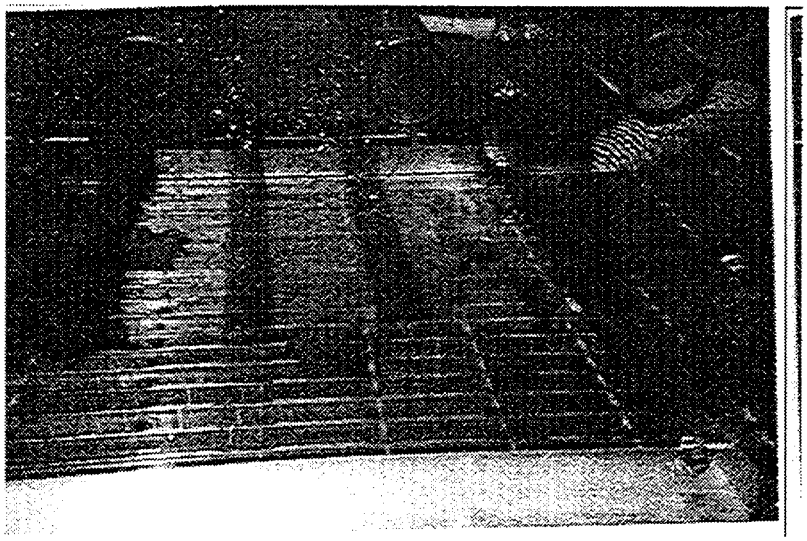

B. After erosion by 30 muniutes of spray flow.

Figure 4-4. Erosion of small air jet generated debris by spray flow (test 13).

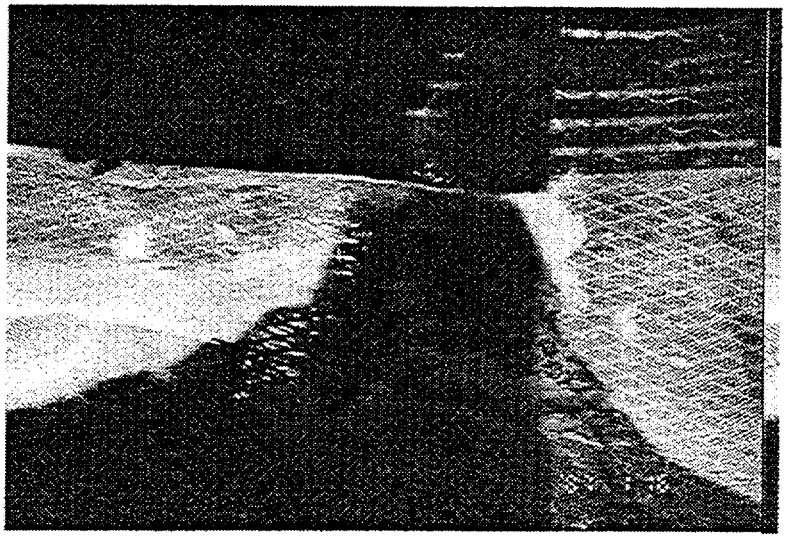

Figure 4-5. Eroded pieces filtered by coarse debris catcher (test 2).

the grate. Visually it can be seen that the piece consisted of several small holes and worn out canvas outer clothing. After 30 minutes of continuous exposure to 175 GPM flow, visual observations exhibited no noticeable erosion of the pieces. Visual observations also suggest that water flows around the blanket, but not through the blanket which would be required to inflict damage. No attempt was made to dry the insulation pieces and perform a mass balance.

Tests C-2, C-3 and C-4 were designed to address the second issue, involving, washdown of small pieces of debris attached to various structures during blowdown. Photographs from the CEESI tests clearly suggest that debris are loosely attached to the surface of interdicting structures due to surface wetness. They also tended to be fairly dry on the outside and wet closer to the structural surface. To simulate this, dry pieces of insulation debris that can be characterized as Fines (see Section 4.2.2) were manually dropped on the pre-wet grating and pipes. These structures were then subjected to water flow. Test C-2 simulated break flow, where as Tests C-3 and C-4 simulated spray flow. Test C-5 is a repeat of C-2, except for the fact that pieces are slightly larger. In all cases, the insulation was completely washed down within the first 5 minutes. No pieces were left behind on the grating, either during spray flow or during break flow

Test C-5 was designed to determine if a large piece is susceptible to being broken down and forced through the grating in a short period of time. A single dry piece of insulation blanket, 6"x4"x1/2" in size, was placed in the middle of the grating and was subjected to break flow of 45 GPM/ft^2. The insulation piece survived approximately 45 minutes of continuous flow, although continuous erosion was noted.

Based on this testing it is concluded that:

1. Partially torn insulation blankets covered with the original canvas clothing are unlikely to be eroded by water flow during washdown. This confirms the BWROG stated conclusion.
2. Fines attached to various wet structures during blowdown as a result of inertial impaction will be washed down by the water flow, irrespective of whether the flow is induced by break overflow or containment sprays. Also, small pieces deposited on the gratings will be washed down completely in the case of break flow. In both cases, transport is complete within few minutes. No conclusions can be drawn related to washdown by condensate drainage

3. Pieces sufficiently larger than the grating (classified as M-O, M-J and L in Section 4.2.2) possess sufficient structure and are not susceptible to being forced through the grating clearances in a short period of time. Erosion (if any) occurs over a longer period of time. It does not reach an asympotic behavior.

4.4.2 Erosion Tests

A total of 21 erosion tests were conducted with the objective of estimating the mass fraction of the insulation

fragments that would be eroded when exposed to break/spray flow for a pre-determined period of time. In all these tests debris fragments of pre-determined size and weight were placed uniformly on the grating and were exposed to break and spray flow. Almost all of the break flow tests were conducted using relatively large debris retaining the original blanket structure as previous tests have shown that small pieces with no original structure do not survive under break flow. The fraction eroded was estimated from the difference in mass between debris placed on the grate and debris that remained on the grating after drying. Table 4-3 presents the results.

4.4.2.1 Effect of Flow Rate (Break versus Spray)

Table 4-4 presents a test-by-test comparison of washdown fractions as a function of test debris size. As shown in this table, under similar test conditions break flows erode a larger fraction of debris than spray flow. Such a dependence is expected considering that break flows discharge considerably larger flow.

4.4.2.2 Effect of Duration Erosion

The effect of time on erosion by break flow was explored in tests E-3, E-4, E-5, E-6 and E-20. Results of these tests are presented in Figure 4-6 as a function of time. From this figure it can be clearly seen that erosion is a linearly increasing function of time, at least over the first three hours. The error bars on the graph represent estimated experimental uncertainty. The spread in the data is due to variability in debris bed formation.

The effect of time on erosion was not explored in the case of sprays because erosion was found to be minimal (except for small and medium pieces).

4.4.2.3 Effect of Bed Thickness (or initial mass)

Theoretical thickness of the bed is a measure of debris loading on the grating (lbm/ft^2). It is computed as:

$$T_t = M/(\rho \cdot A_g) \qquad (4\text{-}1)$$

where:

- T_t = theoretical thickness (ft)
- M = mass of insulation (lbm)
- Ag = cross-section Area of the Grating (ft2)
- ρ = as-fabricated density of insulation (2.4 lbm/ft^3)

Tests E-1 and E-2 measured erosion as a function of theoretical thickness for medium size debris pieces with original structure (M-O) by break flow. As evident from Table 4-2, the fraction eroded is inversely proportional to the bed theoretical thickness. On the other hand, the quantity of insulation eroded is approximately the same in both cases. This suggests a constant rate erosion in the case of large and medium pieces that retain the majority of the original blanket structure.

Tests E-12, E-13, E-14 and E-19 examined erosion of air-blast generated debris by spray washdown. As evident from Table 4-2, no noticeable dependence existed between theoretical thickness and percentage eroded. This is consistent with the visual observation that loosely attached parts of the debris were quickly eroded by the sprays (visual observation suggests that it occurred within the first 15 minutes). The left over debris pieces retained some of the original structure and were not eroded by spray.

4.4.2.4 Effect of Debris Size and Structure on Erosion

Tables 4-5 compares erosion of Medium and Small pieces cut manually from the original blanket with those generated by air jet. As evident from this table, the potential for erosion is smaller for pieces that possess some of the original structure.[1]

Table 4-6 compares erosion potential as a function of debris size. Data suggest that in the case of debris pieces that possess original blanket structure, mass eroded is independent of debris size, but is only dependent on time (somewhat weakly dependent on theoretical thickness). To illustrate this trend, in Table 4-5 rate of erosion (mass eroded per hour per 100-ft^2) is presented as a function of debris size and theoretical thickness. As evident from this table for break flow, the erosion rate is fairly independent of size and thickness and can be bounded by a value 3.0 lbm/100-ft^2-grating/hr.

4.4.2.5 Experimental Data Repeatability

Data repeatability can be best judged by comparing results of similar or identical tests. As shown in Table 4-3, Test E-7 is an exact repeat of Test E-1 and Test E-17 is an exact repeat of Test E-12. In both cases, the fraction eroded was found to be within $\pm$10% of each other. In reviewing the data it should be noted that all measurements are associated with experimental

[1] Manually cut pieces possess strong structure that is typical of original pieces.

Table 4-3. Results of washdown erosion test program.

Test ID	Flow type	Duration (min)	Debris size type	Theo. Thick. (In)	Initial mass (gm)	Final mass (gm)	Mass eroded (gm)	Percent (%)	Comments
C-1	Break	30	M(O)	0.5	Not Meas.	Not Meas.	Not Meas.	Not Meas.	Visually, erosion is insignificant.
C-2	Break	30	S+F	0.5	200	0	175	100	All the insulation was forced through the grating.
C-3	Spray	30	F	0.25	100	0	20	100	Same as above. Insulation only fines.
C-4	Spray	30	F	0.25	100	0	20	100	Same as above. Insulation only fines.
C-5	Break	30	M(O)	0.5	Not Meas.	Not Meas.	Not Meas.	Not Meas.	Erosion was evident. No large-scale break through.
E-1	Break	30	M(O)	0.5	196	172	24	12	All pieces aged. Manually cut from Original blanket.
E-2	Break	30	M(O)	1.0	362	341	21	6	All pieces aged. Manually cut from Original blanket.
E-3	Break	15	L	1.0	360	355	5	1.4	All pieces aged. Manually cut from Original blanket.
E-4	Break	180	L	1.0	362	264	98	27	All pieces aged. Manually cut from Original blanket.
E-5	Break	30	L	1.0	366	343	23	6	All pieces aged. Manually cut from Original blanket.
E-6	Break	60	L	1.0	370	353	18	5	All pieces aged. Manually cut from Original blanket.
E-7	Break	30	M(O)	0.5	180	160	20	11	All pieces aged. Manually cut from Original blanket.
E-8	Break	30	<M(O)	0.5	194	171	23	12	All pieces aged. Manually cut from Original blanket.
E-9	Break	30	S(O)	0.5	185	133	52	28	All pieces aged. Manually cut from Original blanket.
E-10	Break	30	L	2.0	720				Test aborted. Noticed build-up of a water layer on debris.
E-11	Spray	30	M(J)	0.5	184	152	32	17	Debris generated from CEESI Experiments [Ref. 2].
E-12	Spray	30	S(J)	1.0	364	214	151	41	Debris generated from CEESI Experiments [Ref. 2].
E-13	Spray	30	S(J)	0.25	96	51	45	47	Debris generated from CEESI Experiments [Ref. 2].
E-14	Spray	30	S(J)	0.5	187	107	80	43	Debris generated from CEESI Experiments [Ref. 2].
E-15	Spray	30	L	1.0	368	368	<1	<1	Debris generated from CEESI Experiments [Ref. 2].
E-16	Spray	30	<M(O)	0.5	186	182	4	2	All pieces aged. Manually cut from Original blanket.
E-17	Spray	30	S(J)	1.0	368	230	138	38	Debris generated from CEESI Experiments [Ref. 2].
E-18	Spray	60	L	0.5	187	185	<2	<1	All pieces aged. Manually cut from Original blanket.
E-19	Spray	30	M(J)	2.0	715	481	235	33	Debris generated from CEESI Experiments [Ref. 2].
E-20	Break	120	L	1.0	362	300	62	17	All pieces aged. Manually cut from Original blanket.
E-21	Break	30	M(J)	2.0	720	375	345	48	Debris generated from CEESI Experiments [Ref. 2].

Table 4-4. Effect of flow rate (i.e., break versus spray) on erosion of debris.

No.	Test conditions		Break flow		Spray flow	
	Size	Duration	% Erosion	Test ID	% Erosion	Test ID
1	L	30 m	6	E-5	<1	E-15
2	M(O)	30 m	6	E-2	<1	E-18
3	M(J)	30 m	48	E-21	18	E-11

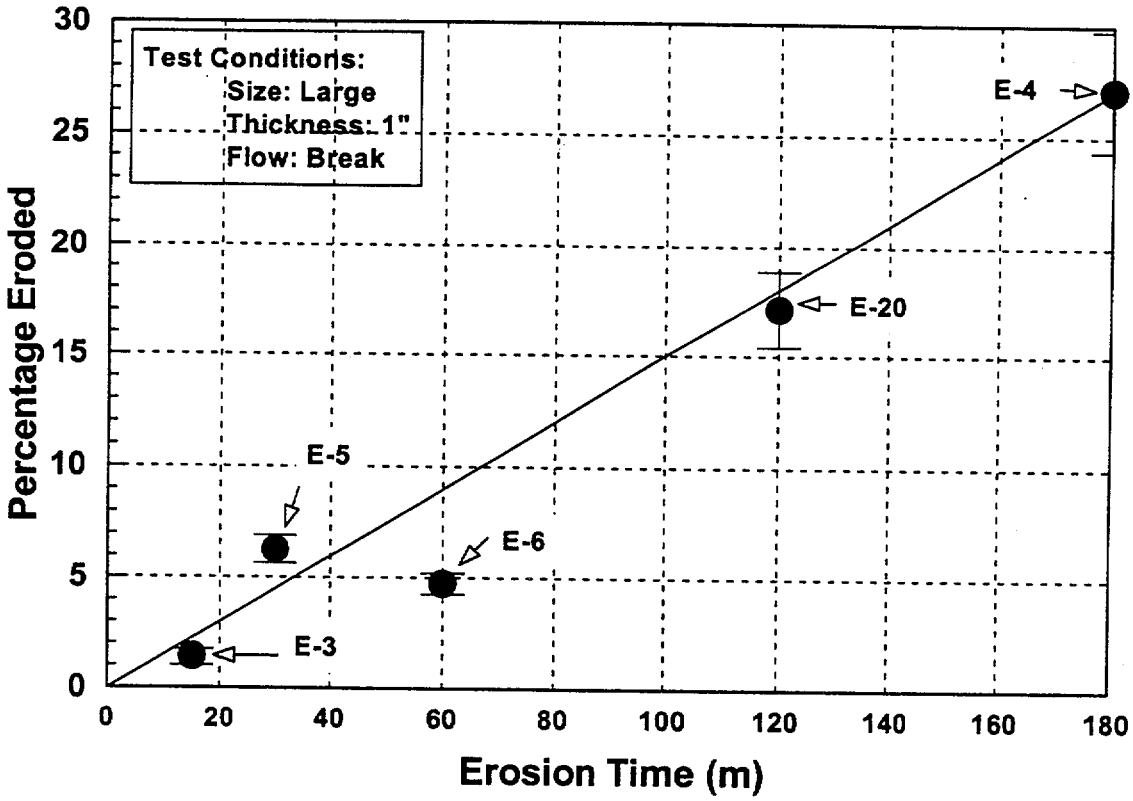

Figure 4-6. Effects of duration of erosion on the percentage of initial blanket eroded.

Table 4-5. Effect of debris size and structure on erosion.

Debris size	Test condition		Air-jet generated		Manually cut pieces	
	Flow type	Duration	Erosion (%)	Test	Erosion (%)	Test
M	Break	30	48	E-21	12	E-1
S	Break	30	100	C-2	28	E-9
M	Spray	30	17	E-11	<1	E-18

Table 4-6. Effect of debris size, debris loading (i.e., thickness) and test duration on erosion.

Test ID	Test Description		Erosion data		Erosion data	
	Theoretical thick. (In)	Debris size type	Duration (m)	Mass eroded (gm)	Percentage of initial mass	lb/100 ft²/hr
E-1	0.5	M(O)	30	24 ± 3	12	2.7 ± 0.33
E-2	1.0	M(O)	30	21 ± 3	6	2.4 ± 0.33
E-3	1.0	L	15	5 ± 3	1.4	1.2 ± 0.75
E-4	1.0	L	180	98 ± 3	27	1.8 ± 0.1
E-5	1.0	L	30	23 ± 3	6	2.7 ± 0.33
E-6	1.0	L	60	18 ± 3	5	1.2 ± 0.2
E-7	0.5	M(O)	60	20 ± 3	11	2.4 ± 0.33
E-8	0.5	<M(O)	30	23 ± 3	12	2.7 ± 0.33
E-20	1.0	L	12	62 ± 3	17	1.8 ± 0.1

uncertainties which are estimated and presented in Section 4.3.3.

4.5 Summary and Conclusions

A total of 26 washdown tests were conducted to quantify the potential for erosion of insulation debris fragments captured on grating as they are subjected to water flow resulting from break overflow and/or from containment sprays. The tests employed several debris fragment sizes and two flow rates. Based on these tests the following conclusions can be drawn:

1. All finer debris that are smaller than the grating, but are captured on grating as a result of inertial capture would be washed down when subjected to break and/or containment sprays. A transport factor of 1.0 should be assigned for such fragments.

2. A significant fraction of the medium pieces (generated by jet impact on insulation blanket) would be eroded and transported to the drywell pool. A transport factor of 1.0 is recommended in the case of break overflow (e.g., following a recirculation line break); on the other hand, for sprays a transport factor of 0.5 appears reasonable.

3. Erosion of larger pieces is dependent both on time and flow rate. At very small flow rates that are typical of containment sprays, erosion of large debris pieces is negligible, especially considering that containment sprays are only operated intermittently. At larger flow rates typical of break flow, erosion can be large. For such conditions an erosion rate of 3.0 lbm/100-ft²/hr is recommended. For the assumed base case scenario (i.e., debris is uniformly distributed on the grating at the end of blowdown, break flow cascades and spreads evenly over a quarter of the grating, and break flow occurs unthrottled for a period of 3 hrs following a LOCA after which the break is isolated and/or throttled), the erosion can be as high as 25% of the large pieces that are separated from the canvas during their generation. For shorter or longer duration, the quantity eroded can be estimated using an erosion rate of 3.0 lbm/100-ft²/hr.

4. The secondary debris generated from erosion of large pieces tends to be very small pieces that are likely to remain suspended in a pool of water with minimal turbulence. Visual observations suggest that they tend to be very small loosely attached clumps of individual fibers.

4.6 References

4.1 Boiling Water Reactor Owners' Group, "Utility Resolution guidance for ECCS Suction Strainer Blockage," NEDO-32686, Rev. 1, 1996.

5. Conclusions

5.1 Air Borne Transport

The conclusions of the study related to short-term (or blowdown) transport can be summarized as follows:

1. Inertial capture is an important mechanism for removal of debris from flow stream provided the drywell structures are wet. Gravitational settling, other mechanism studied in the test program was negligible except for large-canvassed pieces.

2. Surface wetness has a clear influence on the capture of small debris by various drywell structures; when dry, these structures did not capture any small debris. For large debris structural wetness has negligible effect.

3. Capture efficiency of individual structural elements decreases when they are grouped with other structures, except for gratings whose capture efficiency did not change. Video images of debris transport clearly demonstrate that due to wake effects created by the first layer of structures debris particles transport around the structures located downstream of them.

4. Gratings captured more fibrous debris than any other structural components, individually or together with other structures. Under identical conditions of surface wetness, gas velocity, debris size and debris mass, a single grating captured as much debris as structural members assembled to typical BWR congestion levels over a 20-ft length.

5. Bulk flow velocity appears to have little impact on capture efficiency, at least within the range tested (25-150 ft/s). Similarly, three-dimensional local flow patterns appear to have an insignificant effect on capture efficiency as demonstrated by good agreement between CEESI and ARL experimental data for gratings and structural combinations. Note that ARL tests employed flow control devices to straighten the flow before it approached the test objects, where as in CEESI a complex three-dimensional flow transported the debris over the test objects.

6. Mark I and Mark II vents with wetted surfaces can be effective at capturing larger debris. However, their capture efficiency for small debris is typically in the range of 12%.

7. Degradation of large pieces deposited on gratings by inertial capture is negligible when exposed to the remaining blowdown flow that follows. In the tests, negligible break up or disintegration of insulation debris captured on the grating was found when 1/8" to ½" thin pieces of insulation were subjected to up to 140 ft/s of approaching air velocity. The pressure drops resulting from the flow were as high as 0.5 psi.

Capture efficiencies recommended for use to estimate drywell transport fractions during blowdown are provided in Table 5-1. While applying the transport fractions care should be taken to ensure that:

- The capture efficiency should be applied to only that fraction of the debris that is expected to be transported across the structural group during blowdown.
- Appropriate capture efficiency should be selected after determining the surface wetness of the structures.

5.2 Transport During Long-Term ECCS Recirculation

The following conclusions related to long-term transport can be drawn from the experimental data:

1. Small debris deposited on the surface of the structural elements can be easily washed down by containment sprays or break overflow. Recapture of these pieces on any of the structures located down stream is unlikely.
2. Large pieces do not undergo instantaneous degradation even when they are subjected to water flows as high as 50 GPM/ft^2 which is representative of break overflow. Instead they undergo continuous erosion at a rate of 3 lbm/100-ft^2/hr. Erosion of large pieces by spray flow is negligible.
3. No erosion was observed in the case of large pieces covered with canvas lining covering them. It is unlikely that such pieces would be transported during washdown by water flows.

Table 5-1. Capture Fractions Recommended for estimating drywell transport fractions during blowdown (short-term).

Debris size[8]	Wetness	Recommended capture fraction		Rationale
		Lower bound[9]	Best estimate[10]	
Floor Grating (4" x 1.5" clearance)				
Small	Dry[11]	0%	0%	See Figures 3.7-4 and 3.7-6.
	Wet	15%	25%	See Figures 2.7-4 and 3.7-6.
Large	Dry	100%	100%	See Section 3.7.6.2
	Wet	100%	100%	See Section 3.7.6.2
Congested Structures (prototypical of BWR drywells)				
Small	Dry	0%	0%	See Figure 3.7-3
	Wet	0%	10%	See Figure 3.7-3 for best estimate. Engr. Judgement for Lower bound
Large	Dry	0%	0%	CEESI tests showed no evidence of deposition.
	Wet	0%	0%	
Mark II Vent Entrance				
Small	Dry	0%	0%	
	Wet	5%	10%	
Large	Dry	5%	10%	
	Wet	10%	35%	
Mark I Vent Entrance				
Small	Dry	0%	0%	
	Wet	1%	5%	

[8] See size definition plotted in Figure 1-2 for CEESI Tests. Small and Large correspond to photographs 3.6-2 and 3.6-4.
[9] Lower bound refers to the minimum capture observed in the experiments (after accounting for experimental uncertainty) for the conditions specified in the table.
[10] Best estimate represents the average capture fraction measured for the conditions specific in the table.
[11] Dry refers to when the surface of the structure is dry or partially dry. Other models should be used to determine if a particular structure is expected to be dry or wet in the BWR drywell during blowdown.
[12] Beyond a minimum structural wetness capture is negligibly effected by wetness. Other models should be used to determine if a particular structure is expected to be dry or wet in the BWR drywell during blowdown.

NRC FORM 335 (2-89) NRCM 1102, 3201, 3202

U.S. NUCLEAR REGULATORY COMMISSION

BIBLIOGRAPHIC DATA SHEET

(See instructions on the reverse)

1. REPORT NUMBER (Assigned by NRC, Add Vol., Supp., Rev., and Addendum Numbers, if any.)

NUREG/CR-6369, Vol. 2
SEA 97-3105-A:15

2. TITLE AND SUBTITLE

Drywell Debris Transport Study: Experimental Work

3. DATE REPORT PUBLISHED

MONTH	YEAR
September	1999

4. FIN OR GRANT NUMBER

W6325

5. AUTHOR(S)

D.V. Rao, C. Shaffer, B. Carpenter, D. Cremer, and J. Brideau

6. TYPE OF REPORT

Final

7. PERIOD COVERED *(Inclusive Dates)*

8. PERFORMING ORGANIZATION - NAME AND ADDRESS *(If NRC, provide Division, Office or Region, U.S. Nuclear Regulatory Commission, and mailing address; if contractor, provide name and mailing address.)*

Science and Engineering Associates, Inc.
6100 Uptown Blvd. NE
Albuquerque, NM 87110

Subcontractor:
Alden Research Laboratory
30 Shrewsbury Street
Holden, MA 01520

9. SPONSORING ORGANIZATION - NAME AND ADDRESS *(If NRC, type "Same as above"; if contractor, provide NRC Division, Office or Region, U.S. Nuclear Regulatory Commission, and mailing address.)*

Division of Engineering Technology
Officeof Nuclear Regulatory Research
U.S. Nuclear Regulatory Commission
Washington, DC 20555-0001

10. SUPPLEMENTARY NOTES

M. Marshall, NRC Project Manager

11. ABSTRACT *(200 words or less)*

This report describes three test programs undertaken as part of the DDTS to pro vide basic understanding regarding transport of insulation fragments in the drywell following a postulated LOCA. The first two tests focused on transport of debris by blowdown flow. They obtained data related to (a) inertial capture of insulatio n debris on typical BWR drywell structures while they are transported across the structures by the steam flow; and (b) degradati on of large insulation pieces captured on floor gratings when exposed to high velocity steam flow with suspended droplets. The se tests clearly established that wet floor gratings would capture significantly more debris than any other BWR drywell str uctures (e.g., pipes, I-beams and vents). The capture efficiency of all structures was found to be a strong function of debri s size and structural wetness, but a weak function of flow velocity and local flow patterns. Floor gratings possess 100% capture efficiency for insulation pieces larger than 6"x4". These large pieces do not degrade or are not forced through the grating clearan ces (1.5"x4") when subjected to high velocity droplet flow, even though the differential pressure across them is as high as I psid.

The third test program addressed the issue of washdown of debris previously cap tured on floor gratings by break over flow or containment spray flow during ECCS recirculation phase. These tests concluded that majority of the small debris pieces captured on various structures would be washed down by break flow or spray flow. On the other hand, erosion is the only available mechanism by which large pieces deposited on the floor gratings would be transported. In three hours, as much as 25% of the larger pieces can be eroded and transported to the suppression pool.

12. KEY WORDS/DESCRIPTORS *(List words or phrases that will assist researchers in locating the report.)*

BWR Suction Strainers
Drywell Debris Transport
Transport Experiment

13. AVAILABILITY STATEMENT

unlimited

14. SECURITY CLASSIFICATION

(This Page)
unclassified

(This Report)
unclassified

15. NUMBER OF PAGES

16. PRICE

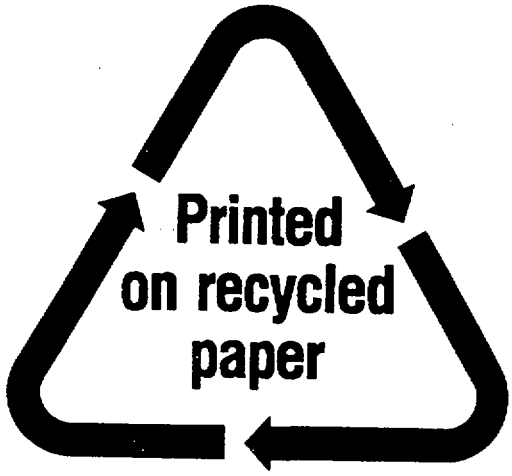

Federal Recycling Program

UNITED STATES
NUCLEAR REGULATORY COMMISSION
WASHINGTON, DC 20555-0001

OFFICIAL BUSINESS
PENALTY FOR PRIVATE USE, $300

SPECIAL STANDARD MAIL
POSTAGE AND FEES PAID
USNRC
PERMIT NO. G-67